SYNTHESIS OF HETEROGENEOUS CATALYST FOR BIODIESEL PRODUCTION

TAN HONG SHEN

UNIVERSITI TUNKU ABDUL RAHMAN

SYNTHESIS OF HETEROGENEOUS CATALYST FOR BIODIESEL PRODUCTION

TAN HONG SHEN

A project report submitted in partial fulfilment of the requirements for the award of Bachelor of Chemical Engineering with Honours

Lee Kong Chian Faculty of Engineering and Science Universiti Tunku Abdul Rahman

April 2024

DECLARATION

I hereby declare that this project report is based on my original work except for citations and quotations which have been duly acknowledged. I also declare that it has not been previously and concurrently submitted for any other degree or award at UTAR or other institutions.

Signature : _____

Name : Tan Hong Shen

ID No. : 1903395

Date : 13 April 2024

APPROVAL FOR SUBMISSION

I certify that this project report entitled **"SYNTHESIS OF HETEROGENEOUS CATALYST FOR BIODIESEL PRODUCTION"** was prepared by **Tan Hong Shen** has met the required standard for submission in partial fulfilment of the requirements for the award of Bachelor of Chemical Engineering with Honours at Universiti Tunku Abdul Rahman.

Approved by,

Signature : *steven*

Supervisor : Dr. Steven Lim

Date : 28.4.2024

Signature : *yeanling*

Co-Supervisor : Dr. Pang Yean Ling

Date : 29.4.24

ACKNOWLEDGEMENTS

I would like to express my sincere gratitude to all those who have contributed to the successful completion of this project.

First and foremost, I am immensely thankful to my supervisor, Dr. Steven Lim, and to my co-supervisor, Dr. Pang Yean Ling, for their invalueable guidance, encouragement, and support throughout this project. Their expertise, patience, knowledge and incredible feedback have been instrumental in the success of this project.

Furthermore, I would also like to extend my heartfelt thanks to my fellow classmates and friends who provided invaluable assistance, support, companionship and constructive ideas. Their presence have been priceless throughout the course of this project.

Additionally, I am also very grateful to Universiti Tunku Abdul Rahman for providing the necessary resources and facilities required for the project. Moreover, I would also like to thank the laboratory staffs for their constant support and guidance throughout the project. Their help has been crucial in facilitating the laboratory works conducted during the project.

Last but not least, I would like to express my deepest appreciation to my parents and sisters for their unwavering love, encouragement, understanding, and consolation throughout this journey. Their constant support has been a source of strength that kept me motivated during challenging moments.

In conclusion, I acknowledge with gratitude the contributions of all individuals and entities mentioned above, without whom the completion of this project would have been impossible.

ABSTRACT

Biodiesel is an intriguing replacement of petroleum diesel, which plays a direct role in advancing Sustainable Development Goal (SDG) 7 ("Affordable and Clean Energy") and SDG 13 ("Climate Action"). However, the current production of biodiesel through the conventional transesterification process is plagued by inefficiency and waste by-product generation. Interesterification poses as a potential alternative to produce biodiesel with more upsides. However, the research of catalyst for interesterification is still lacking, particularly in heterogeneous catalysts. By using two types of biomass, microcrystalline cellulose and corncob, a functional sulfonated carbon-based catalyst was obtained. The catalyst was synthesised through a conventional two-step method consisting of a 2 hours carbonisation step and a 4 hours sulfonation step, where it was determined that the optimal carbonisation temperature is 200 °C and the optimal sulfonation temperature is 100 °C. The synthesised catalysts shown amorphous crystal structure and have no apparent porosity, with the highest observed specific surface area being 1.93 m^2/g. However, the attachment of the functional group, sulfonic group, onto the catalyst surface is successful and comparable with other studies, where the highest sulfonic group density of 1.04 mmol/g was achieved. For the interesterification, methyl acetate and oleic acid was mixed at a molar ratio of 50:1 and reacted at a reaction temperature of 100 °C. As a result, the synthesised catalyst managed to achieve a reasonable optimal biodiesel yield of 82 % at a catalyst loading of 10 wt% and a reaction time of 4 h. While the synthesised catalyst have good thermal stability at the reaction temperature of 100 °C employed in this report, it suffered a noticeable decrease in activity due to leaching as the spent catalyst can only achieve a maximum biodiesel yield of 65 %, signalling that further study is required to improve the stability of the catalyst against leaching. This study provides more insight into the potential of sulfonated carbon-based catalysts from biomass to catalyse the production of biodiesel, which could ultimately help advance the progress of the UN SDGs, in particular SDG 7 and SDG 13.

TABLE OF CONTENTS

LIST OF TABLES

LIST OF FIGURES

LIST OF SYMBOLS / ABBREVIATIONS

AV	Acid Value, mmol/g
C_{KOH}	Concentration of Potassium Hydroxide, mol/L
C_{NaOH}	Concentration of Sodium Hydroxide, mol/L
m	Mass of the Catalyst Used, g
m_{sample}	Mass of the Sample Used, g
MW_{FAME}	Molecular Weight of Fatty Acid Methyl Ester, g/mol
MW_{FFA}	Molecular Weight of Free Fatty Acid, g/mol
MW_{KOH}	Molecular Weight of Potassium Hydroxide, g/mol
V_{KOH}	Volume of Potassium Hydroxide, mL
V_{NaOH}	Volume of Sodium Hydroxide, mL
X	Free Fatty Acid Conversion, %
Y	Fatty Acid Methyl Ester Yield
BET	Brunauer, Emmett and Teller Method
$ClSO_3H$	Chlorosulfonic Acid
FAME	Fatty Acid Methyl Ester
FFA	Free Fatty Acid
FTIR	Fourier-Transform Infrared Spectroscopy
KOH	Potassium Hydroxide
MCC	Microcrystalline Cellulose
NaCl	Sodium Chloride
$NaNO_2$	Sodium Nitrite
NaOH	Sodium Hydroxide
NO_x	Nitrogen Oxides
OPEFB	Oil Palm Empty Fruit Bunch
SDG	Sustainable Development Goal
SEM-EDX	Scanning Electron Microscope with energy dispersive X-ray
SO_3H-	Sulfonic Functional Group
TGA	Thermogravimetric Analysis
XRD	X-ray Diffraction
4-BDS	4-Benzenediazonium Sulfonate

LIST OF APPENDICES

CHAPTER 1

INTRODUCTION

1.1   Renewable Energy

Renewable energy as alternative energy source and eventual replacement for the traditional energy source is well known and had been a focus of study in the past decades. The continual development and application of renewable energy source is deemed a must to hit the United Nations Sustainable Development Goals (SDGs), with hopes of halting overexploitation of the natural resources on the planet Earth (Abbasi, et al., 2022; Shahzad, et al., 2020). The current renewable energy production in the world is dominated by the United States, China, and the United Kingdom, which made up of 48.32 % of the total renewable energy production in the world. Most countries including Malaysia have a much lower renewable energy production capability than the three major producers due to various factors, with the common features among these countries being either a low income economy, small territory, or having an abundance in fossil fuel resource (Li, Luan and Lin, 2022).

Generally, the renewable energy sources in use nowadays around the world includes solar, wind, hydro, tidal, wave, geothermal, biomass and biofuel energies (Miralles-Quirós and Miralles-Quirós, 2018). Since the year 2000, the electricity produced from various renewable energy sources had increased significantly annually, making up roughly 9 % of the global electricity generated (Li, Luan and Lin, 2022). However, despite the increased application and advancement of renewable energy sources, the global carbon dioxide concentration in the air had reached an unprecedented level of 413 ppm, indicating a worsening greenhouse effect (Syafiuddin, et al., 2020). Figure 1.1 shows the world electricity generated by sources in year 2018.
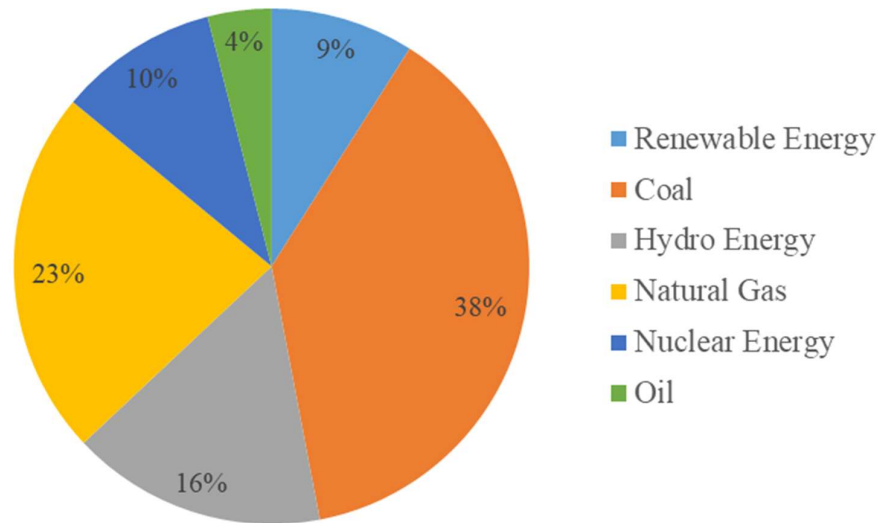
Figure 1.1: Electricity Generated by Source in 2018 (Li, Luan and Lin, 2022).

The emergence of biofuels like biodiesel and bioethanol is seen as a counter to the volatile fossil fuel price and also key in reducing the emissions of greenhouse gas (Miralles-Quirós and Miralles-Quirós, 2018; Shahzad, et al., 2020). In a study by Abbasi, et al. (2022), the use of fossil fuel significantly increases carbon dioxide emissions into the atmosphere in both short and long term, whereas the use of alternative fuel from renewable sources increases carbon dioxide emissions in the short term, but has a lasting positive effect in the long term.

1.2   Biodiesel

In Malaysia, the development of biodiesel had attracted much interest due to the vast plantations of oil palm and production of palm oil, a feedstock for biodiesel production. Biodiesel is a type of fuel derived from biomass which have similar or enhanced properties compared to petroleum diesel. It presents an attractive alternative to petroleum diesel due to the shrinking petroleum reserve in the world (Li, et al., 2023).

Biodiesel has many features that encouraged its usage and further development. Firstly, burning biodiesel produces less emissions of hydrocarbons, carbon monoxide, carbon dioxide and particulate matters. Furthermore, the feedstock for biodiesel production is more resilient and tough, needing less nutrients than the common crops, thereby allowing for the

valorisation of barren land unsuitable for the growth of food crops. Other than that, biodiesel can be used without needing any significant modification to the existing engines and can be blended with petroleum diesel (Dutta, et al., 2021; Li, et al., 2023). Biodiesel is also less toxic than petroleum diesel and has a much higher degradation rate, which allow biodiesel to cause less harm to the environment and human health in case a spillage occurs (Singh, et al., 2020). Compared to petroleum diesel, biodiesel has a higher flash point at 150°C, making the transportation and storage of biodiesel safer than petroleum diesel, which usually has a flash point around 60°C (Syafiuddin, et al., 2020).

However, biodiesel also face several drawbacks. Firstly, the use of first generation feedstock negatively affects food supply as farmers switch from food crops to better priced fuel crops. On the other hand, the use of second generation feedstocks does not affect food supply as it can be grown on less fertile land unsuitable for food crops, but it faces issues with low crop yield similar to some first generation feedstocks. Third and fourth generation feestocks seeks to overcome the issues of the first and second generation feedstock, but its development is still immature, leading to high cost which are economically unfeasible especially for fourth generation feedstocks (Singh, et al., 2020). The need of agricultural land to grow the feedstock also leads to further deforestation, decreasing the carbon storage capacity of the planet. Biodiesel also tends to have a higher viscosity than petroleum diesel, which leads to cold start difficulties and increase in NO_x emissions (Syafiuddin, et al., 2020).

In year 2021, the global biodiesel production totaled 43.4 billion litres, which is lower than the bioethanol produced in the same timeframe amounting to 117 billion litres. The discrepancy between the production of biodiesel and bioethanol is attributed to economic uncertainty surrounding the biodiesel production process, more specifically due to a lack of sufficient and consistent feedstock, in addition to the use of catalysts which are neither efficient nor sustainable (Sreeharsha, Dubey and Mohan, 2023). Malaysia is one of the top biodiesel producer and exporter in the world, accounting for 28 % of the total global biodiesel production and 33 % of the total global biodiesel exports. It was found that the demand for biodiesel is coupled with the price of fossil fuel, where an increase in the price of fossil fuel leads to an increase in biodiesel demand (Dutta, et al., 2021).

1.3 Biodiesel Synthesis Pathway

In the past decades, biodiesel is mostly produced through transesterification pathway industrially. Transesterification is a reaction between triglycerids with alcohols, typically methanol, to produce fatty acid esters, typically fatty acid methyl esters (FAME). In transesterification, the glycerol backbone of the triglyceride is removed and treated as a by-product. The reaction have three stages, which occurs successively, with triglyceride being converted to diglyceride in the first stage, diglyceride being converted to monoglyceride in the second stage, and monoglyceride being converted to glycerol in the final stage. In each stages of the reaction, an alkyl ester, the desired product, is formed (Pandit, et al., 2023). Transesterification requires either strong acid or base as catalyst. Sodium hydroxide, potassium hydroxide and sodium methoxide are examples of strong base catalyst used in transesterification process, whereas hydrochloric acid and sulfuric acid are examples of strong acid catalyst (Pandit, et al., 2023; Prestigiacomo, et al., 2022; Dhawan, Barton and Yadav, 2021). Figure 1.2 visualises the transesterification reaction.
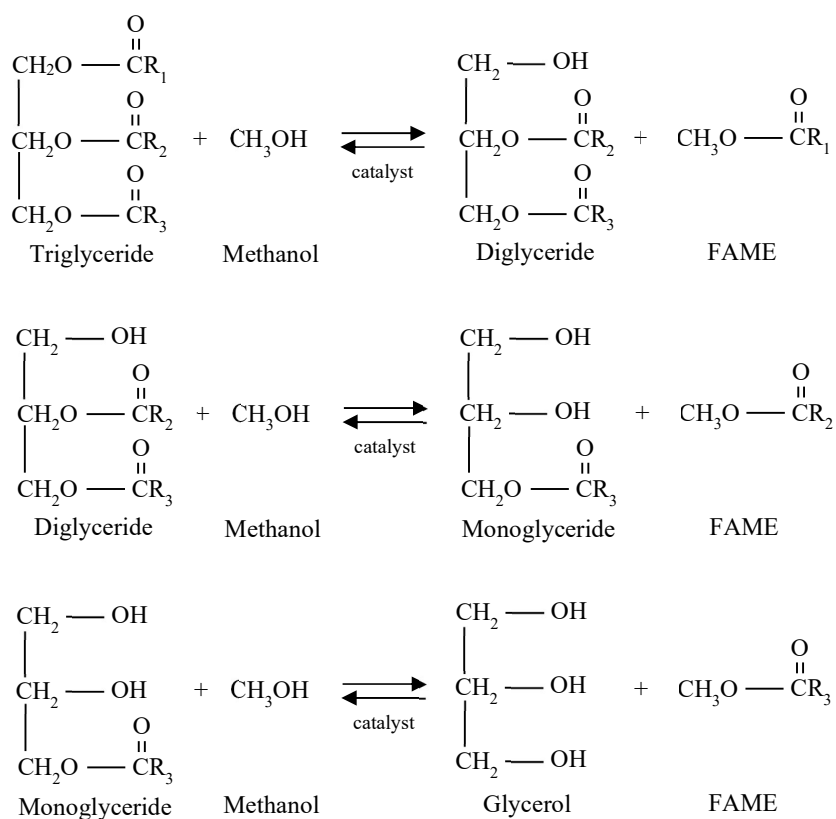
Figure 1.2: Transesterification Reaction (Pandit, et al., 2023).

Another reaction pathway available for the production of biodiesel is interesterification. Interesterification produce fatty acid esters, typically FAME, in a reaction between triglycerides with the acyl donors, typically methyl acetate. In interesterification, the acyl donor exchange its acyl group with the triglyceride, forming triacetin as a by-product. Similar to transesterification, interesterification proceeds in three successive stages, with triglyceride being converted to monoacetindiglyceride in the first stage, monoacetindiglyceride being converted to diacetinmonoglyceride in the second stage, and finally diacetinmonoglyceride being converted to triacetin in the third stage. Fatty acid esters are produced at each of the three stages during interesterification. The study of catalyst for interesterification is not as conclusive and complete as compared to its equivalent for transesterification due to the relative novelty of the reaction. Several studies suggested that interesterification can be carried out without catalyst at extreme temperature and pressure, whereas other studies reported alkaline hydroxide, alkoxide, and octoate as potential homogeneous catalyst; and various sulfuric acid functionalised metal catalyst as potential heterogeneous catalyst (Prestigiacomo, et al., 2022).

Interesterification had gained great interest among scholars as an alternative to the widely used transesterification process, mainly due to the ability of interesterification to overcome the shortcomings of transesterification. Firstly, methanol is immiscible with the reaction media, requiring intensive mixing efforts to overcome the mass transfer limitation (Prestigiacomo, et al., 2022; Wong, et al., 2023). Furthermore, the excess methanol used in transesterification was found to be negatively impacting the stability of heterogeneous catalyst used in reactors (Prestigiacomo, et al., 2022). The glycerol produced in transesterification as by-product also has a low market value, as there is significantly more supply than demand in the chemical market for glycerol. Therefore, glycerol is treated as a waste and needs to be disposed, creating additional costs and giving rise to environmental issues (Dhawan, Barton and Yadav, 2021; Kashyap, Gogate and Joshi, 2019; Prestigiacomo, et al., 2022). Figure 1.3 shows the interesterification reaction.

The following reactions are shown in the figure:

Reaction 1:

$$\text{Triglyceride} + \text{Methyl Acetate} \underset{\text{catalyst}}{\rightleftharpoons} \text{Monoacetindiglyceride} + \text{FAME}$$

Triglyceride:
$$\begin{array}{l} CH_2O \!-\! \overset{O}{\overset{\|}{C}}R_1 \\ CH_2O \!-\! \overset{O}{\overset{\|}{C}}R_2 \\ CH_2O \!-\! \overset{O}{\overset{\|}{C}}R_3 \end{array} + CH_3O \!-\! \overset{O}{\overset{\|}{C}}CH_3 \underset{\text{catalyst}}{\rightleftharpoons} \begin{array}{l} CH_2O \!-\! \overset{O}{\overset{\|}{C}}CH_3 \\ CH_2O \!-\! \overset{O}{\overset{\|}{C}}R_2 \\ CH_2O \!-\! \overset{O}{\overset{\|}{C}}R_3 \end{array} + CH_3O \!-\! \overset{O}{\overset{\|}{C}}R_1$$

Triglyceride Methyl Acetate Monoacetindiglyceride FAME

Reaction 2:

$$\begin{array}{l} CH_2O \!-\! \overset{O}{\overset{\|}{C}}CH_3 \\ CH_2O \!-\! \overset{O}{\overset{\|}{C}}R_2 \\ CH_2O \!-\! \overset{O}{\overset{\|}{C}}R_3 \end{array} + CH_3O \!-\! \overset{O}{\overset{\|}{C}}CH_3 \underset{\text{catalyst}}{\rightleftharpoons} \begin{array}{l} CH_2O \!-\! \overset{O}{\overset{\|}{C}}CH_3 \\ CH_2O \!-\! \overset{O}{\overset{\|}{C}}CH_3 \\ CH_2O \!-\! \overset{O}{\overset{\|}{C}}R_3 \end{array} + CH_3O \!-\! \overset{O}{\overset{\|}{C}}R_2$$

Monoacetin-diglyceride Methyl Acetate Diacetinmonoglyceride FAME

Reaction 3:

$$\begin{array}{l} CH_2O \!-\! \overset{O}{\overset{\|}{C}}CH_3 \\ CH_2O \!-\! \overset{O}{\overset{\|}{C}}CH_3 \\ CH_2O \!-\! \overset{O}{\overset{\|}{C}}R_3 \end{array} + CH_3O \!-\! \overset{O}{\overset{\|}{C}}CH_3 \underset{\text{catalyst}}{\rightleftharpoons} \begin{array}{l} CH_2O \!-\! \overset{O}{\overset{\|}{C}}CH_3 \\ CH_2O \!-\! \overset{O}{\overset{\|}{C}}CH_3 \\ CH_2O \!-\! \overset{O}{\overset{\|}{C}}CH_3 \end{array} + CH_3O \!-\! \overset{O}{\overset{\|}{C}}R_3$$

Diacetin-monoglyceride Methyl Acetate Triacetin FAME

Figure 1.3: Interesterification Reaction (Prestigiacomo, et al., 2022).

Interesterification overcome the abovementioned shortcomings by replacing methanol completely with methyl acetate or ethyl acetate. Methyl acetate and ethyl acetate are both soluble in the reaction media, essentially removing the mass transfer difficulties encountered when using methanol in transesterification. The by-product produced in interesterification is triacetin, which has a much higher market value than glycerol (Prestigiacomo, et al., 2022). Triacetin can be mixed into the biodiesel produced to up to 10 wt% without affecting the quality and performance of the final product (Dhawan, Barton and Yadav, 2021; Kashyap, Gogate and Joshi, 2019; Prestigiacomo, et al., 2022). Additionally, triacetin can also be used as plasticiser in polymer synthesis process and as additive in pharmaceutical and cosmetic industries (Kashyap, Gogate and Joshi, 2019; Prestigiacomo, et al., 2022).

However, interesterification also has its own drawbacks. The most significant drawback reported is the struggle of interesterification to achive

equivalent yield relative to transesterification in a specific timeframe (Dhawan, Barton and Yadav, 2021; Prestigiacomo, et al., 2022). The low yield is attributed to the high reversibility of interesterification reaction (Dhawan, Barton and Yadav, 2021). Interesterification has also been studied mainly with homogeneous catalyst and enzymes, where some studies reported significant difficulties in the recovery and reuse of the catalyst (Dhawan, Barton and Yadav, 2021; Prestigiacomo, et al., 2022). Compared to transesterification, interesterification is not studied as extensively, especially when it comes to the use of heterogeneous catalyst.

1.4   Catalyst for Biodiesel Synthesis

Catalyst used in the production of biodiesel can be either chemical or biological, with the aim to enhance the reaction rate and to achieve a higher yield. Catalyst can be categorised into homogeneous or heterogeneous depending on the state of matter relative to the reaction media (Rocha-Meneses, et al., 2023). Chemical catalyst can be either base catalyst or acid catalyst, with base catalyst being more popular due to its shorter reaction time, higher yield, and relatively mild operating conditions. However, certain base catalyst such as potassium hydroxide and sodium hydroxide is troubled by side reactions that arise with higher free fatty acid content, which lowers its product yield. On the other hand, acid catalyst has a high tolerance for free fatty acid and is unaffected by its presence. However, it has a higher cost, slower reaction time, is corrosive and more harmful to the environment (Changmai, et al., 2020).

Homogeneous catalyst refers to the type of catalyst that operates in the same phase as the reaction media (Pandit, et al., 2023). Homogeneous catalyst had been widely studied and is found to be facilitating high reactivity at a low cost, however, the difficult recovery of the catalyst and tedious purification proces of the biodiesel required makes it economically unsound. As such, heterogeneous catalyst had gained much attention and interest as it can be recovered and reused at ease without significant lose of catalytic activity. Heterogeneous catalyst mostly exist in solid phase where the reaction media is either in liquid phase or gas phase, the main sites of reaction are located at the surface of the catalyst. Heterogeneous catalysts are also less toxic and have little

corrosive power relative to homogeneous catalyst, making it more environmentally friendly (Changmai, et al., 2020).

Heterogeneous base catalyst specifically had gained more attraction in recent times as it exhibits outstanding catalytic activity under mild reaction conditions while overcoming the drawbacks of homogeneous base catalyst. There are several categories of heterogeneous base catalyst being developed, including transition metal oxides, zeolites, alkaline earth metal oxides, biomass-based catalyst, mixed metal oxides, supported catalyst, and hydrotalcite. Despite its advantanges, many heterogeneous base catalysts exhibited poor performance when encountering feedstock rich in free fatty acid. On the other hand, heterogeneous acid catalyst can tolerate a higher free fatty acid or water content. Categories of heterogeneous acid catalyst includes ion exchange resin, sulfacted catalyst, mixed metal oxides and sulfonated carbon-based catalyst (Changmai, et al., 2020).

Sulfonated carbon-based catalyst is to be investigated in this report due to its interesting features of low production cost, simple synthesis pathway, excellent surface chemistry, environmental friendliness, biogenic, good thermal stability and good chemical stability (Changmai, et al., 2020; Sangsiri, Laosiripojana and Daorattanachai, 2022). Sulfonated carbon-based catalyst refers to a group of metal-free solid acid catalyst, which main structure is made up of carbon and exhibits Brønsted acidity equivalent to sulfuric acid. Sulfonated carbon-based catalyst typically consist of a carbon structure functionalised with a sulfonic group (Changmai, et al., 2020).

1.5   Corncob as Catalyst

Corn is an important agricultural crops used to produce both edible and non-edible products, where its global production capacity has reached almost 1150 million tonnes annually with the United States of America and China as the top two producers (Gandam, et al., 2022b). Corncob is a waste that is generated as a by-product from the production of corn to other products, where it was reported that 0.3 tonne of corncob is produced for every 1 tonne of corn processed (Gandam, et al., 2022a). Typically, corncob is simply disposed as waste, used as soil fertiliser, or sometimes directly burned as an energy source (Tinh, et al., 2023).

Compared to other agricultural biomass waste, corncob is distinct in terms of its composition, which has a relatively higher cellulose and hemicellulose (especially xylan) content; and a lower lignin and ash content. It was generally reported that the biomass composition of corncob is made up of 38.9 % cellulose, 28.5 % hemicellulose, and 20.5 % lignin on average, making it particularly attractive in biofuel synthesis related applications (Gandam, et al., 2022a). Additionally, unlike other agricultural biomass waste, corncob can be easily subjected to a wide range of pretreatment methods including chemical, physical, mechanical, biological or combination of any other pretreatment methods (Gandam, et al., 2022b). A fitting pretreatment of corncob may achieve up to 95 % recovery of cellulose, complete hemicellulose solubilisation, and 99 % delignification (Gandam, et al., 2022b; Guo, et al., 2023).

Currently, the efforts to valorise corncob is predominantly directed at using it as the feedstock to produce biofuels, typically bioethanol, and also chemicals such as furfural (Gandam, et al., 2022a; Gandam, et al., 2022b; Tinh, et al., 2023). However, corncob had attracted great interest as a potential catalyst for biodiesel production in recent times, where it is reported that sulfonated corncob-based catalyst can achieve similar biodiesel yield in a shorter reaction time while operating under a milder temperature compared to other available catalyst (Guo, et al., 2023; Naeem, et al., 2021).

1.6   Importance of the Study

As emphasised in the previous section, the continual research and development of renewable energy is of upmost importance to ensure a sustainable future. Biodiesel as a potential alternative to petroleum diesel can brings many benefits and help to achieve the United Nations SDGs by reducing the emissions of greenhouse gas through the replacement of petroleum diesel with biodiesel. As biodiesel replaces petroleum diesel, it is expected to have a direct and significant impact on the advancement of SDG 7 ("Affordable and Clean Energy") and SDG 13 ("Climate Action"). Indirectly, advancement towards SDG 1 ("No Poverty"), SDG 9 ("Industry, Innovation and Infrastructure"), and SDG 15 ("Life on Land").

1.7   Problem Statement

The production of biodiesel in the industry is predominantly through the transesterification process. However, the conventional synthesis process of transesterification to produce biodiesel has several drawbacks due to inefficiency and waste by-product. In particular, the use of methanol as the reactant in transesterification poses as an inefficiency, as the use of methanol requires intensive mixing to achieve a satisfactory homogeneity within the reaction mixture. Additionally, the glycerol produced as the by-product in transesterification also have low market value and is often disposed of as waste.

An interesting alternative, interesterification, which addressed abovementioned drawbacks of transesterification by replacing methanol as the reactant and producing valuable triacetin as by-product rather than glycerol, is not studied as extensively and offers more potential for improvement and optimisation. Specifically, the development of catalyst for interesterification is still relatively new and novel, with most studies focusing on homogeneous catalyst. The use of heterogeneous catalyst offers interesting advantages when compared to homogeneous catalyst, for instance, heterogeneous catalyst does not require additional separation and recovery step from the product stream, thereby cutting the cost associated with catalyst recovery.

Furthermore, the dominant heterogeneous catalyst currently in use in the biodiesel industry, both acidic and basic, are based on various types of metal oxides. While these heterogeneous catalysts had been proven in practical use, the cost of these catalysts are still relatively high due to the presence of metallic content in the catalysts. Therefore, compared to the conventional metallic heterogeneous catalysts, carbon-based heterogeneous catalysts derived from biomass, in particularly waste biomass, represents an opportunity in catalyst cost reduction.

Thus, the successful industrialised use of an effective carbon-based heterogeneous catalyst derived from waste and cheap biomass is expected to greatly reduce the catalyst purchase cost and catalyst separation cost, thereby reducing the production cost of biodiesel and allows for its widespread use. However, the research and development of heterogeneous catalyst for interesterification is lacking and immature.

1.8   Aim and Objectives

The study aims to develop a sulfonated carbon-based catalyst for the interesterification process to produce biodiesel. The objectives are as follows,

1. To synthesize a sulfonated carbon-based catalyst from microcrystalline cellulose and corncob.
2. To characterise the physical and chemical properties of the synthesized catalyst.
3. To compare the catalytic activity of the two catalysts in interesterification reaction with different operating conditions.

1.9   Scope and Limitations of the Study

This study is concerned with the effect of various catalyst synthesis parameters, in particular carbonisation temperature and sulfonation temperature, on the catalytic performance of the sulfonated carbon-based catalyst derived from different biomass, that are microcrystalline cellulose and corncob. Furthermore, this study also intends to characterise the catalyst synthesised to gain a better understanding of the relationship between catalytic activity and the inherent properties of the catalyst in interesterification reaction. Additionally, this study also includes the effect of various interesterification reaction conditions, in particular catalyst loading and reaction time, on the biodiesel yield.

However, the optimisation of the catalyst in this study is limited to the catalytic activity optimisation only, as the stability of the catalyst is excluded and the study does not intend to optimise the stability of the catalyst due to time and equipment constraints. Moreover, the effect of carbonisation time and sulfonation time on the synthesised catalyst, as well as the different method of sulfonated carbon-based catalyst synthesis, the one-step method, is also excluded. Furthermore, the determination of optimal interesterification reaction temperature is also excluded due to time constraints.

CHAPTER 2

LITERATURE REVIEW

2.1   Introduction

In the industrial production of biodiesel, homogeneous catalysts are often favoured due to wide availability, cheapness, fast reaction and highly effective (Zhang, et al., 2021). However, homogeneous catalysts no matter basic or acidic, for example, potassium hydroxide and sulfuric acid, often faces issues with separation and recovery difficulties, environmental pollution, and corrosion to equipments and pipes (Bureros, et al., 2019; Cao, et al., 2021; Sangar, et al., 2019). Additionally, base catalysts face challenges from the occurrence of saponification when using feedstock with high free fatty acid and water content (Bureros, et al., 2019; Lathiya, Bhatt and Maheria, 2018; Lim, et al., 2020; Rocha, Olivera and Franca, 2019). The use of heterogeneous catalyst such as sulfonated carbon-based catalyst overcomes these issues (Bureros, et al., 2019; Cao, et al., 2021; da Luz Corrêa, et al., 2023; Lathiya, Bhatt and Maheria, 2018; Sangar, et al., 2019; Wong, et al., 2020; Zhang, et al., 2021). However, conventional heterogeneous acid catalysts such as zeolites, silica and polystyrene resin face issues with small pore size and low acid density. Moreover, these catalysts are often unstable and expensive (Flores, et al., 2019).

Compared to other heterogeneous catalyst, sulfonated carbon-based catalyst standouts due to its wide range of raw materials which are often cheap waste biomass, and rich surface functional groups including sulfonic groups, carboxyl groups and hydroxyl groups which provided high acidity comparable to sulfuric acid (Cao, et al., 2021; Lathiya, Bhatt and Maheria, 2018; Rocha, Olivera and Franca, 2019; Zhang, et al., 2021). Several carbon sources had been identified as inexpensive and was used to produce sulfonated carbon-based catalyst, including organic carbon compound such as sugar, lignin, carbohydrates and cellulosic materials; agricultural waste; industrial waste; and polymer resin (Changmai, et al., 2020).

In   particular,   sulfonated   carbon-based   catalyst   allows interesterification to operate under mild conditions rather than under supercritical condition or by using enzymatic catalysis. This alternative

possibility provided by sulfonated carbon-based catalyst is important especially in view of industrial scale-up as it promotes energy efficiency and lower operational cost compared to the other two more conventional methods for interesterification (Wong, et al., 2020).

2.2 Synthesis Pathway

Sulfonated carbon-based catalyst can be prepared by two different methods, namely the two-step method and the one-step method. In two-step method, the carbon-based biomass is carbonised to form biochar in the first step, and the produced biochar is then subjected to sulfonation using sulfonating reagent to produce the desired catalyst in the second step (Bureros, et al., 2019; da Luz Corrêa, et al., 2023; Lim, et al., 2020; Souza, et al., 2022; Zhang, et al., 2021). In one-step method, the carbon-based biomass is carbonised while immersed in a sulfonating reagent, directly producing the desired catalyst by simultaneous carbonisation and sulfonation (Flores, et al., 2019; Souza, et al., 2022; Zhang, et al., 2021). The sulfonation process can be achived by using various sulfonation reagent such as SO_3 gas, sulfuric acid, p-toluenesulfonic acid, $ClSO_3H$, SO_3H-functionalised aryl diazoniums and 4-benzenediazonium sulfonate (4-BDS) (Changmai, et al., 2020).

2.2.1 Two-Step Method

The more conventional two-step method to synthesise sulfonated carbon-based catalyst was studied by many researchers using different raw materials. da Luz Corrêa, et al. (2023) used the two-step method to synthesise the sulfonated catalyst from murumuru kernel. Murumuru kernel is a type of agricultural waste from the extraction of butter from murumuru palm fruit that is underexploited. Firstly, the murumuru kernel is crushed into powder under the size of 340 μm. da Luz Corrêa, et al. (2023) then carbonised the murumuru kernel powder at different temperature (450 °C, 600 °C, 750 °C) for 1 h to investigate the effect of carbonisation temperature on the catalyst quality and performance. The biochar produced is then further squashed using mortar and pestle before being subjected to sulfonation. The sulfonation is conducted using concentrated sulfuric acid which was mixed with the biochar at a ratio of 1 g biochar to 10 mL sulfuric acid at 200 °C for 4 h under reflux. The obtained mixture was then

cooled to room temperature and diluted with deionised water, where the precipitated solids was then filtered out. The recovered solids was washed with deionised water until neutral pH was reached before drying at 60 °C for 24 h. The dried solids was retrieved as the sulfonated carbon-based catalyst.

Ibrahim, et al. (2019) studied the potential of corncob as the carbon support for sulfonated carbon-based catalyst. The corncob was mechanically milled into small aggregates sizing between 1 cm to 2 cm in diameter. Differing from the work of da Luz Corrêa, et al. (2023), Ibrahim, et al. (2019) carbonised the corncob through hydrothermal carbonisation rather than the more conventional direct carbonisation. In hydrothermal carbonisation, the biomass was fully immersed in a medium of water during the process at a relatively low temperature compared to direct carbonisation. Ibrahim, et al. (2019) mixed 5 g of corncob aggregates into 100 mL of distilled water, where the mixture was then carbonised at 200 °C for 10 h. The biochar produced was filtered out from the mixture, cooled to room temperature and then washed with distilled water until neutral pH was reached. The washed biochar was then dried at 100 °C for 12 h before being crushed to form fine powder. The fine powder obtained was sulfonated at 150 °C for 8 h through mixing with concentrated sulfuric acid under reflux. The product was filtered, and the recovered biochar was washed with distilled water at 80 °C till a neutral pH was attained. The obtained sulfonated carbon-based catalyst was then dried at 100 °C for 1 h.

Wong, et al. (2020) studied the use of oil palm empty fruit bunch (OPEFB) as the carbon support for sulfonated carbon-based catalyst extensively, placing heavy emphasis on investigating the effect of carbonisation temperature, carbonisation time, sulfonation temperature and sulfonation time on the quality of the catalyst produced. The OPEFB was first mechanically reduced into finer fibres of sizes no greater than 850 μm before being chemically treated with 30 % phosphoric acid at room temperature for 24 h. The chemically activated biomass was then washed and dried. To investigate the effect of carbonisation temperature, the pretreated fibres was carbonised at different temperatures (400 °C, 500 °C, 600 °C, 700 °C, 800 °C). Additionally, to investigate the effect of carbonisation time, the pretreated fibres was carbonised for different duration (1 h, 2 h, 3 h, 4 h, 5 h). The produced biochar was sieved to recover smaller particles of size 300 μm or smaller for the subsequent sulfonation step. The

sulfonation was carried out by mixing the biochar with concentrated sulfuric acid under reflux. The process was performed at different temperature (75 °C, 100 °C, 125 °C, 150 °C, 175 °C, 200 °C) for different duration (3 h, 4 h, 5 h, 6 h, 24 h) to investigate its influence on the catalyst quality. The mixture was cooled to room temperature and diluted with distilled water, where the precipitates formed was then filtered out. The precipitates recovered was washed with distilled water until neutral pH was achieved. The washed precipitates was dried at 80 °C overnight and sulfonated carbon-based catalyst was obtained.

Similar to the work of Wong, et al. (2020), Lim, et al. (2020) also studied the potential of OPEFB as the carbon support for sulfonated carbon-based catalyst using similar steps. However, rather than the conventional direct sulfonation using concentrated sulfuric acid, Lim, et al. (2020) performed sulfonation through the arylation of 4-benzenediazonium sulfonate (4-BDS), which presents as an alternative that offers better catalytic performance. Firstly, the OPEFB was crushed into fine powder. The powder was then chemically activated with 30 % phosphoric acid at room temperature in a ratio of 1 g powder to 1 g acid for 24 h. Lim, et al. (2020) intended to investigate the effects of carbonisation temperatures on catalyst quality, therefore, the pre-treated fibre was subjected to carbonisation at different temperatures (200 °C, 300 °C, 400 °C, 500 °C, 600 °C) for 2.5 h. The sulfonation of biochar through arylation of 4-BDS was more complex than direct sulfonation using concentrated sulfuric acid, where 4-BDS needs to be synthesised first. To synthesise 4-BDS, 15 g of sulfanilic acid was added into 300 mL of 1 M hydrochloric acid solution and mixed well at 5 °C. Then 90 mL of $NaNO_2$ was added drop by drop, after which the mixture was stirred for 1 h while at 5 °C. Afterwards, 4-BDS can be retrieved as a white precipitate after the mixture was allowed to settled. The obtained 4-BDS was then mixed with 200 mL of deionised water, 60 mL of ethanol and 3 g of the biochar at between 3 °C to 5 °C for the sulfonation process. 30 % hypophosphorous acid was added into the mixture in two batch, the first batch of 100 mL was added and stirred for 30 minutes whereas the second batch of 50 mL was added and stirred for 1 h. Sulfonated carbon-based catalyst can then be retrieved as solid in the mixture.

Cao, et al. (2021) studied the possibility of using *Sargassum horneri*, a type of algae that can be commonly found along the coast of China as the carbon support for the sulfonated carbon-based catalyst. The algae recovered was dried at 105 °C to remove the water content before crushing the algae into fine powders. The dried powder was mixed with 30 % phosphoric acid in a mass ratio of 1:10 as a chemical activation step. Cao, et al. (2021) carbonised the algae powder under an atmosphere of nitrogen gas in a tube furnace while varying carbonisation temperature and carbonisation time. The carbonisation temperature investigated in this study includes 200 °C, 250 °C, 300 °C, 350 °C, 450 °C, and 550 °C, whereas the carbonisation time investigated in this study includes 1 h, 2 h, 3 h, and 4 h. The biochar obtained was crushed again into finer powder before being subjected to sulfonation. The crushed biochar was mixed and stirred with concentrated sulfuric acid at 90 °C for 5 h. The resulting mixture was diluted and washed with distilled water at no lower than 80 °C until neutral pH was reached, where the sulfonated carbon-based catalyst can be obtained after drying at 105 °C.

Rocha, Oliveira and Franca (2019) also investigated the use of corncobs as carbon support for the sulfonated carbon-based catalyst. Similar to Lim, et al. (2020), Rocha, Oliveira and Franca (2019) also carried out the sulfonation process by using 4-BDS. Firstly, corncobs are mechanically reduced into powder, where it was then treated with 85 % phosphoric acid at a ratio of 1 g corncob powder to 1 mL phosphoric acid. The mixture was stirred continuously at room temperature for 3 minutes, after which the mixture was filtered and the pre-treated powder was recovered. The corncob powder was then carbonised in a muffle furnace at 500 °C for 1 h. The biochar produced was cooled under an atmosphere of nitrogen gas and then washed with distilled water until a neutral pH was attained. The preparation of 4-BDS was similar to the steps taken by Lim, et al. (2020), firstly, 5.2 g of sulfanilic acid was added and mixed into 300 mL of 1 M hydrochloric acid at a temperature between 3 °C to 5 °C. 33 mL of 1 M $NaNO_2$ solution was added dropwise into the mixture while under constant mixing until a clear solution was obtained. The clear solution was continuously stirred for another hour at 3 °C to 5 °C, where 4-BDS precipitate slowly forms as a white powder in the solution. The 4-BDS recovered was then added into a mixture containing 50 % ethanol and 50 %

water, where the biochar was also added in a ratio of 1 g biochar to 1 g 4-BDS. Subsequently, 50 mL of 50 % hypophosphorous acid was added to the mixture at 3 °C to 5 °C while under constant stirring for 30 minutes. Another 50 mL of 50 % hypophosphorous acid was added to the mixture under the same condition for 1 h, except that the mixture was allowed to settle without constant stirring. The sulfonated carbon-based catalyst can then be recovered from the mixture after filtration, washing and drying.

Lathiya, Bhatt and Maheria (2018) investigated the synthesis of sulfonated carbon-based catalyst from waste orange peel. Similar to the work of Ibrahim, et al. (2019), hydrothermal carbonisation was carried out in this work rather than direct carbonisation. However, in this study by Lathiya, Bhatt and Maheria (2018), the biomass was submerged in potassium hydroxide solution rather than water for simultaneous chemical activation and carbonisation. Firstly, the waste orange peel devoid of water was grinded into fine powder and was mixed with potassium hydroxide solution. To investigate the effect of potassium hydroxide solution dosage on the catalyst morphology and performance, the waste orange peel powder was mixed with the potassium hydroxide solution under different mass ratio (1:1, 1:2, 1:3). Afterwards, the mixture was carbonised at 180 °C for 6 h. The product was washed continuously with deionised water till a neutral pH was attained before drying at 110 °C for 6 h. The sulfonation was carried out by mixing the biochar with concentrated sulfuric acid at a ratio of 1 g biochar to 20 mL concentrated sulfuric acid at 200 °C for 24 h. Sulfonated carbon-based catalyst can then be retrieved by filtering, washing and drying the produced mixture after sulfonation.

Bureros, et al. (2019) studied the use of cacao shells to synthesise sulfonated carbon-based catalyst. Firstly, the cacao shells are milled into smaller aggregates of particle sizes around 840 μm and was directly carbonised at 350 °C for 1 h. The biochar produced from the carbonisation step was mixed with concentrated sulfuric acid at a ratio of 1 g biochar to 20 mL sulfuric acid at different temperatures (80 °C, 100 °C, 120 °C) for different durations (4 h, 6 h, 8 h) to study how the quality of the synthesised catalyst is affected by sulfonation temperature and sulfonation time. The mixture was then cooled to room temperature, diluted and washed with hot distilled water till a neutral pH

was achieved. The precipitates in the mixture was then filtered out, washed and dried, thus sulfonated carbon-based catalyst was obtained.

Sangar, et al. (2019) investigated the potential of cow manure to synthesise sulfonated carbon-based catalyst. The use of cow manure was interesting especially in Malaysia, where it was estimated that 6.64 million kg of cow manure was produced daily in year 2016. While the use of cow manure as fertiliser, pesticides and feedstock to produce biochar and bio-oil was widely investigated, using cow manure to produce catalyst was still a novel topic. Firstly, fresh cow manure was dried for three days under sunlight and in the oven at 100 °C for 24 h to ensure that the water content in cow manure was removed completely. The dried cow manure was carbonised at 500 °C for 2 h for carbonisation. For the sulfonation step, the sulfonating agent used is concentrated sulfuric acid, which is mixed at a ratio of 1 g cow manure to 10 mL sulfuric acid. To study the relationship between sulfonation time and the catalyst quality, sulfonation is carried out at 180 °C for different durations (2 h, 5 h, 10 h) under reflux. The mixture was then filtered and washed until a neutral pH was achieved. Sulfonated carbon-based catalyst can then be recovered after drying in oven.

2.2.2   One-Step Method

Recently, an alternative one-step method had received attention from scholars due to advantages over the conventional two-step method such as much lower preparation time as well as much more energy saving. Zhang, et al. (2021) studied the synthesis of sulfonated carbon-based catalyst through the one-step method by using bamboo powder. Firstly, about 3 g of bamboo powder with particle size no greater than 45 μm was added to 50 mL of concentrated sulfuric acid. Zhang, et al. (2021) aim to investigate the effect of temperature and time on the quality and performance of the catalyst, thus, the mixture was heated to different temperatures (100 °C, 125 °C, 150 °C, 175 °C, 200 °C) for different durations (2 h, 4 h, 6 h, 8 h, 10 h). The mixture was then cooled to room temperature and diluted with deionised water. Afterwards, the solid content in the mixture was recovered using filtration, which was washed using deionised water till a neutral pH was attained. The washed solid was dried at 105 °C for 12 h to recover the sulfonated carbon-based catalyst.

Souza, et al. (2022) also investigated the use of microcrystalline cellulose (MCC) in the synthesis of sulfonated carbon-based catalyst. Firstly, MCC was added into concentrated sulfuric acid slowly while under constant agitation. Souza, et al. (2022) varied the ratio of MCC to concentrated sulfuric acid at 1 g MCC to 10 mL concentrated sulfuric acid and 1 g MCC to 20 mL concentrated sulfuric acid to study its effects on the catalyst synthesised. Similar to the work of Zhang, et al. (2021), Souza, et al. (2022) also inquire into the effects of temperature and time on the catalyst quality and performance. The mixture was heated to different temperatures (100 °C, 125 °C, 150 °C) for different durations (1 h, 2 h, 4 h, 6 h) in an oil bath. The mixture was added directly into cold water and precipitates formed. The mixture was filtered and the recovered precipitates was washed repeatedly until neutral pH was achieved. The precipitates are dried at 100 °C for 12 h and recovered as sulfonated carbon-based catalyst.

Flores, et al. (2019) explored the potential of sugarcane bagasse in synthesising sulfonated carbon-based catalyst. Firstly, the bagasse was dried in oven at 60 °C for 3 days to ensure that the moisture content no more than 10 % in weight. The bagasse was milled and sieved to recover bagasse powder of particle size around 645 μm. Subsequently, around 3 g of bagasse powder was added into 50 mL of concentrated sulfuric acid in a digestion flask. Flores, et al. (2019) investigated the effect of temperature and time on the quality and performance of the synthesised catalyst. The mixture was then heated to different temperatures (150 °C, 200 °C, 250 °C) for different durations (4 h, 6 h, 8 h). The mixture was then cooled to room temperature and then diluted with 180 mL of distilled water slowly while under constant agitation. The precipitates formed in the mixture was recovered by filtration and then washed with water at 90 °C until pH greater than 5 was attained. The washed precipitate was recovered as sulfonated carbon-based catalyst.

2.2.3   Summary

The literatures discussed in section 2.2.1 regarding the two-step synthesis of sulfonated carbon-based catalyst is tabulated in Table 2.1 below as a brief summary.

Table 2.1: Literatures on Synthesis of Sulfonated Carbon-Based Catalyst through Two-Step Method

Biomass	Carbonisation		Sulfonation		Reference
	Temperature °C	Time h	Temperature °C	Time h	
Murumuru kernel	750	1	200	4	da Luz Corrêa, et al., 2023[1a]
Corncob	200	10	150	8	Ibrahim, et al., 2019[2a]
OPEFB	600	3	100	6	Wong, et al., 2020[1a]
OPEFB	200	2.5	5	1.5	Lim, et al., 2020[1b]
Sargassum horneri	300	2	90	5	Cao, et al., 2021[1a]
Corncob	500	1	5	1.5	Rocha, Olivera and Franca, 2019[1b]
Waste Orange Peel	180	6	200	24	Lathiya, Bhatt and Maheria, 2018[2a]
Cacao Shell	350	1	120	4	Bureros, et al., 2019[1a]
Cow Manure	500	2	180	10	Sangar, et al., 2019[1a]

[1] Direct Carbonisation

[2] Hydrothermal Carbonisation

[a] Direct Sulfonation

[b] 4-BDS Method Sulfonation

As shown in most studies regarding the two-step synthesis of sulfonated carbon-based catalyst is mostly done through a combination of direct carbonisation and direct sulfonation using concentrated sulfuric acid. Generally speaking, the biomass is reduced into finer particles as the initial steps. Subsequently, the biomass particles may be pretreated through a chemical activation step as shown in the works of Wong, et al. (2020); Lim, et al. (2020); Cao, et al. (2021); Rocha, Olivera and Franca (2019); and Lathiya, Bhatt and Maheria (2018). The biomass is then subjected to carbonisation through either direct carbonisation or hydrothermal carbonisation. The produced biochar from the previous steps is then sulfonated by using concentrated sulfuric acid, however alternative sulfonating agent such as 4-BDS may also be used. The mixture obtained from sulfonation is cooled to room temperature, where it is diluted, filtered and then washed with hot water until a neutral pH is achieved. The washed sulfonated carbon-based catalyst can then be recovered and stored for future use after drying.

The literatures discussed in section 2.2.2 regarding the one-step synthesis of sulfonated carbon-based catalyst is tabulated in Table 2.2 below as a brief summary.

Table 2.2: Literatures on Synthesis of Sulfonated Carbon-Based Catalyst through One-Step Method

| Biomass | Carbonisation-Sulfonation | | Reference |
| | Temperature | Time | |
	°C	h	
Bamboo	150	4	Zhang, et al., 2021
Microcrystalline Cellulose	125	1	Souza, et al., 2022
Sugarcane Bagasse	150	8	Flores, et al., 2019

All literatures reviewed synthesised sulfonated carbon-based catalyst in a similar manner, with only slight variation in synthesis conditions. Firstly, the biomass is reduced in finer particles. Dissimilar to two-step method, none of the literature reviews used any types of chemical activation as a pretreatment

step. The biomass is then added into concentrated sulfuric acid directly and carbonised at the same time, thereby performing carbonisation and sulfonation simultaneously. Similar to two-step method, the mixture produced is filtered and diluted. The recovered solid is then washed with water till a neutral pH is achieved. Sulfonated carbon-based catalyst can then be recovered after drying.

Both methods of synthesis while differing in steps, was capable of achieving at least reasonable biodiesel yield or free fatty acid conversion. The following Table 2.3 summarises the catalytic performance of the catalysts synthesised in the literatures discussed above.

Table 2.3: Catalytic Performance of Catalysts Synthesised

Biomass	Synthesis Method	Biodiesel Yield (%)	Reference
Murumuru Kernel	Two-Step	98[1]	da Luz Corrêa, et al., 2023
Corncob	Two-Step	92[1]	Ibrahim, et al., 2019
Corncob	Two-Step	88	Rocha, Olivera and Franca, 2019
Cacao Shell	Two-Step	93[1]	Bureros, et al., 2019
OPEFB	Two-Step	50.5	Wong, et al., 2020
OPEFB	Two-Step	98.1	Lim, et al., 2020
Sargassum horneri	Two-Step	96	Cao, et al., 2021
Cow Manure	Two-Step	80.9[1]	Sangar, et al., 2019
Orange Peel	Two-Step	92[1]	Lathiya, Bhatt and Maheria, 2018

Table 2.3: Catalytic Performance of Catalysts Synthesised (Cont.)

Biomass	Synthesis Method	Biodiesel Yield (%)	Reference
Bamboo	One-Step	98[1]	Zhang, et al., 2021
Sugarcane Bagasse	One-Step	90[1]	Flores, et al., 2019
Microcrystalline Cellulose	One-Step	80[1]	Souza, et al., 2022

[1] FFA Conversion in %

2.3   Effect of Carbonisation Temperature

da Luz Corrêa, et al. (2023) found that as the carbonisation temperature increase, the mass yield of the resulting biochar decrease. The mass yield decrease was attributed to the decomposition and release of more volatile components in the biomass during the carbonisation process, where a higher temperature leads to more volatile components being released from the biomass (Bureros, et al., 2019; da Luz Corrêa, et al., 2023; Wong, et al., 2020). The process of releasing volatile components from the biomass is important in the synthesis of carbon-based catalyst, as pores are left behind in the space originally occupied by the volatile components, creating more surface area for the attachment of sulfonic groups in the subsequent sulfonation step (Wong, et al., 2020). This finding is supported by Cao, et al. (2021) and da Luz Corrêa, et al. (2023), where catalyst synthesised at higher carbonisation temperatures yielded catalyst with higher sulfonic group density.

However, it was also widely reported that an excessively high carbonisation temperature has a negative influence on the catalytic performance of the catalyst. Cao, et al. (2021) reported that at higher carbonisation temperature, rigid and large carbon structure containing of multiple polycyclic aromatic carbon sheets which are stacked on top of one another was formed. Formation of such rigid carbon structure was also reported by Lim, et al. (2020), Bureros, et al. (2019) and Flores, et al. (2019), where the carbon structure of the biochar produced becomes gradually more rigid as the carbonisation temperature increases. Such rigid carbon structures are disadvantageous to the

attachment of sulfonic groups onto the catalyst surface (Bureros, et al., 2019; Cao, et al., 2021; Flores, et al., 2019). Lim, et al. (2020) and Wong, et al. (2020) also found that at excessively high temperatures, the biomass faces severe decomposition and disintegration of its carbon structure, where the pore density of the carbon structure decreases due to formation of less numerous and larger pores, thereby reducing the surface area available for sulfonic groups attachment. Such observations and findings are supported by the fact that the sulfonic group density increases initially as the carbonisation temperature increases up until an optimal point, after which the sulfonic group density decreases as carbonisation temperature increases (Bureros, et al., 2019; Cao, et al., 2021).

However, carbonisation at higher temperatures also yields catalyst with higher stability due to the presence of stacked polycyclic aromatic carbon structures that is formed at higher temperatures. The stability of the catalyst produced at higher carbonisation temperature is evident as it retains most of its functional groups after multiple cycles of use in reaction while the catalyst produced at lower carbonisation temperature lost significant amount of its functional groups after usage (da Luz Corrêa, et al., 2023). This phenomenon can be observed from the results from the reusability test in the work of da Luz Corrêa, et al. (2023), where the catalyst synthesised at 750 °C can achieve 94 % conversion in the second cycle of use whereas the catalyst synthesised at 450 °C can only achieve 45 % conversion even though both catalyst achieve similar conversion during the first cycle of use. This result is consistent with the work of Bureros, et al. (2019), where the catalyst synthesised at carbonisation temperature of 350 °C saw its conversion drops from 93 % in the first cycle to only 48 % in the fourth cycle.

Generally, carbonisation is performed at lower temperatures to ensure that the carbonisation process is incomplete. Incomplete carbonisation of biomass at lower temperature produces small and numerous polycyclic aromatic carbon sheets rather than large stacked polycyclic aromatic carbon sheets that are formed from multiple smaller carbon sheets at higher temperature (Cao, et al., 2021; Sangar, et al., 2019). Such polycyclic aromatic carbon sheets favor a higher amount of sulfonic groups attachment onto the catalyst surface (Cao, et al., 2021; Lim, et al., 2020; Wong, et al., 2020). Moreover, incomplete

carbonisation also promotes the formation of more porous carbon structure that provides more surface area for sulfonic groups attachment (Sangar, et al., 2019; Wong, et al., 2020).

2.4   Effect of Carbonisation Time

Wong, et al. (2020) reported that carbonisation time has a very minor role in determining the catalytic activity of the sulfonated carbon-based catalyst produced. Bureros, et al. (2019) also found that the carbonisation time has a very little effect on the catalytic activity, agreeing well with the finding of Wong, et al. (2020). Despite that, Cao, et al. (2021) concluded that as carbonisation time increases, the sulfonic group density and catalytic performance of the catalyst increases, up to a certain optimal point, after which the sulfonic group density and catalytic performance will decrease gradually. The decrease in sulfonic group density and catalytic performance at excessively long carbonisation time was also reported in the work of Wong, et al. (2020) and Lim, et al. (2020). This is attributed to the stacking of polycyclic aromatic carbon sheets which are rigid and inflexible, thus discouraging the attachment of sulfonic groups (Lim, et al., 2020).

2.5   Sulfonation

During sulfonation, in addition to the sulfonic group, carboxyl group and hydroxyl group, both of which are weaker acid groups, are also attached onto the surface of the catalyst (Bureros, et al., 2019; Flores, et al., 2019; Sangar, et al., 2019). Among the functional groups introduced to the catalyst during sulfonation, sulfonic groups are the predominant functional groups that give rise to the catalytic capabilities to the carbon-based catalyst (Souza, et al., 2022). Sangar, et al. (2019) reported that the hydrophilic sulfonic groups, carboxyl groups, and hydroxyl groups that are attached onto the catalyst acts as anchoring sites for the reaction to takes place, thereby increasing the catalytic activity. Bureros, et al. (2019) also suggested that mass transfer of reactants to the catalyst surface and the active sites are boosted with the existence of attached weak acid groups, thereby increasing the catalytic activity. Flores, et al. (2019) suggested a contradicting finding to Sangar, et al. (2019). Flores, et al. (2019) reported that carboxyl groups enhance the catalytic performance by attracting

alcohol towards the catalyst, which is in agreement with Sangar, et al. (2019), however, it was reported that hydroxyl groups reduces the catalytic activity instead as it attracts water towards the catalyst, which pushes the hydrophobic fatty acid away. The adsorption of reactants by the weak acid groups is possible due to the presence of polar constituents in the reactant molecules which have a strong attraction between one another, for example hydroxyl group in alcohol compounds, with the weak acid groups (Bureros, et al., 2019).

2.5.1 Effect of Sulfonation Temperature

Zhang, et al. (2021) found that sulfonation temperature and sulfonic group density shows a positive relationship, where an increase in sulfonation temperature, leads to an increase in sulfonic groups density of the synthesised catalyst, up to an optimal point at 150 °C, beyond which the sulfonic groups density decreases instead. Bureros, et al. (2019) came to the same conclusion as Zhang, et al. (2021), where the sulfonic groups density increases as sulfonation temperature increases. Wong, et al. (2020) reported a contradicting conclusion with Zhang, et al. (2021), where a lower sulfonation temperature favors the attachment of sulfonic groups onto the catalyst surface, yielding a catalyst with higher sulfonic groups density. Flores, et al. (2019) agrees with Wong, et al. (2020) and found that as sulfonation temperature increases, the sulfonic group density decreases.

Wong, et al. (2020) claimed that the decreasing sulfonic groups density at higher sulfonation temperature is due to the relative thermal instability of sulfonic groups in addition to side reactions such as oxidation, condensation and dehydrogenation which are more competitive at higher temperatures. Flores, et al. (2019) reported that at lower sulfonation temperatures, the attachment of functional groups onto the catalyst surface is dominated by sulfonic groups whereas at higher sulfonation temperatures, the attachment of functional groups onto the catalyst surface is dominated by carboxyl groups and hydroxyl groups.

Souza, et al. (2022) also reported that the optimal sulfonation temperature lies within the temperature range of 100 °C to 150 °C for most biomass, where sulfonation temperature outside the optimal range results in decreasing sulfonic groups density. Wong, et al. (2020) also agrees with Souza,

et al. (2022) and reported that sulfonation at a temperature below 100 °C is ineffective in producing a functional catalyst.

Interestingly, Wong, et al. (2020) also reported that while the sulfonic group density of catalyst synthesised at lower sulfonation temperature is higher, it is also more vulnerable to leaching, losing more sulfonic groups than catalysts synthesised at higher sulfonation temperatures, this finding contradicted with the findings of Bureros, et al. (2019) which reported that the stability of the catalyst decreases as sulfonation temperature increases. The findings of Zhang, et al. (2021) may explain the leaching phenomenon encountered in the study of Wong, et al. (2020), where it was reported that at lower sulfonation temperatures, a weaker attachment of sulfonic groups arise, resulting in loose sulfonic groups that are prone to leaching and deactivation.

2.5.2   Effect of Sulfonation Time

Zhang, et al. (2021) reported that as sulfonation time increases, the sulfonic groups density of the synthesised catalyst increases up to an optimal point at 4 h, after which the sulfonic groups density decreases instead. Bureros, et al. (2019) as well found that the catalyst exhibits a a higher sulfonic groups density with a longer sulfonation time, which is in agreement with Zhang, et al. (2021). Furthermore, it was determined that the decrease in sulfonic groups density beyond the optimal sulfonation time is due to the formation of rigid carbon structure that limited the surface area available for sulfonic groups attachment, this is particularly evident at higher sulfonation temperature (Bureros, et al., 2019). Sangar, et al. (2019) also found that increase in sulfonation time correlates to an increase in sulfonic groups density. Whereas Wong, et al. (2020), Flores, et al. (2019) and Souza, et al. (2022) reported that sulfonation time only has a minor influence on the catalytic activity.

Flores, et al. (2019) reported that while longer sulfonation time has little effect on the catalytic performance of the synthesised catalyst, it has a more pronounced effect on the stability of the catalyst, where a longer sulfonation time created a stronger attachment of sulfonic groups onto the catalyst surface, making it more resistant to leaching and deactivation. Sangar, et al. (2019) also reported the increases in attachment strength of the sulfonic groups onto the catalyst surface is attributed to the increase in sulfonation time. Bureros, et al.

(2019) reported that as sulfonation time increases, the stability of catalyst increases as well. However, Wong, et al. (2020) reported that sulfonation time beyond 6 h produced catalyst that are vulnerable to deactivation.

2.6   Sulfonic Group Density

Carbon-based catalyst has little to none catalytic capabilities on its own, thereby, it relies on processes such as sulfonation which grants it catalytic capabilities through the incorporation of sulfonic groups (Flores, et al., 2019; Souza, et al., 2022; Wong, et al., 2020). Various studies had indicated that the catalytic activity of sulfonated carbon-based catalyst is mainly affected by the density of the sulfonic group, the total acid density and the porosity of the carbon structure (Changmai, et al., 2020).

Various works had reported sulfonated carbon-based catalyst with excellent catalytic activity and listed sulfonic group density as an key indicator in determining and predicting the performance of the catalyst. da Luz Corrêa, et al. (2023) had reported a maximum sulfonic group density of 1.70 mmol/g for catalyst synthesised at carbonisation temperature of 600 °C. Zhang, et al. (2021) also reported a maximum sulfonic group density of 1.50 mmol/g at carbonisation-sulfonation temperature of 150 °C for 4 h. Cao, et al. (2021) reported a maximum sulfonic group density at 1.40 mmol/g by performing carbonisation and sulfonation at 300 °C and 90 °C respectively, where carbonisation is carried out for 2 h and sulfonation is carried out for 5 h. Lathiya, Bhatt and Maheria (2018) also reported a maximum sulfonic group density at 1.57 mmol/g. Bureros, et al. (2019) reported a maximum sulfonic group density comparable to other literatures at 1.48 mmol/g by performing sulfonation at 120 °C for 4 h. Flores, et al. (2019) reported a relatively low value of 1.06 mmol/g for sulfonic group density using a carbonisation-sulfonation temperature of 150 °C for 8 h. From the literatures, it can be seen that an average sulfonic groups density value of around of 1.50 mmol/g can be obtained from the synthesis of sulfonated carbon-based catalyst using different biomass and also different synthesis method.

It is generally agreed that sulfonic group density plays a dominant role in determining the catalytic capability of the sulfonated carbon-based catalyst, where a higher sulfonic group density leads to greater catalytic activity.

However, Flores, et al. (2019) and Rocha, Olivera and Franca (2019) also claimed that the effect of sulfonic group density on the catalytic activity is not as dominant as conventionally believed, where a higher sulfonic group density does not translate to a higher catalytic performance, other factors such as catalyst porosity and specific surface area plays a comparable or perhaps even more significant role in giving rise to a greater catalytic activity.

2.7   Porosity

Generally, the porous structure of the catalyst is formed during the carbonisation step, where the porous structure in the catalyst is made up of empty spaces left behind due to the removal of volatile components at high temperature (Cao, et al., 2021; da Luz Corrêa, et al., 2023; Wong, et al., 2020). da Luz Corrêa, et al. (2023) had found that porosity plays an important role in the catalytic performance of the catalyst due to the increased specific surface area available that encourages more contact between reactants and the functional groups active sites attached on the catalyst surface. Rocha, Olivera and Franca (2019) also found a strong positive relationship between specific surface area and porosity, with the catalytic performance of the catalyst, where a catalyst with higher specific surface area and porosity has a higher catalytic activity. Flores, et al. (2019) also came to the same conclusion that specific surface area and pore size plays a significant role in the catalytic performance of the catalyst synthesised. Wong, et al. (2020) also reported that most functional groups attachment onto the catalyst surface occurs within the porous structures of the carbon-based catalyst, with only some functional groups attaching onto the external surface.

However, this finding is disputed by Ibrahim, et al. (2019), who reported that specific surface area and pore properties do not contribute to the catalytic activity in biodiesel production. Zhang, et al. (2021) and Souza, et al. (2022) both reported that the catalyst synthesised has little porosity of note, and attributed the simultaneous carbonisation and sulfonation used in the one-step method of synthesis as the reason for the lack of pores formation. Zhang, et al. (2021) suspected that the temperature used for simultaneous carbonisation and sulfonation is too low for sufficient decomposition and removal of organic components to create enough empty space for pores formation. Souza, et al. (2022) also suggested that the occurrence of sulfonation along with various side

reactions such as oxidation that is caused by the strong sulfonating agent prevented any significant pores formation. Interestingly, despite the lack of porous structure, Zhang, et al. (2021) reported that the synthesised catalyst can achieve an excellent conversion at 98 % whereas Souza, et al., also reported a satisfactory conversion at 80 %.

Moreover, da Luz Corrêa, et al. (2023) found that the porosity of the catalyst is improved after direct sulfonation with concentrated sulfuric acid due to corrosion and oxidation by the strong acid. However, this finding contradicted with the findings of Zhang, et al. (2021), who found that the pore volume is reduced after sulfonation. Ibrahim, et al. (2019) also reported that the pore properties deteriorated after the sulfonation step. Cao, et al. (2021) also found that the pore volume and specific surface area of the catalyst after sulfonation is worse compared to a freshly carbonised biochar. This phenomenon is also reported by Lathiya, Bhatt and Maheria (2018), where the surface morphology of the catalyst is altered by the sulfonation step and a reduction in specific surface area is experienced. Interestingly, while Rocha, Olivera and Franca (2019) also reported a reduction in the specific surface area of the catalyst after sulfonation, it was also reported that the surface morphology and carbon structure of the catalyst is unaffected by sulfonation with concentrated sulfuric acid. Wong, et al. (2020) agrees with the findings of Rocha, Olivera and Franca (2019), that is the surface morphology and carbon structure of the catalyst is unaffected by the direct sulfonation with concentrated sulfuric acid. The reduction in pore volume and specific surface area is attributed to the attachment of large sulfonic groups onto the catalyst surface (Ibrahim, et al., 2019; Rocha, Olivera and Franca, 2019; Zhang, et al., 2021). The cause of reduction of specific surface area and change in surface morphology specifically is suggested to be the collapse of porous carbon structure due to various side reactions such as oxidation and polymerisation in the presence of concentrated sulfuric acid (Cao, et al., 2021; Lathiya, Bhatt and Maheria, 2018; Zhang, et al., 2021).

In many of the literatures reviewed, a chemical activation step is included in the synthesis of sulfonated carbon-based catalyst. Most of the studies used phosphoric acid as the chemical activator in a chemical activation pretreatment step prior to the carbonisation of biomass, such as in the works of

Wong, et al. (2020); Lim, et al. (2020); Cao, et al. (2021); and Rocha, Olivera and Franca (2019). Lathiya, Bhatt and Maheria (2018) also used potassium hydroxide as the chemical activator, where the potassium hydroxide solution doubles as the medium in the hydrothermal carbonisation of the biomass, thus the chemical activation step occurs simultaneous with the carbonisation process. It was reported that the use of phosphoric acid as the chemical activator is effective in enhancing the formation of porous structure in the latter steps and increases the specific surface area of the synthesised catalyst (Cao, et al., 2021). Similarly, Lathiya, Bhatt and Maheria (2018) also reported that the chemical activation process using potassium hydroxide is effective in increasing the specific surface area and promote pores formation during the simultaneous carbonisation process.

2.8   Catalyst Deactivation

In many of the literatures reviewed, it was noticed that the reusability and stability of the sulfonated carbon-based catalyst synthesised became a problem and is a point of emphasis in improving the feasibility of the catalyst for practical usage on an industrial scale. da Luz Corrêa, et al. (2023) reported that all catalysts synthesised can achieve an ideal conversion at around 96 %, however, depending on the carbonisation temperature, the conversion of all catalysts eventually dropped to around 30 % at a different rate with the fastest being reached in 4 cycles. Ibrahim, et al. (2019) also reported a significant reduction in conversion from 92 % achieved by the fresh catalyst to around 20 % to 30 % by used catalysts after only 1 cycle. Souza, et al. (2022) also reported a significant reduction in catalytic activity, where the used catalyst may only achieve around 45 % conversion after 3 cycles as compared to approximately 80 % conversion using fresh catalyst. Cao, et al. (2021) also reported a reduction in conversion from around 96 % using fresh catalyst to only around 55 % after 4 cycles. Bureros, et al. (2019) also reported a significant catalyst deactivation, where the used catalyst may only achieve around 48 % after 3 cycles compared to the fresh catalyst which may achieve a conversion at around 93 %. Zhang, et al. (2019) reported better reusability, where the conversion achieved by the catalyst dropped from 98 % to 79 % after 4 cycles. Flores, et al. (2019) also reported synthesised catalyst with good stability, where the catalyst may still

achieve a conversion at around 80 % compared from the initial conversion at around 87 % using fresh catalyst. Sangar, et al. (2019) also reported a synthesised catalyst with good stability and reusability, the used catalyst may still achieve around 75 % conversion after 7 cycles, with only minor loss of catalytic activity from the initial conversion at around 81 %. Surprisingly, Rocha, Olivera and Franca (2019) reported that the catalyst synthesised is stable and retained its catalytic activity without any noticeable loss after use, where the used catalyst may still achieve around 88 % conversion after 5 cycles.

Most studies agree the leaching of weakly attached sulfonic group is mainly responsible for the loss in catalytic activity (Bureros, et al., 2019; Cao, et al., 2021; da Luz Corrêa, et al., 2023; Flores, et al., 2019; Lathiya, Bhatt and Maheria, 2018; Sangar, et al., 2019; Souza, et al., 2022; Zhang, et al., 2021). In view of this, the washing of catalyst before usage in biodiesel production is particularly important to avoid any significant leaching of sulfonic groups into the reaction medium, thereby causing pollution to the product stream and necessiting intensive purification step, defeating the purpose of using heterogeneous catalyst over homogeneous catalyst (Flores, et al., 2019). Most of the literatures reviewed uses methanol, ethanol, n-hexane and hot water (at least 80 °C) to washes the stored and recovered catalyst before use to remove the loosely attached sulfonic groups on the catalyst surface. However, the use of n-hexane in removing the loosely attached sulfonic groups is ineffective largely due to its non-polarity that has little affinity with the sulfonic groups, hence the significant loss of catalytic activity shown in many of the literatures reviewed (Bureros, et al., 2019). Moreover, Flores, et al. (2019) also reported that the use of hot water to remove the loosely attached sulfonic groups are insufficient and leads to assessment results that inaccurately reflects the actual performance of the catalyst. Bureros, et al. (2019) and Flores, et al. (2019) suggested the use of methanol to remove the loosely attached sulfonic groups which are more effective due to the high affinity between the polar methanol with the hydrophilic sulfonic groups.

Additionally, the side reaction of sulfonic groups with methanol to form sulfonate esters also deactivates the sulfonic groups as a catalytic active sites (da Luz Corrêa, et al., 2023; Flores, et al., 2019; Lathiya, Bhatt and Maheria, 2018; Rocha, Olivera and Franca, 2019; Souza, et al., 2022; Zhang, et al., 2021).

It was reported that loosely attached sulfonic groups are much more prone to deactivation through side reaction with methanol (Rocha, Olivera and Franca, 2019; Wong, et al., 2020; Zhang, et al., 2021).

Various strategies were proposed to reactivate the used catalyst. Ibrahim, et al. (2019) attempted to reactivate the catalyst by washing with n-hexane and methanol, which proved to be ineffective in reactivating the catalyst. Ibrahim, et al. (2019) also tried washing the catalyst with n-hexane followed by concentrated sulfuric acid, which is also ineffective. Ibrahim, et al. (2019) and Souza, et al. (2022) found that the reactivation of catalyst is the most effective by resulfonating the catalyst with concentrated sulfuric acid, which is capable of producing reactivated catalysts that have comparable catalytic activity to freshly synthesised catalysts. The resulfonation of used catalyst achieved its objective by replenishing leached sulfonic groups and reactivating the deactivated sulfonic groups by hydrolysing the sulfonate esters formed. Besides reactivating the used catalyst, Ibrahim, et al. (2019) also suggested thermal treatment of fresh catalyst at a low temperature of 100 °C for 2 h which proved to be effective in improving the stability of the fresh catalyst, however, significant catalyst deactivation still occurs after multiple cycles.

Moreover, da Luz Corrêa, et al. (2023) reported that the sulfonic groups decompose at a temperature between 220 °C and 290 °C. Souza, et al. (2022) reported a wider temperature range than da Luz Corrêa, et al. (2023) with the decomposition of sulfonic groups occurring at between 175 °C and 450 °C. Wong, et al. (2020) also reported a similar sulfonic groups decomposition range from 200 °C to 350 °C. Rocha, Olivera and Franca (2019) reported a higher sulfonic groups decomposition range at between 350 °C and 600 °C. Lathiya, Bhatt and Maheria (2018) reported a sulfonic groups decomposition temperature range far wider than any other literatures at between 190 °C and 700 °C. Therefore, the reaction temperature when using such sulfonated carbon-based catalyst must be carefully controlled as to prevent the decomposition of sulfonic groups. Additionally, it was reported that the catalyst suffers from mass loss that can be attributed to moisture content at a temperature up to 100 °C (da Luz Corrêa, et al., 2023; Lathiya, Bhatt and Maheria, 2018; Rocha, Olivera and Franca, 2019; Souza, et al., 2022; Wong, et al., 2020).

2.9   Catalyst Characterisation

Various characterisation test such as SEM-EDX, FTIR, XRD, and BET are used in the literatures reviewed to characterise the catalyst.

2.9.1   Scanning Electron Microscope with Energy Dispersive X-ray (SEM-EDX)

It was reported that the biochars produced after carbonisation have a typical surface morphology expected in a lignocellulosic biomass, that is rough surface without any obvious structure (da Luz Corrêa, et al., 2023). However, it was reported that after sulfonation, the biochars carbonised at higher temperatures exhibited obvious changes in morphology that includes an increase in porosity, likely due to corrosion and oxidation by the concentrated sulfuric acid (da Luz Corrêa, et al., 2023).

Ibrahim, et al. (2019) also reported that the biochar produced consists of non-porous structure with smooth surface, which is attributed to the degradation and destruction of plant cell walls. After sulfonation, the surface morphology exhibits an obvious change where the surface becomes much rougher (Ibrahim, et al., 2019).

Souza, et al. (2022) reported catalyst samples that have no obvious porosity, with surface morphology in the form of rigid aggregates. The lack of porosity even after sulfonation is likely due to the simultaneous carbonisation and sulfonation process, where the sulfonation and partial oxidation reactions can interfere and disrupt the pores formation by interacting with the carbon surface during the development of the carbon structure (Souza, et al., 2022).

On the other hand, regarding the elemental composition of the sample using energy dispersive X-ray, it was reported that as the carbonisation temperature increases, the relative carbon composition of the biochar product increases while the relative oxygen composition decreases (da Luz Corrêa, et al., 2023; Lim, et al., 2020). This phenomenon may be explained by the release of various volatile oxygenated species that originally exist in the biomass structure during the carbonisation process, where as the carbonisation temperature increases, more volatile oxygenated species is removed from the biomass structure (da Luz Corrêa, et al., 2023; Lim, et al., 2020). Furthermore, it was observed that after the sulfonation process, the relative oxygen

composition increases again, together with the emergence of sulfur in the elementary composition of the catalyst sample (da Luz Corrêa, et al., 2023). This may be explained by the nature of the sulfonation process which utilises concentrated sulfuric acid as a sulfonating agent, where the concentrated sulfuric acid is also a strong oxidising agent, thus, favouring the formation of oxygenated groups during the sulfonation process (da Luz Corrêa, et al., 2023).

The results obtained by the literatures reviewed in this report are summarised and tabulated in Table 2.4.

Table 2.4: Catalyst Sample EDX Results Reported

Biomass	Elements			Reference
	C	O	S	
Murumuru Kernel	67.49	24.11	8.37	da Luz Corrêa, et al., 2023
Corncob	68.09	25.59	7.35	Ibrahim, et al., 2019
Microcrystalline Cellulose	66.90	30.10	3.00	Souza, et al., 2022
OPEFB	64.01	32.47	3.52	Lim, et al., 2020
Waste Orange Peel	43.44	37.81	3.68	Lathiya, Bhatt and Maheria, 2018
Cow Manure	60.50	31.78	4.20	Sangar, et al., 2019

2.9.2 Fourier-Transform Infrared Spectroscopy (FTIR)

da Luz Corrêa, et al. (2023) reported using Fourier-Transform Infrared Spectroscopy (FTIR) that the characteristic bands at around 1593 cm^{-1} is indicative of the C=C bonds in aromatic rings, whereas characteristic bands at around 1704 cm^{-1} is evidence of the presence of C=O bond in various carboxylic groups. Furthermore, Souza, et al. (2022) has reported that the absorption band at around 1580 cm^{-1} is associated with the C=C bonds of aromatic rings whereas the absorption band at around 1150 cm^{-1} is associated with the O=S=O bond of

the sulfonic groups. Zhang, et al. (2021) also reported that the characteristic bands at around 1704 cm^{-1} belongs to C=O bond in carboxylic groups and further indicate the presence of polycyclic aromatic carbon structure. Additionally, it was reported that the infrared absorption bands at around 1040 cm^{-1} and 1170 cm^{-1} are associated with symmetrical and asymmetrical O=S=O bonds respectively, which belong to the sulfonic functional groups, indicating the successful sulfonation (Cao, et al., 2021; da Luz Corrêa, et al., 2023; Zhang, et al., 2021).

Wong, et al. (2020) performed an intensive study using FTIR, it was reported that absorption bands at around 2800 cm^{-1} to 3600 cm^{-1} are associated with O–H bonds of phenolic structures, while the absorption bands at between 1100 cm^{-1} and 1200 cm^{-1} are associated with the symmetrical and asymmetrical O=S=O bonds. Moreover, the successful implantation of the sulfonic group, –SO$_3$H, can be determined from the absorption band at around 1296 cm^{-1}, while the bonding between the sulfonic group and the carbon surface, C–S, can be determined from the characteristic bands at between 670 cm^{-1} and 715 cm^{-1}. The findings of Wong, et al. (2020) agrees well with the work of Souza, et al. (2022), where the absorption band at around 1580 cm^{-1} associated with the C=C bonds is indicative of the presence of polycyclic aromatic carbon structure. Wong, et al. (2020) also agrees with da Luz Corrêa, et al. (2023) and Zhang, et al. (2021) where the presence of characteristic bands at around 1700 cm^{-1} indicates the presence of C=O bonds, which is of either carbonyl or carboxylic functional groups.

Similarly, Lim, et al. (2020) reported that the absorption bands at around 1580 cm^{-1} belongs to C=C bonds of aromatic carbon structure, while S=O bonds can be observed at between 1020 cm^{-1} and 1090 cm^{-1}. Furthermore, it was reported that –SO$_3$H group can be determined from absorption bands at between 1150 cm^{-1} and 1270 cm^{-1}. Lim, et al. (2020) also agrees with other studies on the presence of C=O bonds at around 1700 cm^{-1}, which is indication of the presence of carbonyl groups. Additionally, Cao, et al. (2021) found that the characteristic bands observed at around 3389 cm^{-1} is indicative of the presence of phenolic O–H bonds, while the characteristic bands at 1707 cm^{-1} and 1612 cm^{-1} are attributed to the presence of carboxylic C=O bonds and amorphous aromatic C=C bonds respectively. Furthermore, Cao, et al. (2021)

also determined that the characteristic bands at around 633 cm^{-1} is indicative of the C–S bond, which is another evidence of successful sulfonic groups implantation. As a summary, the reviewed FTIR results are tabulated in Table 2.5 below.

Table 2.5: FTIR Results Summary

Absorption Band Wavelength (cm^{-1})	Bonding
633 – 715	C–S
1020 – 1090	S=O
1040	Symmetrical O=S=O
1170	Asymmetrical O=S=O
1100 – 1200	O=S=O
1150 – 1296	–SO$_3$H
1580 – 1612	C=C
1700	C=O
2800 – 3600	O–H

2.9.3   X-Ray Diffraction (XRD)

Zhang, et al. (2021) conducted X-ray Diffraction analysis (XRD) on raw cellulose and reported that the strong diffraction peak at around $2\theta = 22°$ is indicative of the (002) diffraction crystal plane of cellulose, whereas the broad diffraction peak at around $2\theta = 15°$ is indicative of the (101) diffraction crystal plane of cellulose, and the relatively smaller diffraction peak at around $2\theta = 35°$ is indicative of the (040) diffraction crystal plane of cellulose. Furthermore, Zhang, et al. (2021) also found that a weak and broad diffraction peak at between $2\theta = 35°$ to $2\theta = 45°$ found in catalyst sample is an indication of the formation of stacked polycyclic aromatic carbon sheets, which is formed from the organic carbon structure after sulfonation process. Ibrahim, et al. (2019) agrees with the finding of Zhang, et al. (2021) where the diffraction peak at around $2\theta = 23°$ is indicative of the carbon crystal plane of (002). Additionally, Ibrahim, et al. (2019) also attributed the diffraction peak at $2\theta = 45°$ to the presence of the carbon crystal plane of (101). Furthermore, Ibrahim, et al. (2019) also attributed the broad peak at $2\theta = 25°$ to the presence and formation of

polycyclic aromatic carbon sheets that is arranged in a random fashion, resulting in the formation of amorphous crystal structure that is more disordered compared to the catalyst precursor, which have a more defined crystal structure. Souza, et al. (2022) agrees well with Zhang, et al. (2021) and Ibrahim, et al. (2019), where the diffraction peak at around $2\theta = 24°$ is associated with the (002) crystalline plane of graphitic structures. Additionally, Souza, et al. (2022) also found that the diffraction peak at around $2\theta = 41°$ belongs to the (100) carbon crystal plane of the polycyclic aromatic carbon sheets.

Other than that, Rocha, Olivera and Franca (2019) and Cao, et al. (2021) had also reported that the strong diffraction peaks at between $2\theta = 20°$ to $2\theta = 30°$ corresponds to the (002) crystalline plane of amorphous aromatic carbon structures, while the weaker diffraction peaks at between $2\theta = 40°$ to $2\theta = 50°$ are attributed to the (101) crystalline plane of graphitic carbon structures. Cao, et al. (2021) claimed that the strengthening diffraction peaks at between $2\theta = 20°$ to $2\theta = 30°$ and the increasing amorphousness as a result of sulfonation process is favourable to the implantation of sulfonic groups onto the carbon structures. Additionally, Sangar, et al. (2019) also noted that the broad diffraction peaks at $2\theta = 25°$ is attributed to the (002) diffraction planes of graphitic structures, which is made up of unorganised polycyclic aromatic carbon structures. The XRD results that was reviewed in this report are summarised in Table 2.6.

2.9.4 Brunauer, Emmett and Teller (BET) Surface Area Analysis

Wong, et al. (2020) reported that the catalyst produced has a high specific surface area of 141.54 m^2/g with significant micropores number along with minor mesopores presence. Rocha, Olivera and Franca (2019) reported an even higher specific surface area of 730.8 m^2/g with predominantly mesopores make-up. Lathiya, Bhatt and Maheria (2018) reported a lower specific surface area of 44 m^2/g with mesopores domination.

Table 2.6: XRD Results Summary

Diffraction Peaks (°)	Crystalline Plane	Description	Summary
15	(040)	Sharp	Cellulose
22 – 24	(002)	Sharp	Graphitic carbon structure, cellulose
20 – 30	(002)	Broad	Amorphous polycyclic aromatic carbon sheets
35	(040)	Weak, Sharp	Cellulose
40 – 50	(101)	Broad	Amorphous polycyclic aromatic carbon sheets

Compared to the specific surface area reported by the other researchers mentioned above, Zhang, et al. (2021) reported a significantly lower specific surface area at 2.60 m^2/g. Zhang, et al. (2021) stated that the low specific surface area is due to the attachments of functional groups which reduces the surface area, as well as due to the various reactions that occurred during sulfonation, which collapsed the porous structure of the catalyst. Similarly, Ibrahim, et al. (2019) also reported a low specific surface area at 8.40 m^2/g. However, Ibrahim, et al. (2019) also stated that the sulfonation process has little effect on the specific surface area and the pore volumes. Lim, et al. (2020) had also reported a specific surface area of 2.85 m^2/g, which was attributed to the nature of the catalyst precursor used. Cao, et al. (2021) had also reported a relatively low specific surface area of 7.34 m^2/g. Table 2.7 shows the summary for the specific surface area reviewed in this section.

Table 2.7: Specific Surface Area Reported

Biomass	Synthesis Method	Specific Surface Area (m^2/g)	References
Corncob	Two-Step	730.8	Rocha, Olivera and Franca, 2019
OPEFB	Two-Step	141.54	Wong, et al., 2020
Waste Orange Peel	Two-Step	44	Lathiya, Bhatt and Maheria, 2018
Corncob	Two-Step	8.40	Ibrahim, et al., 2019
Sargassum horneri	Two-Step	7.34	Cao, et al., 2021
OPEFB	Two-Step	2.85	Lim, et al., 2020
Bamboo	One-Step	2.60	Zhang, et al., 2021

2.9.5 Thermogravimetric Analysis (TGA)

By using thermogravimetric analysis (TGA), Souza, et al. (2022) found that the mass loss at below 175 °C is attributed to moisture loss, while the sulfonic groups decomposition occurs at between 175 °C and 450 °C, and further mass loss above 450 °C was attributed to the loss of oxygenated groups and graphitic structures. Furthermore, Wong, et al. (2020) also noted that the mass loss below 100 °C is due to the loss in moisture content, whereas the mass loss at between 200 °C and 350 °C is attributed to the decomposition of sulfonic groups and other oxygenated groups. Lim, et al. (2020) also concluded that the mass loss below 150 °C is caused by the loss of moisture content in the catalyst sample, while subsequent mass loss is due to further structural decomposition caused by carbonisation. Similarly, Cao, et al. (2021) found that the sulfonic groups decompose at a temperature range in between 200 °C and 250 °C. Rocha, Olivera and Franca (2019) agrees with Wong, et al. (2020) and Lathiya, Bhatt and Maheria (2018) that the mass loss at below 100 °C is due to the loss in

moisture content, but reported a higher decomposition temperature of sulfonic groups at between 350 °C and 600 °C. Moreover, Lathiya, Bhatt and Maheria (2018) reported that the decomposition of sulfonic groups occur at temperature at higher than 190 °C.

2.10   Application in Interesterification Process

As discussed in the previous chapter, the research and development on interesterification is lacking, especially in terms of using heterogeneous catalyst. This is evident when only one of the literatures reviewed in this chapter synthesised biodiesel through interesterification reaction using sulfonated carbon-based catalyst, with all other literatures studying the sulfonated carbon-based catalyst by synthesising biodiesel through transesterification.

Wong, et al. (2020) reacted methyl acetate and oleic acid in a 500 mL round bottom flask at a molar ratio of 50:1. To study the effect of catalyst loading on the biodiesel yield, Wong, et al. (2020) added the synthesised sulfonated carbon-based catalyst at different mass ration (0 wt%, 2 wt%, 4 wt%, 7 wt%, 10 wt%, 12 wt%). The reactants are reacted at 100 °C for 8 h while under constant agitation. Furthermore, the reaction is carried out under reflux. After the reaction is completed, the reaction medium is cooled to room temperature by quenching to halt the reaction. The catalyst is then filtered out and recovered for further use, whereas the reaction medium is left alone to allow excess methyl acetate to evaporate. Wong, et al. (2020) reported that as catalyst loading increases, the biodiesel yield increases up to an optimal point at 10 wt%, after which the biodiesel yield decreases. Although synthesising biodiesel through transesterification, Cao, et al. (2021), Rocha, Olivera and Franca (2019) and Sangar, et al. (2019) also reported such trend as Wong, et al. (2020). The increase in biodiesel yield is attributed to the increase in catalytic active sites available to facilitate the reaction, whereas the decrease in biodiesel yield is attributed to mass transfer limitation introduced by the excessive catalyst in the reaction medium.

CHAPTER 3

METHODOLOGY AND WORK PLAN

3.1 Material and Apparatus

The experiment proposed involve the production of the sulfonated carbon-based catalyst from both microcrystalline cellulose and corncob, the production of biodiesel from oleic acid, and the subsequent characterisation of the synthesised catalyst. Throughout the experiment, several materials and apparatus were needed. The materials used are listed in Table 3.1, whereas the apparatus used are listed in Table 3.2.

Table 3.1: Material List

Material	Grade	Supplier	Use
Ortho-Phosphoric acid	85 %	Merck	As the chemical activator for the biomass in the pretreatment step
Sulfuric acid	95 – 97%	Merck	As the sulfonating agent in the sulfonation step
Oleic acid	90 %	Sigma-Aldrich	As the reactant for the interesterification process
Methyl Acetate	98 %	Sigma-Aldrich	As the reactant for the interesterification process
Potassium Hydroxide	≥ 85 %	Friendemann Schmidt	As the precursor to the titrant in the acid value determination test of the oil sample
Ethanol	95 %	Sigma-Aldrich	As the precursor to the titrant and also as the titrand in the acid value determination test of the oil sample

Table 3.1: Material List (Cont.)

Material	Grade	Supplier	Use
Sodium Hydroxide	≥ 99 %	R & M Chemicals	As the titrant in the sulfonic group density test of the synthesised catalyst
Sodium Chloride	99 %	Sigma-Aldrich	As the titrand in the sulfonic group density of the synthesised catalyst
Phenolphthalein	1 g/L	R & M Chemicals	As the indicator in all titration steps

Table 3.2: Apparatus List

Apparatus	Detail	Use
Oven	Memmert	To dry the biomass and the synthesised catalyst
Muffle Furnace	LT furnace	To conduct carbonisation of the biomass
Sieve	300 μm mesh size	To sieve the biomass and catalyst
Vacuum Pump	Rocker 300	To perform vacuum filtration to recover the synthesised catalyst after sulfonation
pH Meter	Sartorius PB-10	To measure the pH value during catalyst washing steps
Heating Mantle	Mtops	To maintain temperature during interesterification process
Ultrasonic Oscillator	Kudos SK5200GT	To mix the catalyst with NaCl solution for the sulfonic group density test

Table 3.2: Apparatus List (Cont.)

Apparatus	Detail	Use
Scanning Electron Microscope Equipped with Energy Dispersive X-ray (SEM-EDX)	Hitachi S-3400N	To investigate the surface morphology and elemental composition of the synthesised catalyst
X-ray Diffractometer (XRD)	Sidmazu XRD-6000	To investigate the crystalline phase of the synthesised catalyst
Fourier Transform Infrared Spectrometer (FTIR)	Nicolet IS10	To investigate the sulfonic groups attachment on the synthesised catalyst
Thermogravimetric Analyser (TGA)	Perkin Elmer STA8000	To investigate the effect of temperature on the synthesised catalyst
Surface Analyser	Micromeritics 3Flex	To investigate the specific surface area and pore distribution

3.2 Overview Experiment Flow Chart

The overview of the experiment methodology is shown in Figure 3.1 below as a general guideline.
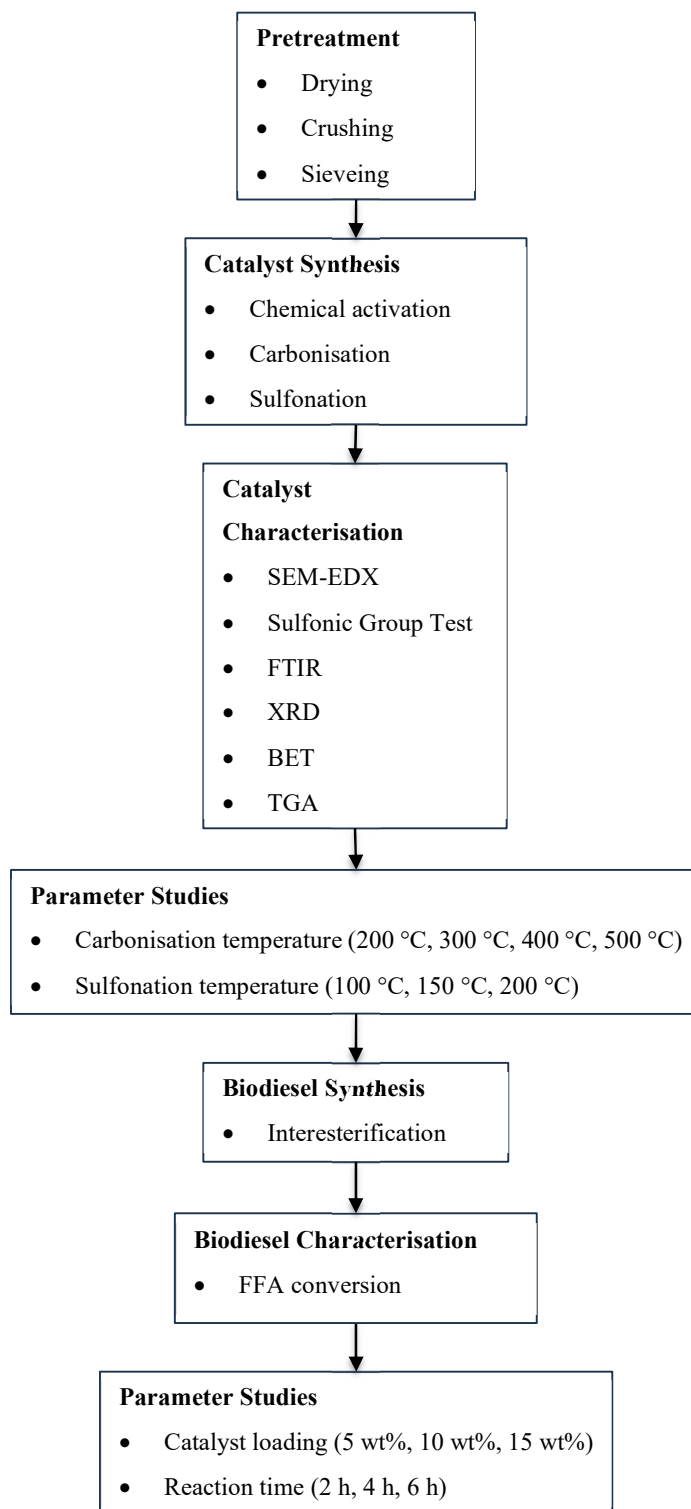
Pretreatment

- Drying
- Crushing
- Sieveing

Catalyst Synthesis

- Chemical activation
- Carbonisation
- Sulfonation

Catalyst Characterisation

- SEM-EDX
- Sulfonic Group Test
- FTIR
- XRD
- BET
- TGA

Parameter Studies

- Carbonisation temperature (200 °C, 300 °C, 400 °C, 500 °C)
- Sulfonation temperature (100 °C, 150 °C, 200 °C)

Biodiesel Synthesis

- Interesterification

Biodiesel Characterisation

- FFA conversion

Parameter Studies

- Catalyst loading (5 wt%, 10 wt%, 15 wt%)
- Reaction time (2 h, 4 h, 6 h)

Figure 3.1: Overview Experiment Flow Chart

3.3 Pretreatment of Biomass

The collected biomass was washed with water before being subjected to drying in the oven overnight at 80 °C to remove the moisture content. The dried biomass was then crushed and grinded into smaller particle sizes of no larger than 300 μm using a pestle and mortar. The crushed biomass was then sieved to recover particles that fulfils the specified size. The recovered biomass was then impregnated with 30 % phosphoric acid by adding the biomass into 30 % phosphoric acid at a mass ratio of 1:7, and stirring the mixture for 24 h under atmospheric condition. The chemically activated biomass was then washed with water until a neutral pH is achieved and then dried overnight at 80 °C in an oven. The dried biomass was collected and stored for further use. The raw biomass before chemical pretreatment was denoted as 'RM' and 'RC' respectively for microcrystalline cellulose and corncob, whereas the chemically activated biomass was denoted as 'M' and 'C' respectively.

3.4 Carbonisation of Biomass

The dried biomass was subjected to carbonisation by using a furnace at 200 °C for 2 h. The produced biochar from the carbonisation process was then collected and stored for the subsequent steps. To investigate the effect of carbonisation temperature on the catalyst produced, the carbonisation step was repeated at different temperatures (300 °C; 400 °C; 500 °C). The denotations of the biochar samples are shown in Table 3.3.

Table 3.3: Biochar Samples Denotations

Biomass	Carbonisation Temperature (°C)			
	200	300	400	500
Microcrystalline Cellulose	M-200	M-300	M-400	M-500
Corncob	C-200	C-300	C-400	C-500

3.5 Sulfonation of Biochar

The biochar was mixed with concentrated sulfuric acid at a ratio of 1 g biochar to 20 mL concentrated sulfuric acid. The mixture was agitated continuously while the temperature is maintained at 100 °C for 4 h. The resulting mixture was allowed to cool to room temperature and then diluted with distilled water. The diluted mixture was then filtered by using vacuum filtration. The solids recovered from the vacuum filtration was washed with methanol until a neutral pH is achieved. To study the relationship between sulfonation temperature and catalyst quality, the sulfonation step was repeated for biochar that shown the highest sulfonic group density at different temperatures (150 °C; 200 °C). Table 3.4 shows the denotations of the sulfonated carbon-based catalyst synthesised.

Table 3.4: Catalyst Samples Denotations

Biochar	Sulfonation Temperature (°C)		
	100	150[1]	200[1]
M-200	M-200-100	M-200-150	M-200-200
M-300	M-300-100	M-300-150	M-300-200
M-400	M-400-100	M-400-150	M-400-200
M-500	M-500-100	M-500-150	M-500-200
C-200	C-200-100	C-200-150	C-200-200
C-300	C-300-100	C-300-150	C-300-200
C-400	C-400-100	C-400-150	C-400-200
C-500	C-500-100	C-500-150	C-500-200

[1] Only selected biochar samples were tested

3.6 Catalyst Characterisation

The produced catalyst are characterised by using various techniques to understand its properties such as sulfonic groups density, elemental composition, surface morphology, crystallinity, specific surface area and thermal stability. The following subsections outline the characterisation steps.

3.6.1   Sulfonic Group Density Test

The sulfonic group density test used to determine the sulfonic group density of the synthesised catalyst. The test was adapted from the works of Cao, et al. (2021) and da Luz Corrêa, et al. (2023). First of all, 0.05 g of the catalyst was mixed with 15 mL of 2 M NaCl solution for 30 minutes under ultrasonic oscillation. Then, the catalyst was filtered off and recovered, while the filtrate was added with 3 drops of phenolphthalein before being subjected to titration using 0.02 M NaOH solution. The sulfonic group density may be calculated using Equation 3.1.

$$Sulfonic\ group\ density\ (mmol/g) = \frac{C_{NaOH}V_{NaOH}}{m} \tag{3.1}$$

where

C_{NaOH} is the concentration of NaOH used in M

V_{NaOH} is the volume of NaOH used in mL

m is the mass of the catalyst used in g

All of the synthesised catalyst samples were subjected to sulfonic group density test.

3.6.2   SEM-EDX

Scanning Electron Microscopy-Energy Dispersive X-ray (SEM-EDX) was used to in the investigation of the effect of carbonisation and sulfonation on the surface morphology and elemental composition of the analysed samples. By using SEM under 20 kV and 500 × magnification, the surface morphology of the catalyst was observed and recorded. Furthermore, by using EDX, the elemental composition of the catalyst can be measured and the readings can be used as an indication of chemical groups attachment on the catalyst. One of the key parameters to look out for is the change in sulfur content after the sulfonation process. By comparing the sulfur content in the biochar before sulfonation and in the synthesised catalyst, the effectiveness of the sulfonation process can be gauged from the degree of increase in the sulfur content (Bureros, et al., 2019; Flores, et al., 2019; Lathiya, Bhatt and Maheria, 2018).

To investigate the effects of carbonisation and sulfonation on the surface morphology and elemental composition, the biomass, biochar, and selected catalyst were subjected to analysis using SEM-EDX.

3.6.3   FTIR

Fourier Transform Infrared Spectroscopy (FTIR) was used to identify the chemical species adsorbed onto the catalyst surface, verifying the findings of SEM-EDX. The infrared spectrum of absorption produced from scanning at between 400 cm^{-1} and 2000 cm^{-1} was used to identify the functional groups attached to the catalyst surface, most importantly the identification of sulfonic groups. The presence of sulfonic groups may be identified by stretching vibrations at between 1020 cm^{-1} to 1090 cm^{-1} and between 1150 cm^{-1} to 1270 cm^{-1} due to the presence of S=O stretching and SO_3H stretching respectively. Moreover, the successful formation of polycyclic aromatic carbon sheet from incomplete carbonisation can be identified from the presence of aromatic C=C stretching vibrations at around 1580 cm^{-1} (Lim, et al., 2020). The catalyst sample with the best performance was subjected to FTIR analysis.

3.6.4   XRD

X-ray diffraction (XRD) is a highly versatile non-destructive method of characterisation that was used to study parameters such as elemental composition and also crystalline phase. By studying the diffraction pattern generated by XRD at full spectrum, the crystalline phase of the samples can be identified via the peaks that exist in the pattern. To investigate the effect of sulfonation on the structure of the sample, selected biochar and sulfonated catalyst sample with the best performance were subjected to XRD analysis.

3.6.5 BET Surface Analysis

By using the Brunauer, Emmett and Teller (BET) method, the specific surface area of the synthesised catalyst and the biochar produced were measured using a surface analyser. As discussed in the previous chapter, it is largely expected that the synthesised catalyst should have a lower specific surface area compared to the biochar. The reduction in specific surface area is attributed to the attachment of sulfonic groups, therefore it can be seen as an implication of successful sulfonation process. However, it should be noted that depending on the biomass used to synthesise the catalyst, the specific surface area of the resulting biochar and catalyst may differ. All raw materials and selected catalyst samples were subjected to BET surface analysis to investigate the effect of carbonisation and sulfonation on the specific surface area of the sample.

3.6.6 TGA

The thermogravimetric analysis (TGA) is a method of thermal analysis in which the changes in physical and chemical properties of materials are measured either as a function of temperature or a function of time. In this study, the weight loss of the analysed catalyst sample is temperature dependent, where the weight loss at a specific temperature range may be attributed to the loss of a specific ranges of structures or compounds within the catalyst. As such, the thermal degradation characteristic of the catalyst may be investigated by subjecting the samples to TGA from 30 °C to 1000 °C at 10 °C/min. The catalyst sample with the best performance was subjected to TGA.

3.7 Biodiesel Synthesis

The interesterification process conducted was based on the work of Wong, et al. (2020). Methyl acetate and oleic acid was added at a molar ratio of 50:1. The synthesised catalyst was added to the reaction medium at 5 wt%. To investigate the effect of catalyst loading on the biodiesel yield, the catalyst loading used was varied as it is reported that excess catalyst loading beyond an optimal amount result in decrease in catalytic activity due to mass transfer limitation (Wong, et al., 2020; Cao, et al., 2021). The reaction mixture was heated to 100 °C and maintained at this temperature for 4 h under reflux with constant agitation. Similarly, to investigate the effect of interesterification time, the

interesterification process was carried for different duration to determine the optimal time. The reaction mixture was then quenched in water to reach room temperature. The catalyst was then recovered from the reaction mixture by vacuum filtration. The recovered catalyst was washed with methanol continuously until a neutral pH is achieved, and then dried at 80 °C overnight. The dried catalyst was stored for possible use in further reusability study. Figure 3.2 shows the typical reflux apparatus setup that will be employed to synthesise the biodiesel in this study.
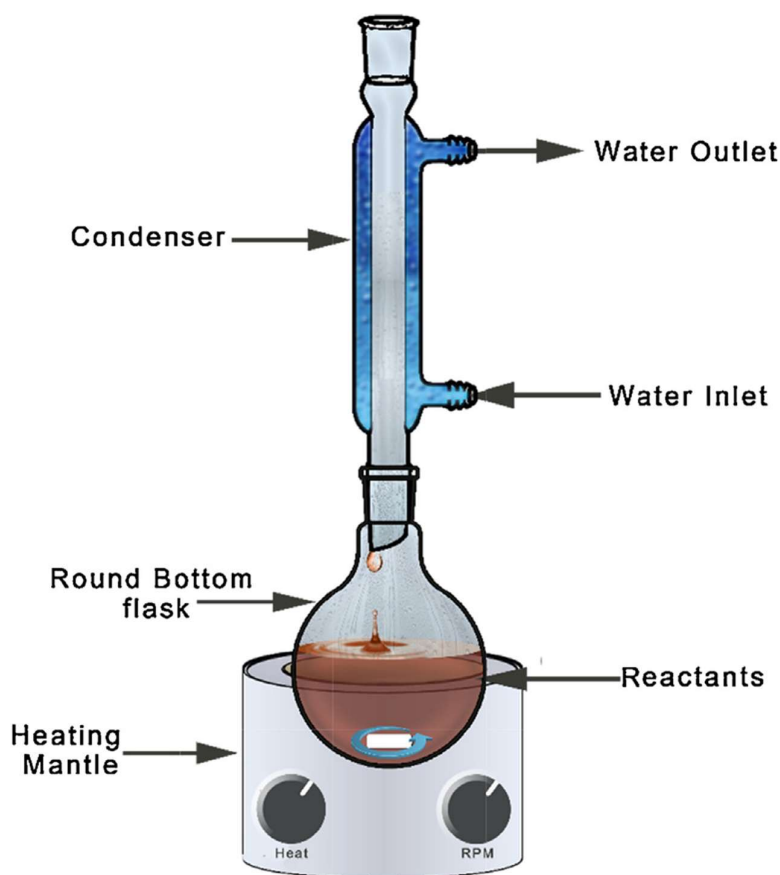
Figure 3.2: Experimental Setup (Aditha, et al., 2016).

3.7.1 Catalyst Loading

To study the effect of catalyst loading on the biodiesel yield through interesterification, different catalyst loading (5 wt%, 10 wt%, 15 wt%) was used to conduct interesterification. In the investigation of effect of methyl acetate to oleic acid molar ratio, the interesterification time is held constant at 4 h.

3.7.2   Interesterification Time

To study the effect of interesterification time on the biodiesel yield, different esterification time (2 h, 4 h, 6 h) was used to conduct the interesterification process using the optimal methyl acetate to oleic acid molar ratio determined from the prior test.

3.8   Catalyst Performance

The catalyst performance was determined based on the conversion of free fatty acid and the yield of FAME obtained, based on the work of Bureros, et al. (2019). The free fatty acid conversion was calculated using Equation 3.2.

$$X\ (\%) = \frac{AV_0 - AV_1}{AV_0} \times 100\ \%$$
(3.2)

where

AV_0 is the initial acid value of the oleic acid in mg KOH/g sample

AV_1 is the final acid value of the oleic acid in mg KOH/g sample

The FAME yield was calculated using Equation 3.3.

$$Y = X \times \frac{MW_{FAME}}{MW_{FFA}}$$
(3.3)

where

MW_{FAME} is the molecular weight of FAME (methyl oleate) in g/mol

MW_{FFA} is the molecular weight of FFA (oleic acid) in g/mol

In accordance with ISO 660, the acid value of the initial and final oleic acid may be determined by titration with ethanolic potassium hydroxide. Firstly, in a 100 mL conical flask, 0.2 g of the sample was added. Then, 0.5 mL of phenolphthalein was added to 50 mL of ethanol and the solution was heated to boil. The solution was added into the conical flask with the sample while the temperature was still at least 70 °C. The mixture was then titrated with ethanolic potassium hydroxide until a persistent colour change of no shorter than 15 s

which is explicit but slight occurs. By using Equation 3.4, the acid values was calculated.

$$AV \ (mg \ KOH/g \ sample) = \frac{V_{KOH} \times C_{KOH} \times MW_{KOH}}{m_{sample}} \qquad (3.4)$$

where

V_{KOH} is the volume of potassium hydroxide solution used in mL

C_{KOH} is the concentration of potassium hydroxide solution used in mol/L

MW_{KOH} is the molecular weight of potassium hydroxide solution in g/mol

m_{sample} is the mass of the sample used in g

3.8.1   Reusability Study

To investigate the stability of the catalyst, selected catalyst samples were subjected to reusability test by reusing the recovered catalyst in further interesterification process. The recovered catalyst from the previous tests was sieved again to ensure the desired catalyst particle size of 300 μm is maintained. Furthermore, the catalyst was then weighed and the volume of reactants used in the interesterification process was adjusted appropriately to maintain the optimal catalyst loading determined in the prior tests and the interesterification process was conducted for the optimal interesterification time as determined before. After the interesterification process, the free fatty acid conversion and FAME yield was calculated again for comparison. A total of 2 cycles were conducted to study the stability of the catalyst.

CHAPTER 4

RESULTS AND DISCUSSION

4.1 Parameter Studies for Catalyst Synthesis

The carbonisation temperature and sulfonation temperature were varied to investigate the effect of these synthesis parameters on the catalytic performance of the catalyst synthesised. To study the effects, several characterisation techniques, such as Scanning Electron Microscopy-Energy Dispersive X-ray (SEM-EDX), surface analysis, X-ray Diffraction (XRD), Fourier Transform Infrared Spectroscopy (FTIR) and sulfonic group density test, were conducted on the samples produced. Among the characterisation studies performed as mentioned above, the most important parameter that was directly used to determine the optimum catalyst synthesis parameters was sulfonic group density, as the density of functional group on a catalyst has a direct relationship with the biodiesel yield.

4.1.1 Effect of Carbonisation Temperature

The raw biomass samples, RC and RM, and all biochar samples (C-200; C-300; C-400; C-500; M-200; M-300; M-400; M-500) carbonised at different temperatures were subjected to Scanning Electron Microscopy-Energy Dispersive X-ray (SEM-DEX) to study the effects of carbonisation temperature on the surface morphology of the biomass samples, as well as the change in elemental composition of the biomass samples. Figure 4.1 and Figure 4.2 below show the images taken using SEM under 2000 × magnifications for corncob and microcrystalline cellulose (MCC) respectively, while images taken under 500 × and 1000 × magnification were presented in Appendix A for more comparison.
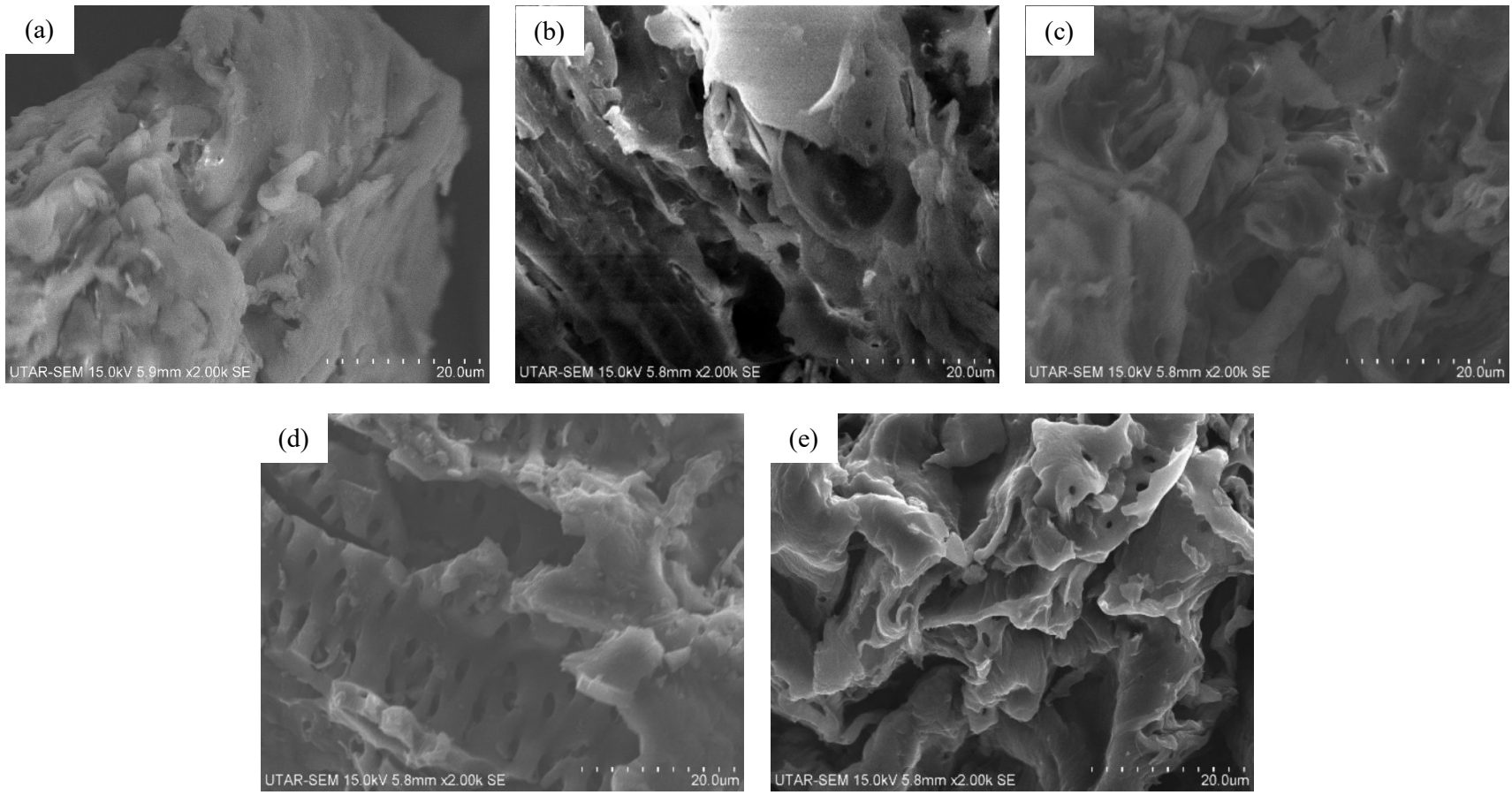
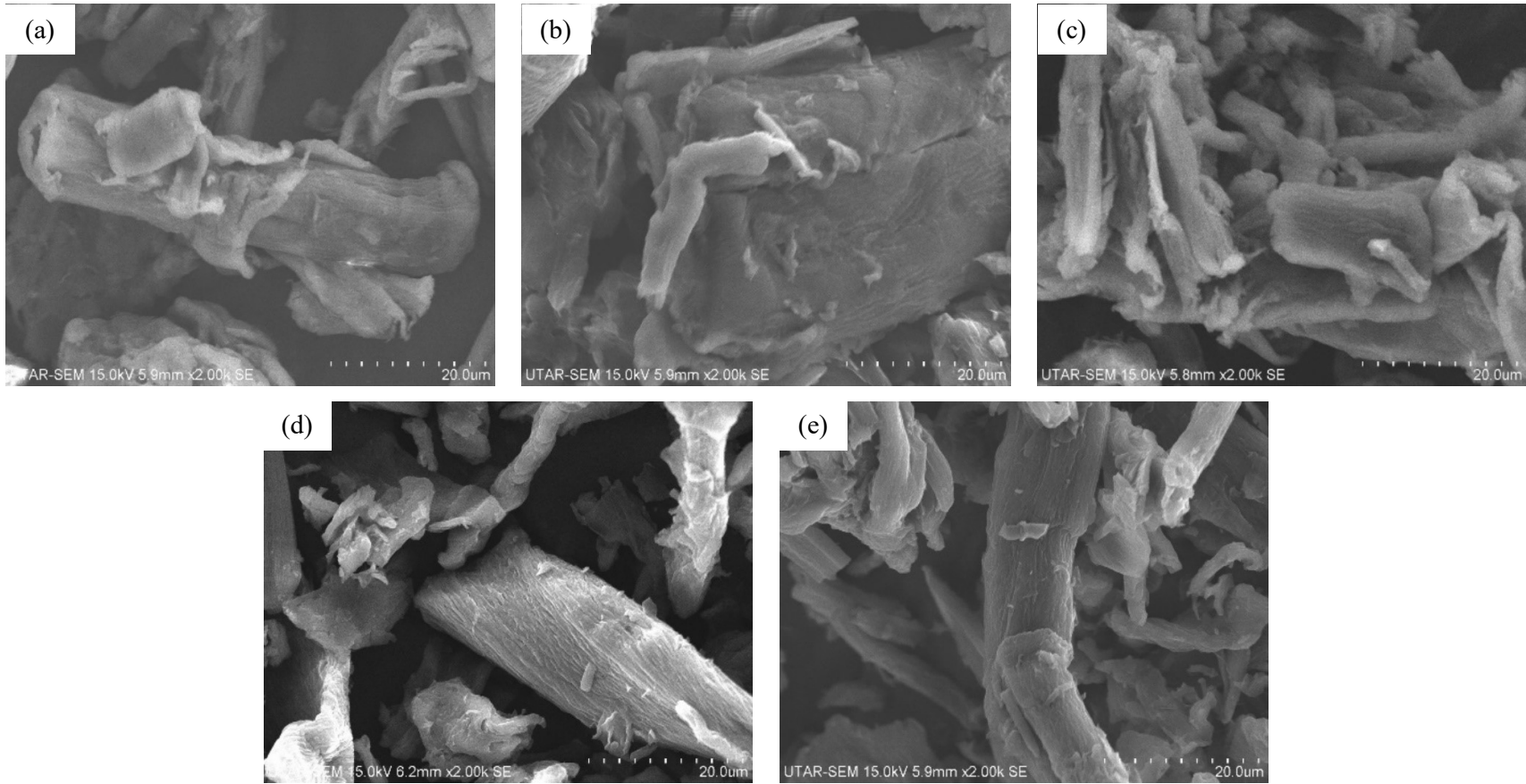Figure 4.1: SEM Images of (a) RC, (b) C-200, (c) C-300, (d) C-400, and (e) C-500

Figure 4.2: SEM Images of (a) RM, (b) M-200, (c) M-300, (d) M-400, and (e) M-500

As can be seen in Figure 4.1 and Figure 4.2, both RC and RM samples were non-porous and have no defined surface structure. As observed in Figure 4.1, corncob-based samples exhibits increased porosity as the carbonisation temperature increases, albeit still not considered highly porous structure at the higher carbonisation temperatures. This was likely attributed to the escape of volatile organic compounds in the raw material at higher temperatures, which was agreeable with the works of Bureros, et al., (2019), da Luz Corrêa, et al., (2023) and Wong, et al., (2020). On the other hand, MCC-based samples do not have the same apparent behaviour as corncob-based samples. As can be observed in Figure 4.2, all MCC-based samples has a rodlike structure which remains intact as the carbonisation temperature increases.

Additionally, the MCC-based samples also did not have any apparent porosity even with increasing carbonisation temperature. The same phenomenon was seen in the work of Souza, et al. (2022), which reasoned that the lack of porosity may be due to the interference of sulfonation and partial oxidation reactions which disrupt and collapse pores structure. However, this reasoning was invalid under the circumstances of this report as the samples were biochars which have not been sulfonated. Another more probable explanation to this phenomenon was provided by Kuznetsov, et al. (2015), who found that MCC activated with phosphoric acid has no apparent porosity even when carbonised at temperatures up to 700 °C. It was determined that various water-soluble compounds such as phosphate esters were formed at lower carbonisation temperatures at between 200 °C and 400 °C, while at higher carbonisation temperatures less soluble polyphosphate compounds were formed instead. These compounds blocked the pores in the biochar produced, and can only be removed at a significant amount through thermal degradation at a high carbonisation temperature of 800 °C. Therefore, the apparent non-porosity observed in this study may be explained by the formation of various phosphate-related compounds formed from the residual phosphoric acid in the activated biomass. As such, it could be suggested that the current method of washing using distilled water is insufficient in removing all residual phosphoric acid, leading to the apparent non-porosity in the biochar samples.

Additionally, Table 4.1 and Table 4.2 belows shows the elemental composition of the corncob-based samples and MCC-based samples examined using EDX, respectively.

Table 4.1: Elemental Composition of Corncob-Based Samples

Samples	Element	Composition	
		Wt%	At%
RC	C	54.8	62.1
	O	43.9	37.4
	P	0.6	0.3
	S	0.6	0.3
C-200	C	66.2	73.2
	O	30.5	25.4
	P	1.9	0.8
	S	1.4	0.6
C-300	C	67.7	74.0
	O	30.9	25.4
	P	0.7	0.3
	S	0.7	0.3
C-400	C	75.8	81.1
	O	22.9	18.4
	P	1.1	0.5
	S	0.3	0.1
C-500	C	74.5	80.2
	O	23.6	19.1
	P	1.1	0.4
	S	0.8	0.3

Table 4.2: Elemental Composition of MCC-Based Samples

Samples	Element	Composition	
		Wt%	At%
RM	C	**55.9**	**63.0**
	O	**43.2**	**36.7**
	P	0.7	0.3
	S	0.2	0.1
M-200	C	**52.4**	**59.7**
	O	**46.4**	**39.7**
	P	0.7	0.3
	S	0.5	0.2
M-300	C	**68.7**	**74.9**
	O	**30.1**	**24.6**
	P	1.1	0.5
	S	0.1	0.0
M-400	C	**76.8**	**81.9**
	O	**22.1**	**17.7**
	P	0.6	0.3
	S	0.5	0.2
M-500	C	**78.2**	**83.2**
	O	**20.2**	**16.1**
	P	1.4	0.6
	S	0.3	0.1

As can be seen from Table 4.1 and Table 4.2, both corncob-based samples and MCC-based samples exhibits the same overall trend, where as the carbonisation temperature increases, the relative composition of carbon increases, while the relative composition of oxygen decreases, as expected due to the release of more volatile oxygenated compounds from the carbon mainbody. This trend was also reported in the work of da Luz Corrêa, et al., (2023) and Lim, et al. (2020). Interestingly, it can be observed that both biomass samples experienced two significant stages of elemental composition change from its raw biomass state to being carbonised at 500 °C. The first major stage

of elemental composition change occurs at a broader range of carbonisation temperature of up to 300 °C, whereas the second major stage of elemental composition change occurs at between carbonisation temperature of 300 °C and 400 °C. According to Amer and Elwardany (2020), the first stage which occurs at between 100 °C and 300 °C was likely consisting of the removal of moisture content and the degradation of hemicellulose, while the second stage that occurs at between 300 °C and 400 °C was likely owing to the degradation of cellulose and lignin, subsequently producing a biochar with a greater relative carbon composition.

Furthermore, the produced biochars were sulfonated at 100 °C to study the effect of different carbonisation temperatures on the sulfonic group density of the synthesised catalysts. Figure 4.3 shows the sulfonic group density of the catalysts synthesised at different carbonisation temperatures, while Table 4.3 summarises the sulfonic group density values.
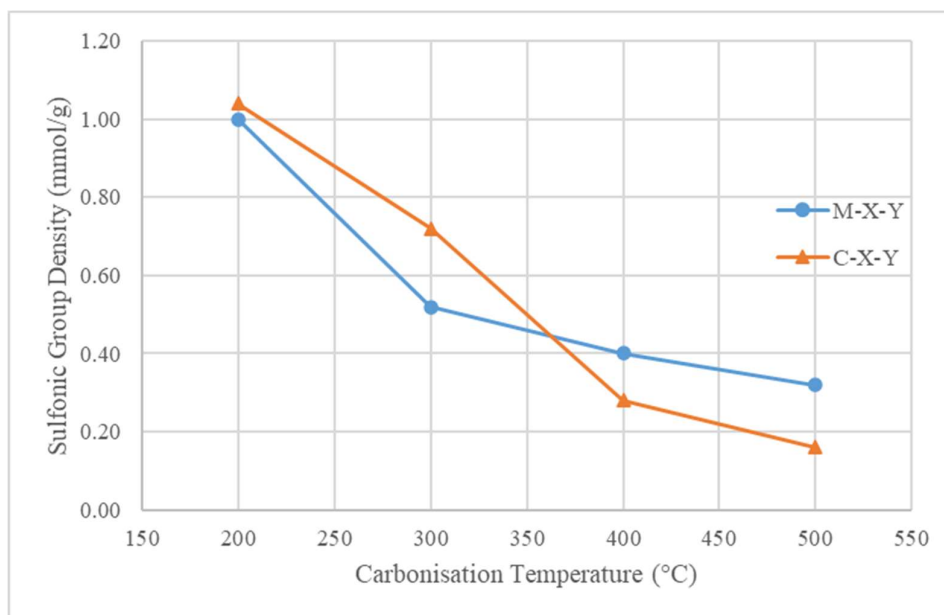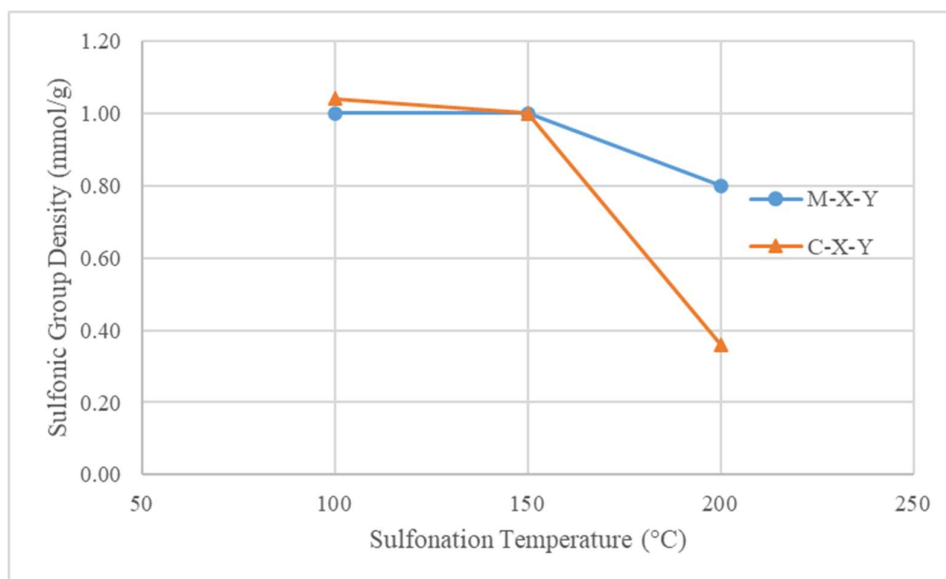

Figure 4.3: Sulfonic Group Density of Catalysts Synthesised against Carbonisation Temperature

Table 4.3: Sulfonic Group Density of Catalysts Synthesised at Different
Carbonisation Temperatures

Samples	Carbonisation Temperature (°C)	Sulfonic Group Density (mmol/g)
M-200-100	200	1.00
M-300-100	300	0.52
M-400-100	400	0.40
M-500-100	500	0.32
C-200-100	200	1.04
C-300-100	300	0.72
C-400-100	400	0.28
C-500-100	500	0.16

As can be seen from Figure 4.3 and Table 4.3, the sulfonic group density of the catalysts synthesised exhibits a negative correlationship for both types of biomass-based catalyst, where the increasing carbonisation temperature leads to decreasing sulfonic group density. This phenomenon was expected, as similar trends were reported in the studies of Bureros, et al. (2019), Cao, et al. (2021), Flores, et al. (2019), and Lim, et al. (2020), which found that at higher carbonisation temperature, the degree of rigidity of the carbon structures formed becomes higher, as evidenced by the increasing presence of stacked polycyclic aromatic carbon sheets found in the catalysts which were carbonised at a higher temperature. The higher degree of rigidity of these carbon structures produced at higher carbonisation temperatures was found to be discouraging to the implantation of sulfonic groups onto the carbon surface, thus leading to lower sulfonic group density on the catalyst synthesised (Bureros, et al., 2019; Cao, et al., 2021; Flores, et al., 2019). Additionally, the results shown in Figure 4.3 and Table 4.3 may also be explained by the structural decomposition induced in the carbon structure by the higher carbonisation temperatures, which collapsed the pores, thus decreasing the specific surface area available for the implantation of the sulfonic groups onto the surface of the catalyst (Lim, et al., 2020; Wong, et al., 2020). As the biochar samples synthesised at 200 °C exhibits the highest sulfonic group density attachment after sulfonation for both corncob- and MCC-

based samples, the optimal carbonisation temperature was determined to be 200 °C. The subsequent parameter study of effect of sulfonation temperature on the catalytic performance of the catalysts was conducted using biochar samples carbonised at 200 °C, which were C-200 and M-200.

4.1.2   Effect of Sulfonation Temperature

The selected biochar samples, C-200, and M-200, were subjected to sulfonation with concentrated sulfuric acid at different temperatures to determine the optimum sulfonation temperature based on the sulfonic group density of the synthesised catalyst samples. Figure 4.4 and Table 4.4 show the sulfonic group density of the catalyst samples synthsised at different sulfonation temperatures.

Figure 4.4: Sulfonic Group Density of Catalysts Synthesised against Sulfonation
        Temperature

Table 4.4: Sulfonic Group Density of Catalysts Synthesised at Different Sulfonation Temperatures

Samples	Sulfonation Temperature (°C)	Sulfonic Group Density (mmol/g)
M-200-100	100	1.00
M-200-150	150	1.00
M-200-200	200	0.80
C-200-100	100	1.04
C-200-150	150	1.00
C-200-200	200	0.36

As can be observed from Figure 4.4 and Table 4.4, both corncob-based catalyst samples and MCC-based catalyst samples presented similar behaviour when sulfonated at different temperatures, where the sulfonic group density remains almost constant when sulfonated at 100 °C and 150 °C, but dropped considerably when sulfonated at 200 °C.

This was probably due to the relative thermal instability of sulfonic groups, which starts to decompose at a higher temperature. This finding was agreeable with the findings in the works of Zhang, et al. (2021), Bureros, et al. (2019), Wong, et al. (2020), Flores, et al., (2019), Souza, et al. (2022), which all found that the increases in sulfonation temperatures leads to an increase in the sulfonic group density, up to an optimal point, beyond which the sulfonic group density declines instead. In particular, Souza, et al. (2022) and Wong, et al. (2020) determined that the optimum sulfonation temperature for most biomass lies in between 100 °C and 150 °C, which coincided with the results shown in Figure 4.4 and Table 4.4, where the sulfonic group density at 100 °C and 150 °C was the highest in both corncob-based and MCC-based catalyst samples.

Furthermore, as suggested by Wong, et al. (2020), the ineffective sulfonation at higher temperatures beyond the optimal point, as can be seen in Figure 4.4 and Table 4.4 at 200 °C, may also be due to the more competitive side reactions at higher temperatures, such as oxidation, condensation and dehydrogenation.

While the sulfonic group density of the catalyst samples sulfonated at 100 °C and 150 °C were similar, ultimately the sulfonation temperature of 100 °C was selected as the optimum sulfonation temperature in consideration of the lower energy requirement. As such, the catalyst samples, M-200-100, and C-200-100, were deemed the optimal catalyst samples used for the subsequent characterisation studies in addition to parameter studies for interesterification reaction to produce biodiesel.

4.2   Characterisation Study of Catalyst

The following sections contain various characteristics studies including XRD, SEM-EDX, FTIR, and BET, of the selected catalyst samples, C-200-100 and M-200-100. Furthermore, the indications and findings of these characteristics studies were discussed and interpreted to obtain a better understanding of the synthesis process and the resulting catalyst samples synthesised.

4.2.1   XRD

To study the crystallinity of the synthesised catalysts, M-200-100 and C-200-100 were subjected to X-ray Diffraction analysis (XRD). Figure 4.5, Figure 4.6, Figure 4.7, and Figure 4.8 show the diffraction pattern for C-200, C-200-100, M-200, and M-200-100 respectively.
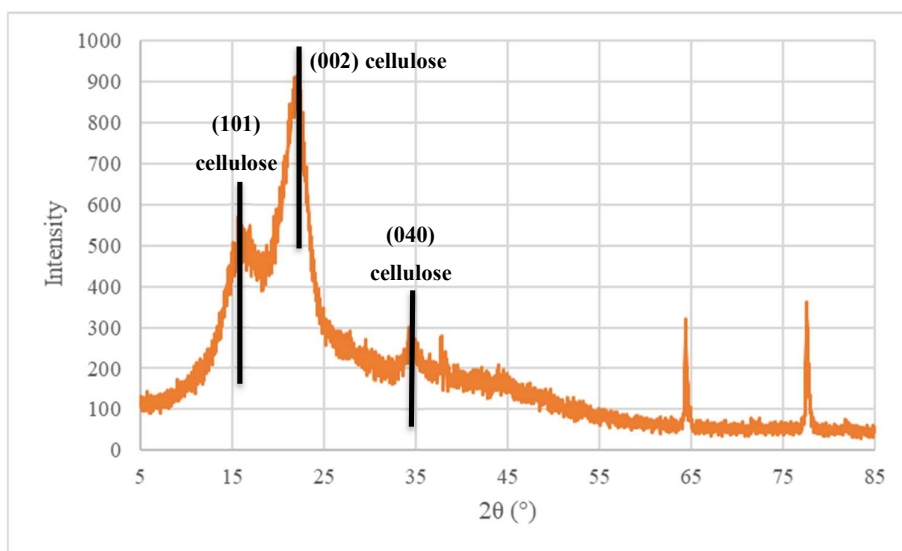
Figure 4.5: XRD Diffraction Pattern of C-200
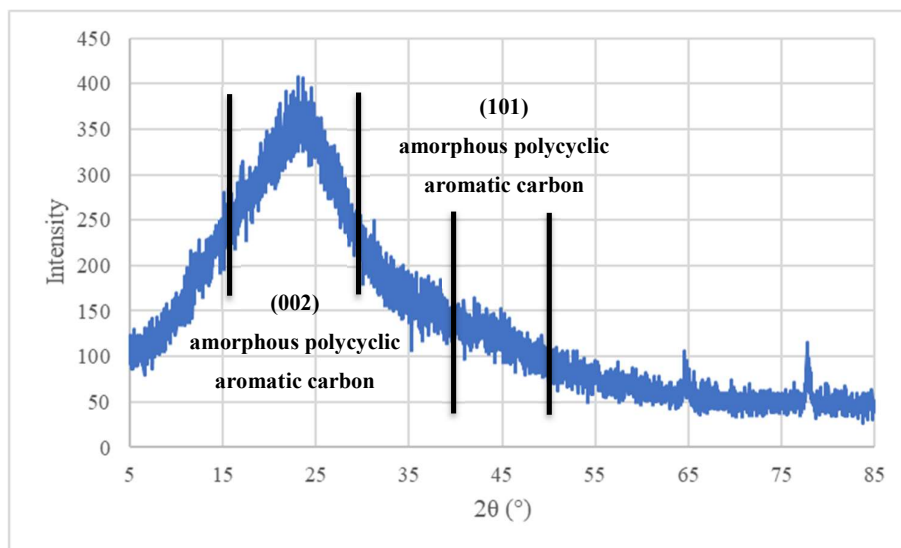
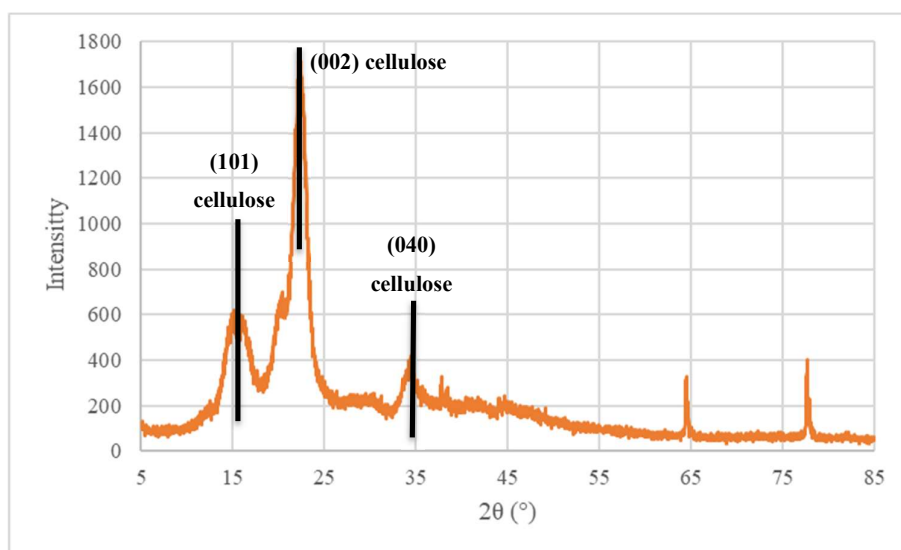Figure 4.6: XRD Diffraction Pattern of C-200-100

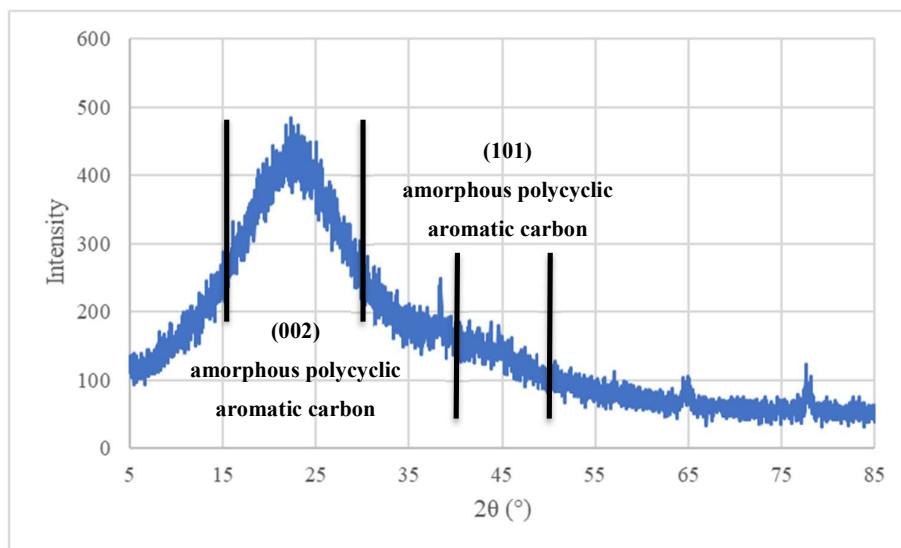Figure 4.7: XRD Diffraction Pattern of M-200

Figure 4.8: XRD Diffraction Pattern of M-200-100

As can be seen from Figure 4.5 and Figure 4.7, both C-200 and M-200 samples exhibited a diffraction pattern typically seen in cellulose-based compounds. The strong peak at around $2\theta = 22°$ seen in both Figure 4.5 and Figure 4.7 was indicative of the (002) diffraction plane of cellulose, while the weaker peaks at around $2\theta = 15°$ and $2\theta = 35°$ observed in both diffraction patterns were indicative of the (101) and (040) diffraction plane of cellulose respectively. These observations were in good agreement with the XRD diffraction pattern published in the work of Zhang, et al. (2021). The presence of these cellulose indicating peaks suggested that the carbonisation of biomass at 200 °C was insufficient for complete carbonisation, as cellulose was not completely degraded after carbonisation, supplementing the SEM-EDX results shown in section 4.1.1 above, where the biochars produced at 200 °C still retains a higher relative oxygen composition and have no apparent porosity.

Furthermore, as can be observed in Figure 4.6 and Figure 4.8, no significant sharp peaks can be seen, while the most prominent diffraction peak was observed in the form of a broad diffraction peak at between $2\theta = 15°$ to $2\theta = 30°$, indicating that both C-200-100 and M-200-100 catalyst samples were amorphous with no defined crystallinity. The presence of this broad peak at between $2\theta = 15°$ to $2\theta = 30°$ was indicative of the (002) diffraction plane of amorphous polycyclic aromatic carbon sheets, where the polycyclic aromatic carbon sheets were positioned in an unorganised fashion. This broad diffraction peak was also observed in the XRD diffraction pattern of sulfonated carbon-

based catalyst in the works of Cao, et al. (2021), Ibrahim, et al. (2019), Rocha, Olivera and Franca (2019) and Sangar, et al. (2019). Furthermore, the presence of a weak and broad diffraction peak at between around $2\theta = 40°$ and $2\theta = 50°$ was indicative of the (101) diffraction plane of amorphous polycyclic aromatic carbon sheets, affirming that the carbon matrix of the catalyst samples were made up of amorphous polycyclic aromatic carbon sheets. The presence of this weak and broad peak was also reported by Cao, et al. (2021) and Rocha, Olivera and Franca (2019) in the XRD diffraction pattern of sulfonated carbon-based catalyst. The high amorphousness of the catalyst samples were conducive to the attachment of sulfonic groups onto the catalyst surface, allowing more sulfonic groups to attach onto the catalyst, increasing the sulfonic group density (Cao, et al., 2021).

Interestingly, the transition of the diffraction pattern of biochars to catalysts as can be seen in Figure 4.5 to Figure 4.6 and Figure 4.7 to Figure 4.8, show that the catalyst samples gained its amorphousness after sulfonation. The loss of crystallinity in the samples after sulfonation may indicate that further carbonisation were carried out simultaneously with the sulfonation process, where the remaining cellulose in the biochar samples due to the incomplete carbonisation at 200 °C was decomposed; analogous to the one-step synthesis method mentioned in Chapter 2, where carbonisation and sulfonation were conducted simultaneously.

4.2.2 SEM-EDX

Additionally, the selected catalyst samples of C-200-100 and M-200-100 were also subjected SEM-EDX analysis to study the surface morphology and elemental composition of the catalyst samples. Figure 4.9 and Figure 4.10 show the SEM images of C-200-100 and M-200-100 under 2000 × and 5000 × magnification, respectively.
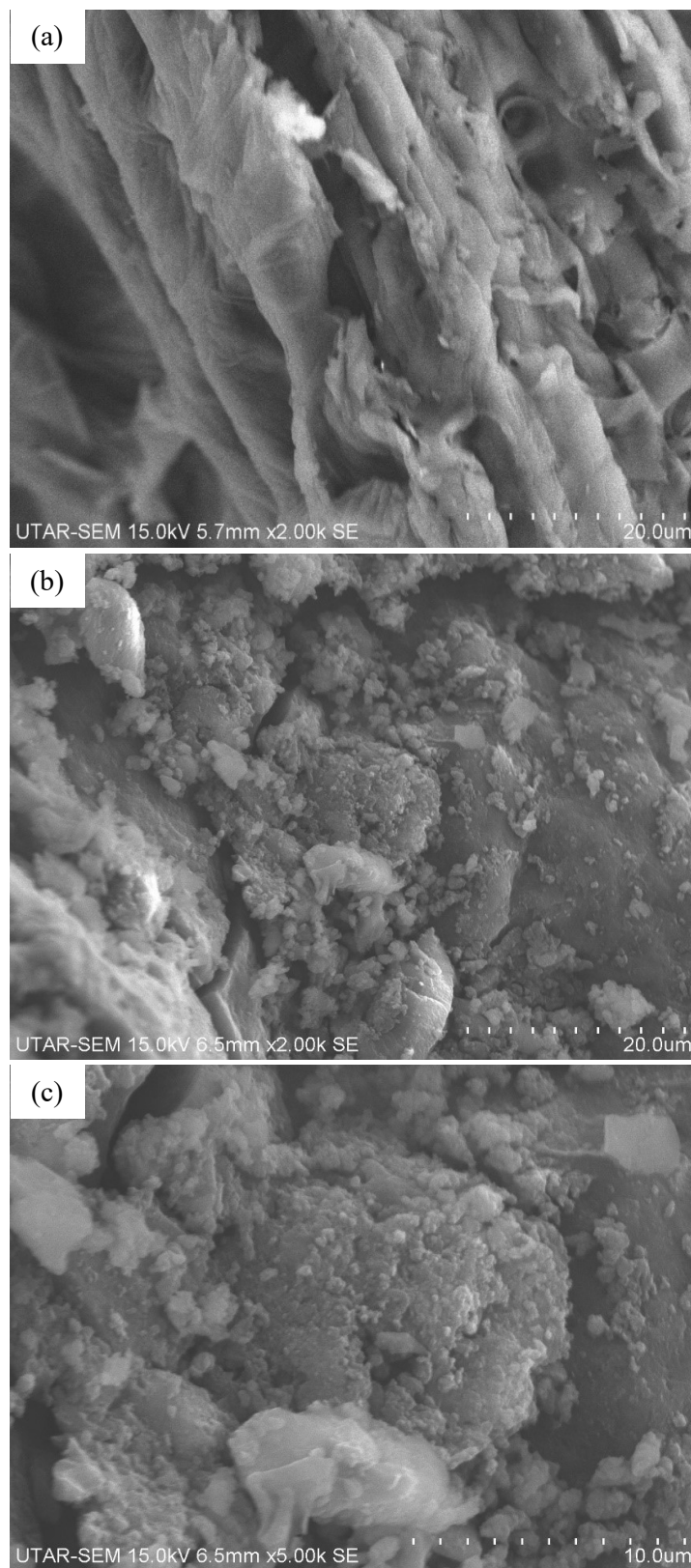
Figure 4.9: SEM Images of (a) C-200, (b) C-200-100 under 2000 × magnification, and (c) C-200-100 under 5000 × magnification
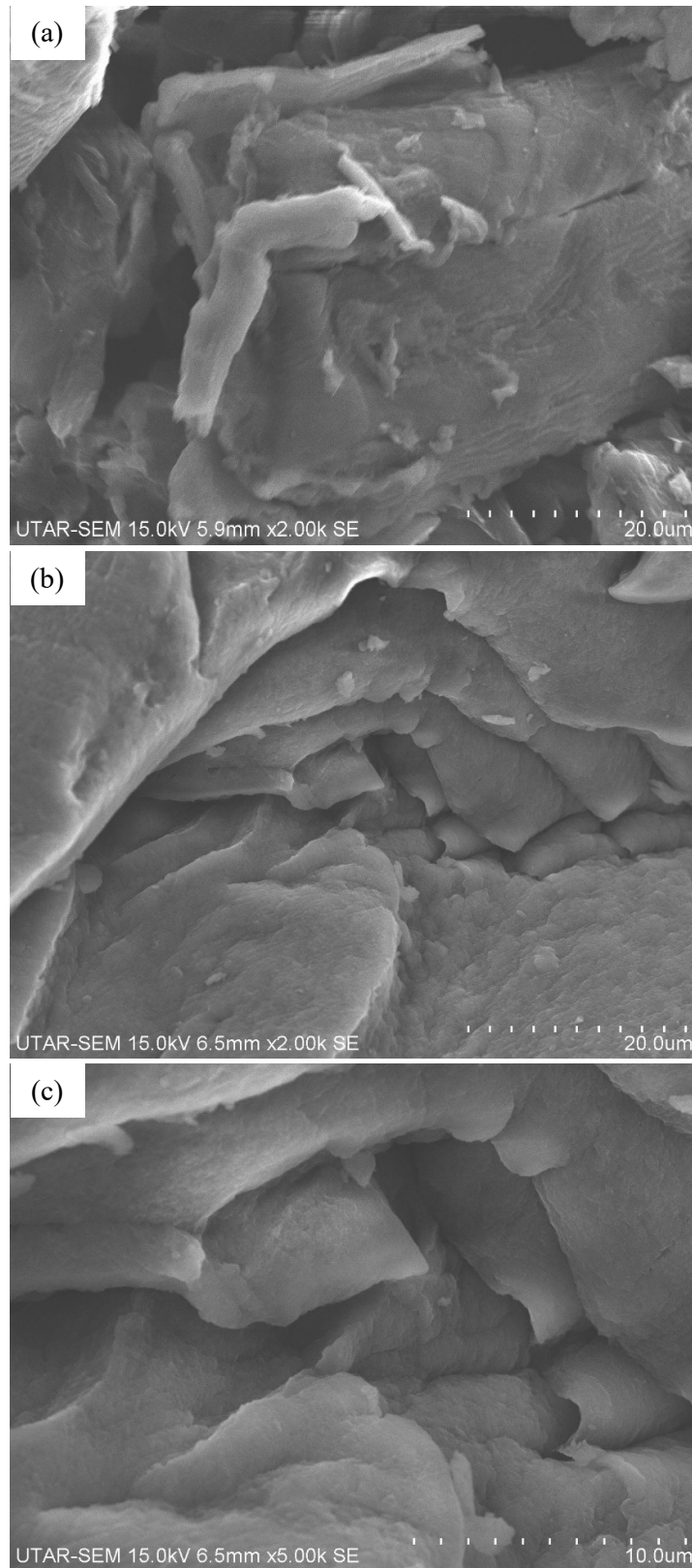
Figure 4.10: SEM Images of (a) M-200, (b) M-200-100 under 2000 ×
magnification, and (c) M-200-100 under 5000 × magnification

As can be observed in Figure 4.9(a) and Figure 4.9(b), while the C-200 sample exhibits a certain degree of porosity, the C-200-100 sample have no apparent porosity while showing a very rough surface with no defined structures. On the other hand, as shown in Figure 4.10(a) and Figure 4.10(b), the rod-like structure seen in M-200 sample disappeared in M-200-100, which shows a layered structure with smooth surface with no apparent porosity. The lack of apparent porosity in both corncob-based and MCC-based catalyst samples may be due to several factors.

Firstly, the disappearance of apparent porosity originally observed in C-200 samples after sulfonation may be due to the destruction and collapse of the pores structure caused by the violent side reactions such as oxidation and polymerisation during the sulfonation process due to the use of concentrated sulfuric acid as the sulfonating agent. Similar reasoning was given by Cao, et al. (2021), Zhang, et al. (2021), and Lathiya, Bhatt and Maheria (2018) to explain the lose of porosity and specific surface area observed in carbon-based catalysts after the sulfonation process using concentrated sulfuric acid.

Secondly, the lack of apparent porosity in both catalyst samples after sulfonation may also be explained by the simultaneous carbonisation and sulfonation process. Concluding from the XRD diffraction patterns of the biochars and catalysts samples analysed above, while it was determined that the carbonisation temperature of 200 °C was insufficient for complete carbonisation and satisfactory pores formation, it was also found that the carbonisation process likely continued during the sulfonation process as the carbon structure of the biochars were converted into predominantly polycyclic aromatic carbon sheets after sulfonation, which were normally only observed in samples carbonised to a certain degree. While it may be assumed that pores formation would occurs during the continued carbonisation process in presence of the sulfonation process, it has been reported for two reasons that disputed this assumption. First of all, the temperature employed during the sulfonation process was too low for any significant decomposition and removal of volatile oxygenated compounds to create spaces for pore formation (Zhang, et al., 2021). Furthermore, the presence of ongoing sulfonation process alongside the carbonisation process prevented any pores formation of note due to the interference by various

reactions including sulfonation and partial oxidation (Souza, et al., 2022). Table 4.5 shows the elemental composition of C-200-100 and M-200-100.

Table 4.5: Elemental Composition of C-200-100 and M-200-100

Samples	Element	Composition	
		Wt%	At%
C-200	C	66.2	73.2
	O	30.5	25.4
	P	1.9	0.8
	S	1.4	0.6
C-200-100	C	51.8	62.5
	O	34.4	31.2
	P	0.5	0.3
	S	13.3	6.0
M-200	C	52.4	59.7
	O	46.4	39.7
	P	0.7	0.3
	S	0.5	0.2
M-200-100	C	62.2	70.6
	O	31.3	26.7
	P	0.5	0.2
	S	6.0	2.6

As can be observed from Table 4.5, the catalyst samples (C-200-100 and M-200-100) both experienced an increase in relative sulfur composition, which was indicative of a successful sulfonation, verifying the presence of sulfonic groups on the catalyst surface. Furthermore, compared to C-200 sample, the C-200-100 have a lower relative carbon composition as well as a higher relative oxygen composition. This phenomenon may be explained by the use of concentrated sulfuric acid as the sulfonating agent, which was a strong oxidising agent that promotes the formation of other oxygenated compounds (da Luz Corrêa, et al., 2023). On the other hand, the MCC-based samples do not follow the explanation provided above by da Luz Corrêa, et al. (2023), as the relative composition of oxygen decreased when it was expected to increase as can be

seen in Table 4.5. The deviation may be caused by the incomplete carbonisation during the initial carbonisation step and the subsequent occurrence of simultaneous carbonisation and sulfonation step as explained previously in the report, where the rate of oxygenated products being degraded and released due to carbonisation outpaced the rate of oxygenated products formation due to sulfonation, hence, resulting in an overall reduction in relative oxygen composition. Furthermore, the elemental composition of M-200-100 obtained in this study was also comparable to the elemental composition of MCC-based sulfonated catalyst reported in the work of Souza, et al. (2022). Table 4.6 shows the comparison between the elemental composition of catalyst synthesised in this study and other studies.

Table 4.6: Comparison of Elemental Composition of Sulfonated Catalyst

Biomass	Elements			Reference
	C	O	S	
Corncob	52.06	34.57	13.37	This Study
MCC	62.51	31.46	6.03	This Study
Murumuru Kernel	67.49	24.11	8.37	da Luz Corrêa, et al., 2023
Corncob	68.09	25.59	7.35	Ibrahim, et al., 2019
MCC	66.90	30.10	3.00	Souza, et al., 2022
OPEFB	64.01	32.47	3.52	Lim, et al., 2020
Waste Orange Peel	43.44	37.81	3.68	Lathiya, Bhatt and Maheria, 2018
Cow Manure	60.50	31.78	4.20	Sangar, et al., 2019

4.2.3   FTIR

Fourier-Transform Infrared (FTIR) analysis was used to prove and verify the attachment of sulfonic groups on the catalyst samples. Figure 4.11 shows the FTIR spectrum of C-200-100 and M-200-100 samples. Observing from Figure 4.11, the absorption band at around 1700 cm^{-1} was indicative of the presence of C=O bond which was associated with either carboxylic or carbonyl groups. Furthermore, an absorption band at between around 1580 cm^{-1} and 1620 cm^{-1} was indicative of the presence of the C=C bond which was associated with aromatic carbon rings. Both of these observations suggested the presence of polycyclic aromatic carbon structures, as reported by Cao, et al. (2021), Zhang, et al. (2021), Wong, et al. (2020) and Souza, et al. (2022).

Additionally, the absorption bands at around 1020 cm^{-1} and 1150 cm^{-1} were indicative of the symmetrical and asymmetrical O=S=O bonds respectively, the presence of both of these peaks indicates the successful implantation of sulfonic groups onto the catalyst surface. Moreover, the absorption band at between around 1150 cm^{-1} and 1270 cm^{-1} was a direct indication of the successful implantation of sulfonic groups as it was associated with –SO$_3$H group (Lim, et al., 2020; Wong, et al., 2020). Besides, the absorption band at between around 650 cm^{-1} and 700 cm^{-1} was associated with the C–S bonds, indicating a successful implantation of sulfonic groups onto the catalyst carbon structure surface (Cao, et al., 2021; Wong, et al., 2020).

Furthermore, the broad absorption band at between around 2800 cm^{-1} and 3600 cm^{-1} was indicative of the O–H bonds of the phenolic groups (Wong, et al., 2020). The presence of the O–H bonds associated with phenolic groups indicates that the carbonisation process was incomplete, as a typical carbon-based sample which were significantly carbonised should have minimal presence of O–H bonds associated with phenolic groups. In addition, as can be observed from Figure 4.11, the transmittance of the sulfonic group related absorption bands of C-200-100 spectrum was much lower than its counterparts of M-200-100 spectrum, which indicates that the concentration of sulfonic groups in C-200-100 sample was higher than the M-200-100 sample according to the Beer-Lambert Law. This was in agreement with the EDX findings above, where the sulfur concentration in C-200-100 was greater than in M-200-100.
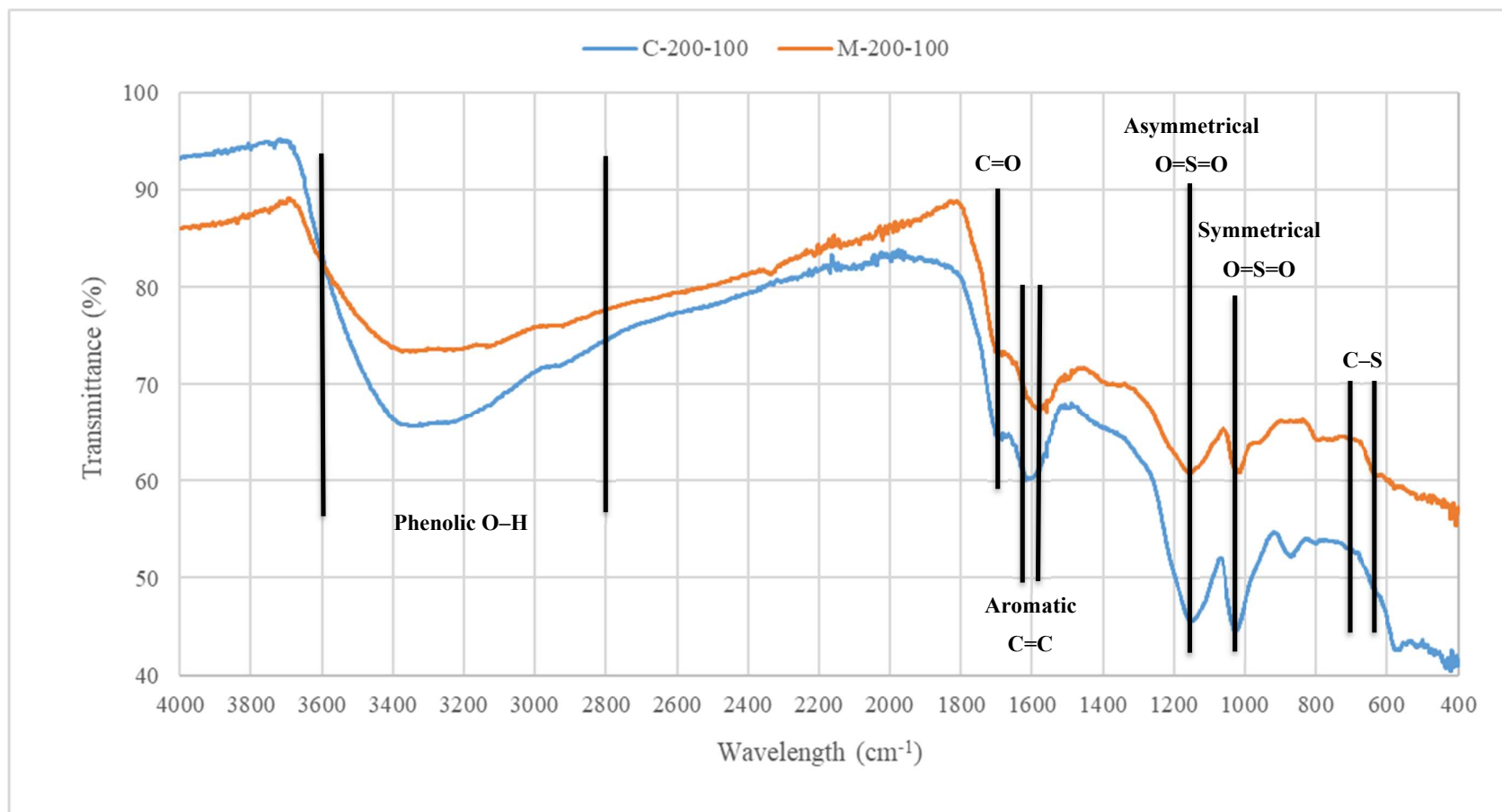
Figure 4.11: FTIR Spectrum of C-200-100 and M-200-100

4.2.4   BET Surface Analysis

To study the specific surface area of the synthesised catalyst samples, and also the effects of the synthesis process on the specific surface area, the raw biomass, RC and RM, and the catalyst samples, C-200-100 and M-200-100, were subjected to BET surface analysis. Table 4.7 shows the BET surface analysis results.

Table 4.7: BET Surface Analysis Results

Samples	BET Surface Area (m^2/g)
RC	1.0350
C-200-100	1.9314
RM	1.1647
M-200-100	1.4399

As can be seen from Table 4.7, the specific surface area of the catalyst samples had only increased marginally after carbonisation and sulfonation process, suggesting that the synthesis process did not produce a catalyst sample with any apparent porosity. This finding was in line with the XRD and SEM findings mentioned above, where the carbonisation temperature at 200 °C was insufficient for any significant pores formation as only a little amount of volatile oxygenated compounds were decomposed and released, while the subsequent continued carbonisation during the sulfonation process also failed to create pores due to interference from other reactions that occurs during the sulfonation. Table 4.8 shows the comparison of the specific surface area reported in other studies with the specific surface area reported in this report.

Table 4.8: Specific Surface Area Reported

Biomass	Specific Surface Area (m²/g)	References
Corncob	1.93	This Study
MCC	1.44	This Study
Corncob	730.8	Rocha, Olivera and Franca, 2019
OPEFB	141.54	Wong, et al., 2020
Waste Orange Peel	44	Lathiya, Bhatt and Maheria, 2018
Corncob	8.40	Ibrahim, et al., 2019
Sargassum horneri	7.34	Cao, et al., 2021
OPEFB	2.85	Lim, et al., 2020
Bamboo	2.60	Zhang, et al., 2021

4.2.5 TGA

Thermogravimetric analysis (TGA) was used to determine the thermal stability of the catalyst samples, C-200-100 and M-200-100. Figure 4.12 and Figure 4.13 shows the temperature-dependent mass loss curve of C-200-100 and M-200-100 respectively.
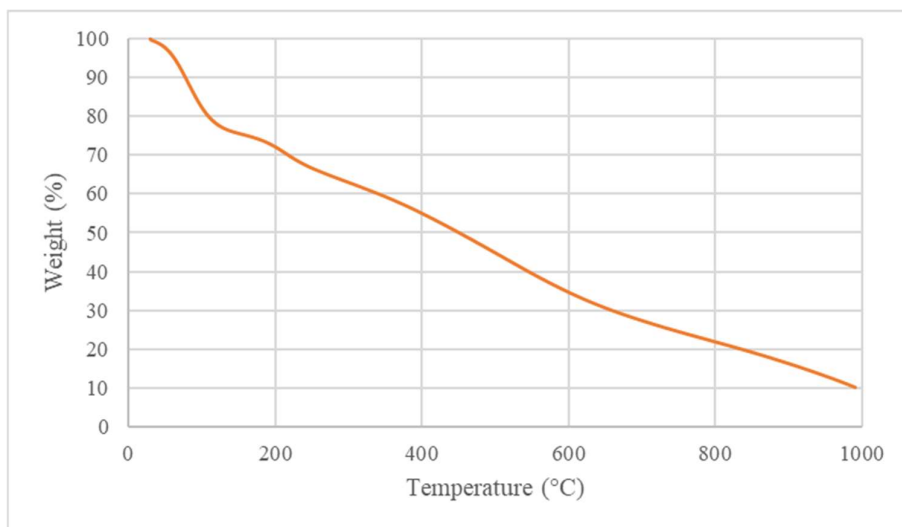
Figure 4.12: Temperature-Dependent Mass Loss Curve for C-200-100
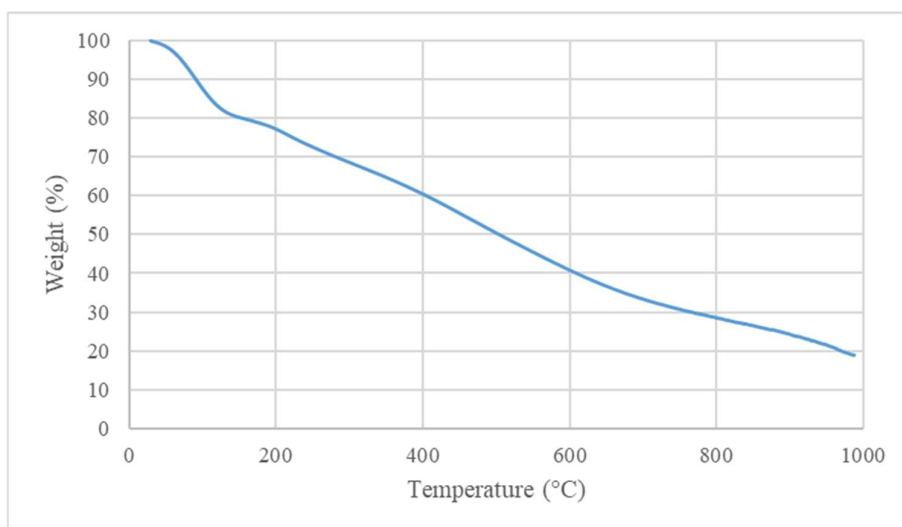
Figure 4.13: Temperature-Dependent Mass Loss Curve for M-200-100

As can be observed from Figure 4.12 and Figure 4.13, a significant mass loss stage can be observed at the range in between around 50 °C and 120 °C. This can be attributed to the loss of inherent moisture content in the catalyst sample, this reasoning was in agreement with the work of Souza, et al. (2022) and Lim, et al. (2020).

Additionally, the mass loss became insignificant in the range between around 120 °C and 200 °C. This indicates that the catalyst can perform with good thermal stability up to 200 °C, which was deemed acceptable for the application in this study, as interesterification can be carried out at a temperature lower than 200 °C.

However, beyond the 200 °C mark, both the C-200-100 and M-200-100 samples experienced a steady and gradual mass loss. This phenomenon likely due to the low carbonisation temperature employed in the synthesis process, which made the carbonisation process incomplete. This finding was in good agreement with the findings of XRD, SEM, and FTIR mentioned above, which pointed out that the carbonisation temperature of 200 °C only managed a lower degree of carbonisation. Therefore, as can be seen in Figure 4.12 and Figure 4.13, the gradual mass loss beyond 200 °C was most likely due to the structural decomposition as usually observed in high temperature carbonisation processes, where the oxygenated groups along with the sulfonic groups were decomposed and released from the samples. This reasoning was in good agreement with the work of Lim, et al. (2020).

4.3 Parameter Studies for Interesterification

Two parameters were studied to determine the optimum conditions for the interesterification reaction using the catalyst synthesised in this report; these parameters were catalyst loading and reaction time. The principle parameter used for determination of the optimal reaction parameters was the conversion of oleic acid and subsequently the biodiesel yield.

4.3.1 Effect of Catalyst Loading on Biodiesel Yield

The catalyst loading was varied at 5 wt%, 10 wt%, and 15 wt% while the reaction time was held constant at 4 h. The following Table 4.9 and Figure 4.14 show the effect of catalyst loading on biodiesel yield.

Table 4.9: Effect of Catalyst Loading on Biodiesel Yield

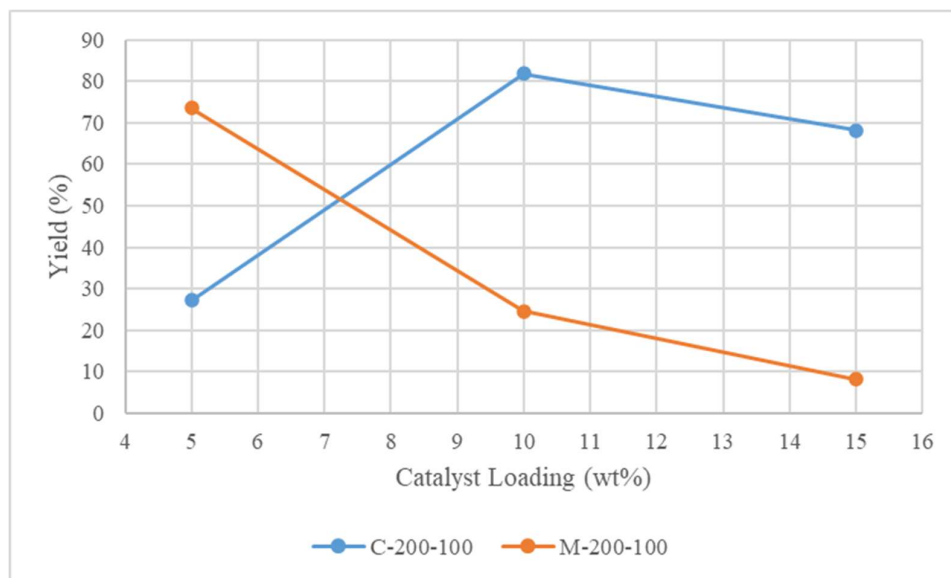| Sample	Catalyst Loading (wt%)	Yield (%)
Control	0	3
C-200-100	5	27
	10	82
	15	68
M-200-100	5	74
	10	25
	15	8

Figure 4.14: Effect of Catalyst Loading on Biodiesel Yield

As shown in Table 4.9, the highest yield can be achieved at different catalyst loading for C-200-100 and M-200-100, where C-200-100 achieved a yield of 82 % at a catalyst loading of 10 wt%, while M-200-100 achieved a yield of 74 % at a catalyst loading if 5 wt%. Additionally, as can be seen from Figure 4.14, the biodiesel yield increases initially as the C-200-100 loading increases, and decreases past the optimal catalyst loading at 10 wt%, whereas the biodiesel yield decreases as the M-200-100 loading increases. The increases in biodiesel yield as the catalyst loading increases can be explained by the increases in active sites available for reactions between the reactants with the catalyst (Wong, et al., 2020; Lim, et al., 2020). Additionally, the decrease in biodiesel yield past the optimal point can be explained by the additional mass transfer limitation imposed on the reaction kinetics introduced by the excessive catalyst loading (Cao, et al., 2021; Wong, et al., 2020). The determined optimal catalyst loading of 10 wt% for C-200-100 and 5 wt% for M-200-100, were then used for the subsequent reaction time study.

4.3.2   Effect of Reaction Time on Biodiesel Yield

The reaction time was varied at 2 h, 4 h, and 6 h while the catalyst loading was held constant at the optimal value determined for C-200-100 and M-200-100 respectively. The following Table 4.10 and Figure 4.15 show the effect of reaction time on biodiesel yield.

Table 4.10: Effect of Catalyst Loading on Biodiesel Yield

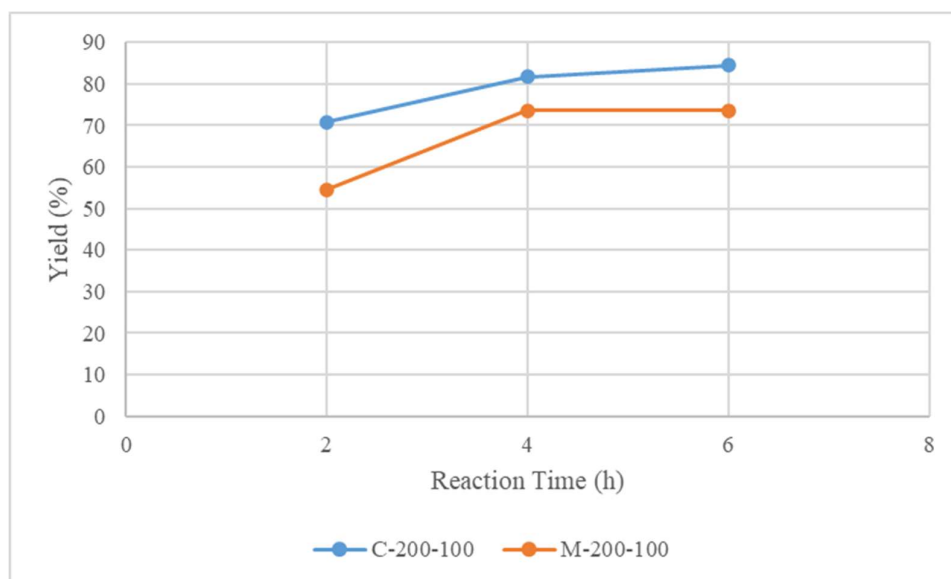| Sample	Reaction Time (h)	Yield (%)
Control	4	3
C-200-100	2	71
	4	82
	6	84
M-200-100	2	54
	4	74
	6	74

Figure 4.15: Effect of Reaction Time on Biodiesel Yield

As shown in Table 4.10, an optimal yield of 84 % was obtained at a reaction time of 6 h for C-200-100, while an optimal yield of 74 % was obtained at a reaction time of 4 h and 6 h for M-200-100. Additionally, as can be seen from Figure 4.13, both C-200-100 and M-200-100 samples exhibited similar performance, where the biodiesel yield increases as reaction time increases, and then plateaued after the 4 h mark with only minimal increment. The stagnancy in yield gain was likely due to the reversible nature of the reaction, where the forward reaction to produce biodiesel was hindered by the reverse reaction, indicating that the interesterification reaction had reached its equilibrium state (Cao, et al., 2021; Ibrahim, et al., 2019; Zhang, et al., 2020). In consideration of the minimal biodiesel yield gain after extending the reaction time, the optimal

reaction time for both corncob-based and MCC-based catalysts were determined to be 4 h, as it was deemed more energy efficient. As such the reaction time of 4 h was used in the subsequent reusability study.

4.4   Reusability Study

The spent catalyst samples recovered after one reaction cycle were reused using the optimal reaction conditions determined in the previous sections. Table 4.11 below shows the biodiesel yield using spent catalysts after one reaction cycle.

Table 4.11: Biodiesel Yield of Spent Catalysts After One Reaction Cycle under Optimal Reaction Conditions

Sample	Description	Yield (%)
C-200-100	Fresh	82
	Spent	65
M-200-100	Fresh	74
	Spent	44

As can be observed from Table 4.11, both the spent catalyst samples after one reaction cycle shown a worse catalytic performance than its fresh counterparts. As suggested by multiple studies (Bureros, et al., 2019; Cao, et al., 2021; da Luz Corrêa, et al., 2023; Flores, et al., 2019; Lathiya, Bhatt and Maheria, 2018; Sangar, et al., 2019; Souza, et al., 2022; Zhang, et al., 2021), the apparent deactivation of the sulfonated catalysts were most likely due to the leaching of weakly attached sulfonic groups. The significant decrease in catalytic activity suggests that the current catalyst washing method used in this study was inadequate in removing the weakly attached sulfonic groups.

4.5   Results Analysis

As can be seen in the previous sections, the corncob-based catalyst held an overall edge over the MCC-based catalyst, both in terms of catalytic performance and reusability, despite undergoing similar synthesis procedures. The difference in performance can be explained through the characteristics studies outlined in the previous section 4.2.

Firstly, the better catalytic performance of corncob-based catalyst can be explained by the higher sulfonic group density found in corncob-based catalyst over MCC-based catalyst, as shown in the EDX results and indicated by the FTIR spectrums.

Secondly, the better catalytic performance of corncob-based catalyst may also be explained by its better surface morphology, as can be observed from the SEM images, where the corncob-based catalyst has a rougher surface compared to the MCC-based catalyst. This explanation was also supported by the BET surface analysis results, where the corncob-based catalyst has a higher specific surface area, albeit minor.

Thirdly, the better reusability of corncob-based catalysts may also be associated with its better surface morphology, which was suspected to have a better leaching resistant properties.

Interestingly, while it was reported by da Luz Corrêa, et al. (2023), Flores, et al. (2019) and Rocha, Olivera and Franca (2019) that the specific surface area and porosity of the catalyst plays an important role in the catalytic performance of the catalyst, both the corncob-based and MCC-based catalysts synthesised in this study achieved a reasonable conversion despite owning little porosity and specific surface area. This finding was also in agreement with the works of Ibrahim, et al. (2019), Souza, et al. (2022) and Zhang, et al. (2021), where the synthesised catalysts managed to achieve at least reasonable catalytic activity despite having little porosity and specific surface area of note. Furthermore, Ibrahim, et al. (2019) also directly stated that the specific surface area and other related pore properties do not contribute to the catalytic activity of the sulfonated catalysts. This discovery suggests that the specific surface area and porosity may not play a role as significant as suggested by the studies mentioned above, where the catalytic performance was likely predominantly dependent on the sulfonic group density, with specific surface area and porosity playing a minor role. Table 4.12 below compares the sulfonic group density and conversion of this study with other studies.

Table 4.12: Sulfonic Group Density and Conversion Summary

Biomass	Sulfonic Group Density (mmol/g)	Biodiesel Yield (%)	References
C-200-100	1.04	82	This Study
M-200-100	1.00	74	This Study
Murumuru Kernel	1.70	96[1]	da Luz Corrêa, et al., 2023
Bamboo	1.50	98[1]	Zhang, et al., 2021
Sargassum horneri	1.40	96	Cao, et al., 2021
Waste Orange Peel	1.57	92[1]	Lathiya, Bhatt and Maheria, 2018
Cacao Shell	1.48	93[1]	Bureros, et al., 2019
Sugarcane Bagasse	1.06	90[1]	Flores, et al., 2019

[1] FFA Conversion in %

CHAPTER 5

CONCLUSIONS AND RECOMMENDATIONS

5.1   Conclusions

In conclusion, a functional sulfonated carbon-based catalyst for the interesterification process to produce biodiesel was successfully synthesised from microcrystalline cellulose and corncob through a conventional two-step method. It was determined that the optimal carbonisation and sulfonation temperature is 200 °C and 100 °C respectively based on the sulfonic group density, which was found to be the predominant factor in the catalytic performance of the sulfonated carbon-based catalyst.

Furthermore, the synthesised catalyst samples were also successfully characterised using XRD, SEM-EDX, FTIR, BET surface analysis and TGA. It was found that the sulfonic groups were successfully implanted onto the catalyst surface, with a maximum sulfonic group density of 1.04 mmol/g and 1.00 mmol/g found in corncob-based catalyst and microcrystalline cellulose-based catalyst respectively. Moreover, it was also discovered that the carbon structure of the synthesised catalysts consisted of amorphous polycyclic aromatic carbon sheets, which were reported to be favourable for sulfonic groups attachment. Furthermore, it was found that the synthesised catalysts have little porosity and specific surface area, with a specific surface area of 1.93 m^2/g and 1.44 m^2/g found in corncob-based catalyst and microcrystalline cellulose-based catalyst respectively. Additionally, it was also determined that the synthesised catalysts can perform with good thermal stability at the interesterification reaction temperature studied in this report.

Furthermore, it was also found that the optimal catalyst loading for corncob-based catalyst and microcrystalline cellulose-based catalyst is 10 wt% and 5 wt% respectively, as additional catalyst loading proved detrimental to the interesterification reaction due to mass transfer limitation. It was also determined that the optimal reaction time for the interesterification reaction using the catalyst synthesised in this study is 4 h, as any longer reaction time only shows minimal gain in biodiesel yield.

Despite the non-porous nature of the catalysts synthesised, it was also found that the catalytic activity of the sulfonated carbon-based catalysts is mainly dependent on the sulfonic group density rather than the porosity and specific surface area. This is shown by the biodiesel yield at 82 % and 74 % obtained by the corncob-based and microcrystalline cellulose-based catalyst synthesised in this study respectively, despite the marginal porosity and specific surface area.

Additionally, it was also found that the corncob-based catalysts have a better overall performance compared to microcrystalline cellulose-based catalysts in terms of both catalytic activity and reusability. The greater catalytic performance of corncob-based catalysts may be attributed to its higher sulfonic groups attachment as well as its superior surface morphology. All in all, the synthesised sulfonated carbon-based catalysts presents a promising direction of research with untapped potential. With more research and development, the sulfonated carbon-based catalysts may poses as a cheap and effective alternative compared to the conventional catalysts. It would also allows for the synthesis of biodiesel through interesterification rather than transesterification at the industrial scale, which should increase the profitability of the biodiesel industry while at the same time reducing the cost of biodiesel, thereby advancing the UN SDGs, in particular SDG 7 and SDG 13.

5.2   Recommendations for Future Work

Over the course of this study, several issues were identified but due to scope limitations, these issues can not be addressed. The following outlines the recommendations for future work in similar topics.

1. The selection of optimal synthesis parameters should factor in the stability of the catalysts synthesised, in addition to the sulfonic group density, which only concerns the catalytic activity of the catalysts.
2. Hot water or other washing agents such as n-hexane should be considered to be used for the samples washing steps in order to leach as much as practically possible amount of attached phosphoric acid and

sulfonic groups, with aim to avoid interference to the experimental results.

3. The chemically activated biomass should be included in characterisation studies to gain a better understanding of the role of the activating agent in the subsequent steps of synthesis.

4. A complete sets of samples including raw biomass, activated biomass, biochar and catalyst should be subjected to all characterisation studies for a complete comparison and discussion.

5. The prepared chemicals should be spent as soon as possible to avoid degradation.

6. One-step synthesis method of sulfonated carbon-based catalyst should be considered and explored as it can potentially cut down the time and energy requirement for the sulfonated carbon-based catalyst synthesis process while yielding catalysts of comparable performance.

7. Method of regeneration for the spent catalyst such as resulfonation using concentrated sulfuric acid may be explored to determine the practical feasibility of the catalyst in industrial use.

8. The effect of carbonisation and sulfonation time on the catalytic performance of the catalyst may be explored to gain a better understanding of the optimal synthesis conditions for sulfonated carbon-based catalyst.

REFERENCES

Abbasi, K.R., Shahbaz, M., Zhang, J., Irfan, M, and Alvarado, R., 2022. Analyze the Environmental Sustainability Factors of China: The Role of Fossil Fuel Energy and Renewable Energy. *Renewable Energy*, [e-journal] 187, pp.390-402. https://doi-org.libezp2.utar.edu.my/10.1016/j.renene.2022.01.066.

Amer, M., and Elwardany, A., 2020. Biomass Carbonization. In: M. Al Qubeissi, A. El-kharouf, and H.S. Soyhan, eds. *Renewable Energy: Resources, Challenges and Applications*. London: IntechOpen. pp.211-233.

Bureros, G.M.A., Tanjay, A.A., Cuizon, D.E.S., Go, A.W., Cabatingan, L.K., Agapay, R.C., and Ju, Y.H., 2019. Cacao Shell-derived Solid Acid Catalyst for Esterification of Oleic Acid with Methanol. *Renewable Energy*, [e-journal] 138, pp.489-501. https://doi-org.libezp2.utar.edu.my/10.1016/j.renene.2019.01.082.

Cao, M., Peng, L., Xie, Q., Xing, K., Lu, M., and Ji, J., 2021. Sulfonated Sargassum Horneri Carbon as Solid Acid Catalyst to Produce Biodiesel via Esterification. *Bioresource Technology*, [e-journal] 324, pp.1-8. https://doi-org.libezp2.utar.edu.my/10.1016/j.biortech.2020.124614.

Changmai, B., Vanlalveni, C., Ingle, A.P., Bhagat, R., and Rokhum, S.L., 2020. Widely Used Catalysts in Biodiesel Production: A Review. *RSC Advances*, [e-journal] 68, pp.41625-41679. https://doi.org/10.1039/D0RA07931F.

da Luz Corrêa, A.P., da Silva, P.M.M., Gonçalves, M.A., Bastos, R.R.C., da Rocha Filho, G.N., and da Conceição, L.R.V., 2023. Study of the Activity and Stability of Sulfonated Carbon Catalyst from Agroindustrial Waste in Biodiesel Production: Influence of Pyrolysis Temperature on Functionalization. *Arabian Journal of Chemistry*, [e-journal] 16(8), pp.1-18. https://doi-org.libezp2.utar.edu.my/10.1016/j.arabjc.2023.104964.

Dhawan, M.S., Barton, S.C., and Yadav, G.D., 2021. Interesterification of Triglycerides with Methyl Acetate for the Co-production Biodiesel and Triacetin using Hydrotalcite as a Heterogeneous Base Catalyst. *Catalysis Today*, [e-journal] 375, pp.101-111. https://doi-org.libezp2.utar.edu.my/10.1016/j.cattod.2020.07.056.

Dutta, A., Bouri, E., Saeed, T., and Vo, X.V., 2021. Crude Oil Volatility and the Biodiesel Feedstock Market in Malaysia during the 2014 Oil Price Decline and the COVID-19 Outbreak. *Fuel*, [e-journal] 292, pp.1-9. https://doi-org.libezp2.utar.edu.my/10.1016/j.fuel.2021.120221.

Flores, K.P., Omega, J.L.O., Cabatingan, L.K., Go, A.W., Agapay, R.C., and Ju, Y.H., 2019. Simultaneously Carbonized and Sulfonated Sugarcane Bagasse as Solid Acid Catalyst for the Esterification of Oleic Acid with Methanol. *Renewable Energy*, [e-journal] 130, pp.510-523. https://doi-org.libezp2.utar.edu.my/10.1016/j.renene.2018.06.093.

Gandam, P.K., Chinta, M.L., Pabbathi, N.P.P., Baadhe, R.R., Sharma, M., Thakur, V.K., Sharma, G.D., Ranjitha, J., and Gupta, V.K., 2022a. Second-generation Bioethanol Production from Corncob - A Comprehensive Review on Pretreatment and Bioconversion Strategies, Including Techno-economic and Lifecycle Perspective. *Industrial Crops and Products*, [e-journal] 186, pp.1-24. https://doi-org.libezp2.utar.edu.my/10.1016/j.indcrop.2022.115245.

Gandam, P.K., Chinta, M.L., Pabbathi, N.P.P., Velidandi, A., Sharma, M., Kuhad, R.C., Tabatabaei, M., Aghbashlo, M., Baadhe, R.R., and Gupta, V.K., 2022b. Corncob-based Biorefinery: A Comprehensive Review of Pretreatment Methodologies, and Biorefinery Platforms. *Journal of the Energy Institute*, [e-journal] 101, pp.290-308. https://doi-org.libezp2.utar.edu.my/10.1016/j.joei.2022.01.004.

García-Franco, A., Godoy, P., de la Torre, J., Duque, E., and Ramos, J.L., 2021. United Nations Sustainability Development Goals Approached from the Side of Biological Production of Fuels. *Microbial Biotechnology*, [e-journal] 14(5), pp.1871-1877. https://doi.org/10.1111/1751-7915.13912.

Guo, Y., Delbari, S.A., Namini, A.S., Le, Q.V., Park, J.Y., Kim, D., Varma, R.S., Jang, H.W., T-Raissi, A., Shokouhimehr, M., and Li, C., 2023. Recent Developments in Solid Acid Catalysts for Biodiesel Production. *Molecular Catalysis*, [e-journal] 547, pp.1-30. https://doi-org.libezp2.utar.edu.my/10.1016/j.mcat.2023.113362.

Ibrahim, S.F., Asikin-Mijan, N., Ibrahim, M.L., Abdulkareem-Alsultan, G., Izham, S.M., and Taufiq-Yap, Y.H., 2020. Sulfonated Functionalization of Carbon Derived Corncob Residue via Hydrothermal Synthesis Route for Esterification of Palm Fatty Acid Distillate. *Energy Conversion and Management*, [e-journal] 210, pp.1-12. https://doi-org.libezp2.utar.edu.my/10.1016/j.enconman.2020.112698.

Kashyap, S.S., Gogate, P.R., and Joshi, S.M., 2019. Ultrasound Assisted Intensified Production of Biodiesel from Sustainable Source as Karanja Oil using Interesterification Based on Heterogeneous Catalyst (γ-alumina). *Chemical Engineering and Processing - Process Intensification*, [e-journal] 136, pp.11-16. https://doi-org.libezp2.utar.edu.my/10.1016/j.cep.2018.12.006.

Kuznetsov, B.N., Chesnokov, N.V., Tsyganova, S.I., Mikova, N.M., and Ivanchenko, N.M., 2015. Production and Properties of Porous Carbon Materials from Chemically Modified Microcrystalline Cellulose. *Russian Journal of Applied Chemistry*, [e-journal] 88, pp.442-448. https://doi.org/10.1134/S1070427215030131.

Lathiya, D.R., Bhatt, D.V., and Maheria, K.C., 2018. Synthesis of Sulfonated Carbon Catalyst from Waste Orange Peel for Cost Effective Biodiesel Production. *Bioresource Technology Reports*, [e-journal] 2, pp.69-76. https://doi-org.libezp2.utar.edu.my/10.1016/j.biteb.2018.04.007.

Li, Y., Wen, Y., Chen, B., Fu, X., and Wu, Y., 2023. The Dilemma and Potential Development of Biodiesel in China - In View of Production Capacity and Policy. *Energy for Sustainable Development*, [e-journal] 75, pp.60-71. https://doi-org.libezp2.utar.edu.my/10.1016/j.esd.2023.05.005.

Li, Z., Luan, R., and Lin, B., 2022. The Trend and Factors Affecting Renewable Energy Distribution and Disparity Across Countries. *Energy*, [e-journal] 254(B), pp.1-11. https://doi-org.libezp2.utar.edu.my/10.1016/j.energy.2022.124265.

Lim, S., Yap, C.Y., Pang, Y.L., and Wong, K.M., 2020. Biodiesel Synthesis from Oil Palm Empty Fruit Bunch Biochar Derived Heterogeneous Solid Catalyst using 4-benzenediazonium Sulfonate. *Journal of Hazardous Materials*, [e-journal] 390, pp.1-9. https://doi-org.libezp2.utar.edu.my/10.1016/j.jhazmat.2019.121532.

Miralles-Quirós, J.L., and Miralles-Quirós, M.M., 2019. Are Alternative Energies a Real Alternative For Investors?. *Energy Economics*, [e-journal] 78, pp.535-545. https://doi-org.libezp2.utar.edu.my/10.1016/j.eneco.2018.12.008.

Naeem, M.M., Al-Sakkari, E.G., Boffito, D.C., Gadalla, M.A., and Ashour, F.H., 2021. One-pot Conversion of Highly Acidic Waste Cooking Oil into Biodiesel over a Novel Bio-based Bi-functional Catalyst. *Fuel*, [e-journal] 283, pp.1-16. https://doi-org.libezp2.utar.edu.my/10.1016/j.fuel.2020.118914.

Pandit, C., Banerjee, S., Pandit, S., Lahiri, D., Kumar, V., Chaubey, K.K., Al-Balushi, R., Al-Bahry, S., and Joshi, S.J., 2023. Recent Advances and Challenges in the Utilization of Nanomaterials in Transesterification for Biodiesel Production. *Heliyon*, [e-journal] 9(4), pp.1-16. https://doi-org.libezp2.utar.edu.my/10.1016/j.heliyon.2023.e15475.

Prestigiacomo, C., Biondo, M., Galia, A., Monflier, E., Ponchel, A., Prevost, D., Scialdone, O., Tilloy, S., and Bleta, R., 2022. Interesterification of Triglycerides with Methyl Acetate for Biodiesel Production Using a Cyclodextrin-derived SnO@γ-Al$_2$O$_3$ Composite as Heterogeneous Catalyst. *Fuel*, [e-journal] 321, pp.1-15. https://doi-org.libezp2.utar.edu.my/10.1016/j.fuel.2022.124026.

Rocha, P.D., Oliveira, L.S., and Franca, A.S., 2019. Sulfonated Activated Carbon from Corn Cobs as Heterogeneous Catalysts for Biodiesel Production using Microwave-assisted Transesterification. *Renewable Energy*, [e-journal] 143, pp.1710-1716. https://doi-org.libezp2.utar.edu.my/10.1016/j.renene.2019.05.070.

Rocha-Meneses, L., Hari, A., Inayat, A., Yousef, L.A., Alarab, S., Abdallah, M., Shanableh, A., Ghenai, C., Shanmugam, S., and Kikas, T., 2023. Recent Advances on Biodiesel Production from Waste Cooking Oil (WCO): A Review of Reactors, Catalysts, and Optimization Techniques Impacting the Production. *Fuel*, [e-journal] 348, pp.1-19. https://doi-org.libezp2.utar.edu.my/10.1016/j.fuel.2023.128514.

Sangar, S.K., Lan, C.S., Razali, S.M., Farabi, M.S.A., and Taufiq-Yap, Y.H., 2019. Methyl Ester Production from Palm Fatty Acid Distillate (PFAD) using Sulfonated Cow Dung-derived Carbon-based Solid Acid Catalyst. *Energy Conversion and Management*, [e-journal] 196, pp.1306-1315. https://doi-org.libezp2.utar.edu.my/10.1016/j.enconman.2019.06.073.

Sangsiri, P., Laosiripojana, N., and Daorattanachai, P., 2022. Synthesis of Sulfonated Carbon-based Catalysts from Organosolv Lignin and Methanesulfonic Acid: Its Activity toward Esterification of Stearic Acid. *Renewable Energy*, [e-journal] 193, pp.113-127. https://doi-org.libezp2.utar.edu.my/10.1016/j.renene.2022.05.012.

Shahzad, S.J.H., Bouri, E., Kayani, G.M., Nasir, R.M., and Kristoufek, L., 2020. Are Clean Energy Stocks Efficient? Asymmetric Multifractal Scaling Behaviour. *Physica A: Statistical Mechanics and its Applications*, [e-journal] 550, pp.1-14. https://doi-org.libezp2.utar.edu.my/10.1016/j.physa.2020.124519.

Souza, M.C.G., Batista, A.C.F., Cuevas, R.F., da Silva Filho, W.J.F., Balanta, M.A.G., Champi, A., and de Assunção, R.M.N., 2022. Simultaneous Carbonization and Sulfonation of Microcrystalline Cellulose to Obtain Solid Acid Catalyst and Carbon Quantum Dots. *Bioresource Technology Reports*, [e-journal] 19, pp.1-11. https://doi-org.libezp2.utar.edu.my/10.1016/j.biteb.2022.101193.

Sreeharsha, R.V., Dubey, N., and Mohan, S.V., 2023. Orienting Biodiesel Production Towards Sustainability and Circularity by Tailoring the Feedstock and Processes. *Journal of Cleaner Production*, [e-journal] 414, pp.1-20. https://doi-org.libezp2.utar.edu.my/10.1016/j.jclepro.2023.137526.

Syafiuddin, A., Chong, J.H., Yuniarto, A., and Hadibarata, T., 2020. The Current Scenario and Challenges of Biodiesel Production in Asian Countries: A Review. *Bioresource Technology Reports*, [e-journal] 12, pp.1-8. https://doi-org.libezp2.utar.edu.my/10.1016/j.biteb.2020.100608.

Tinh, N.T., Dan, D.K., Phuong, N.T., Dat, N.M., Khang, P.T., Bao, P.P., Bao, L.M., Nhan, D.D., Khoa, N.N., Hanh, N.T., Hoa, D.N., Viet, V.N.D., Danh, T.T., Chau, P.T.L., Phong, M.T., and Hieu, N.H., 2023. Sustainable Synthesis of Cellulose-derived Magnetic Iron Oxide/Sulfonated Graphene Oxide-like Material from Corncob for Conversion of Hemicellulose to Furfural. *Fuel*, [e-journal] 343, pp.1-15. https://doi-org.libezp2.utar.edu.my/10.1016/j.fuel.2023.127870.

Wong, W.Y., Lim, S., Pang, Y.L., Shuit, S.H., Chen, W.H. and Lee, K.T., 2020. Synthesis of Renewable Heterogeneuos Acid Catalyst from Oil Palm Empty Fruit Bunch for Glycerol-free Biodiesel Production. *Science of The Total Environment*, [e-journal] 727, pp.1-12. https://doi-org.libezp2.utar.edu.my/10.1016/j.scitotenv.2020.138534.

Wong, W.Y., Lim, S., Pang, Y.L., Shuit, S.H., Lam, M.K., Tan, I.S., and Chen, W.H., 2023. A Comprehensive Review of the Production Methods and Effect of Parameters for Glycerol-free Biodiesel Production. *Renewable and Sustainable Energy Reviews*, [e-journal] 182, pp.1-17. https://doi-org.libezp2.utar.edu.my/10.1016/j.rser.2023.113397.

Zhang, B., Gao, M., Geng, J., Cheng, Y., Wang, X., Wu, C., Wang, Q., Liu, S., and Cheung, S.M., 2021. Catalytic Performance and Deactivation Mechanism of a One-step Sulfonated Carbon-based Solid-acid Catalyst in an Esterification Reaction. *Renewable Energy*, [e-journal] 164, pp.824-832. https://doi-org.libezp2.utar.edu.my/10.1016/j.renene.2020.09.076.

APPENDICES

Appendix A: SEM Images
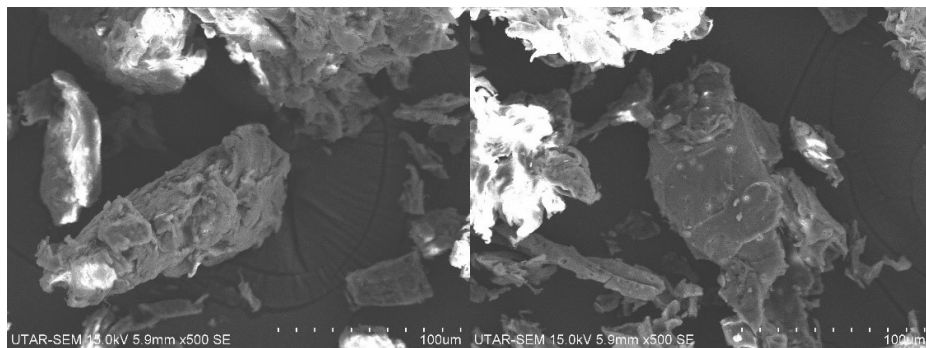
Figure A-1: RC under 500 × Magnification
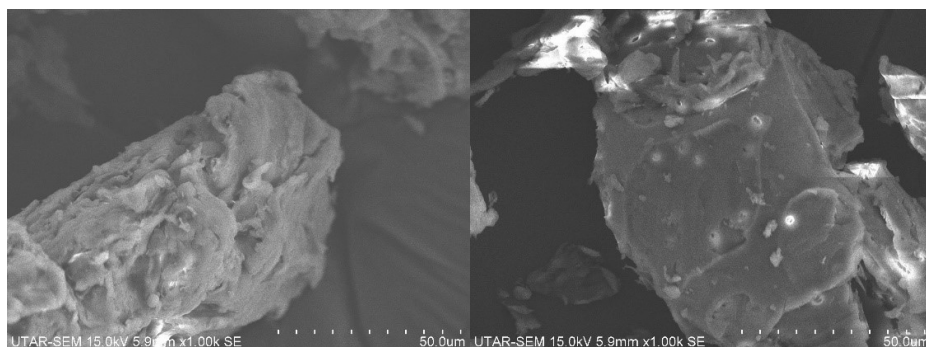
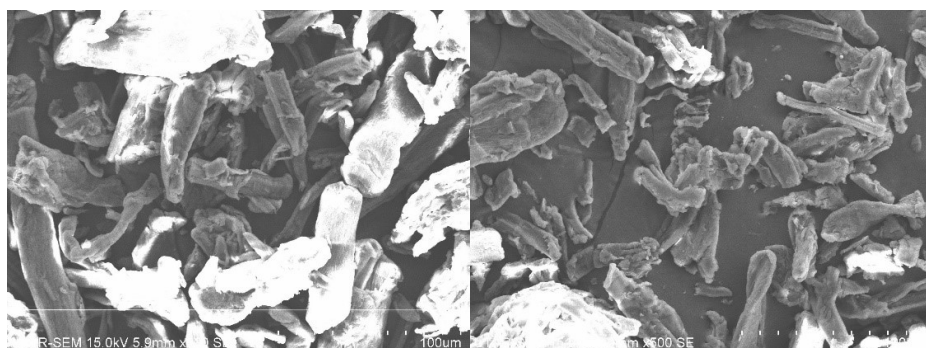Figure A-2: RC under 1000 × Magnification

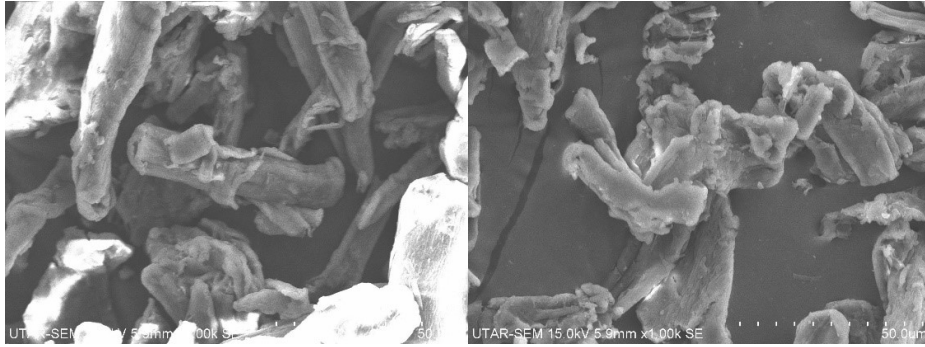Figure A-3: RM under 500 × Magnification

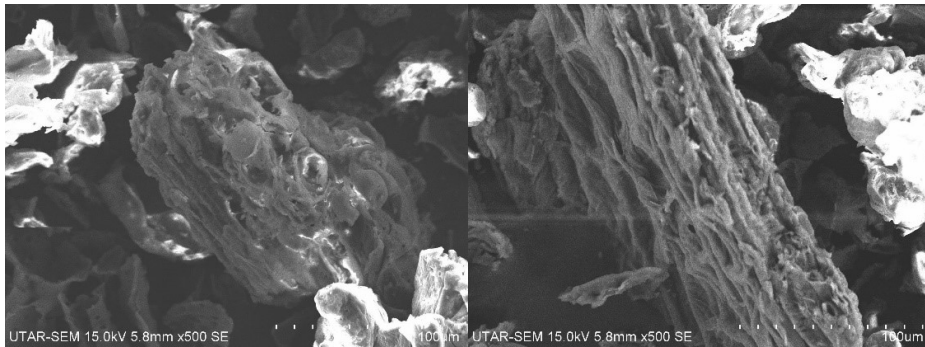Figure A-4: RM under 1000 × Magnification

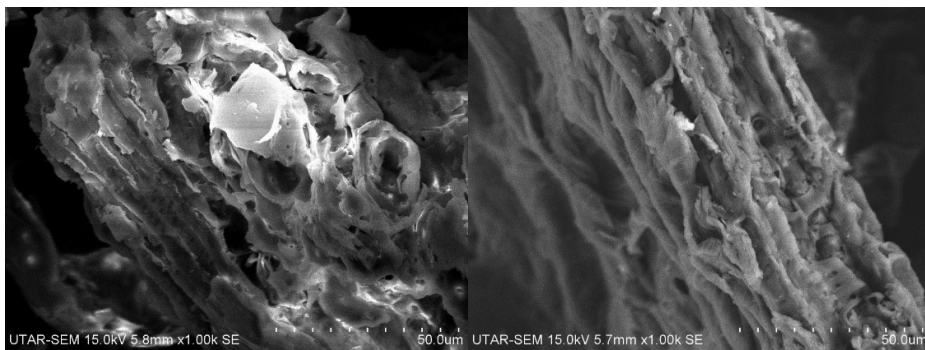Figure A-5: C-200 under 500 × Magnification
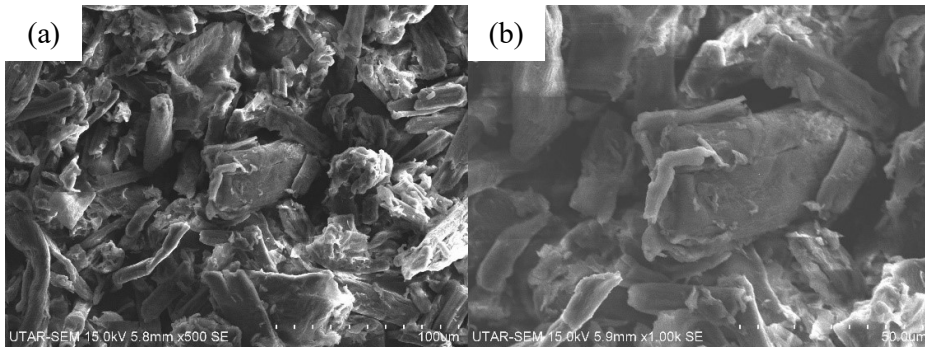

Figure A-6: C-200 under 1000 × Magnification

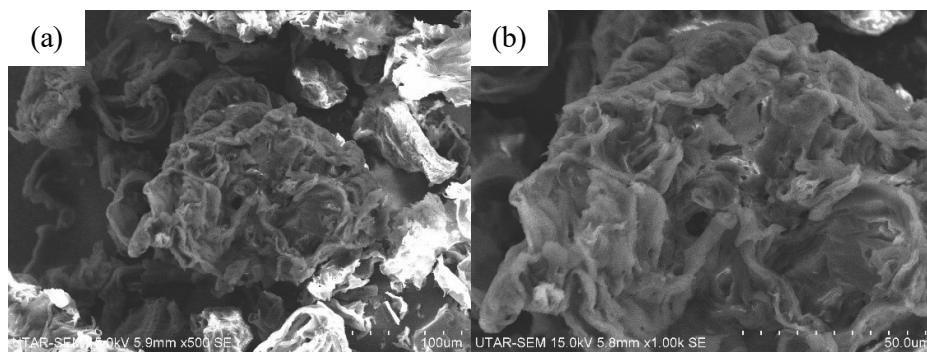Figure A-7: M-200 under (a) 500 × and (b) 1000 × Magnification

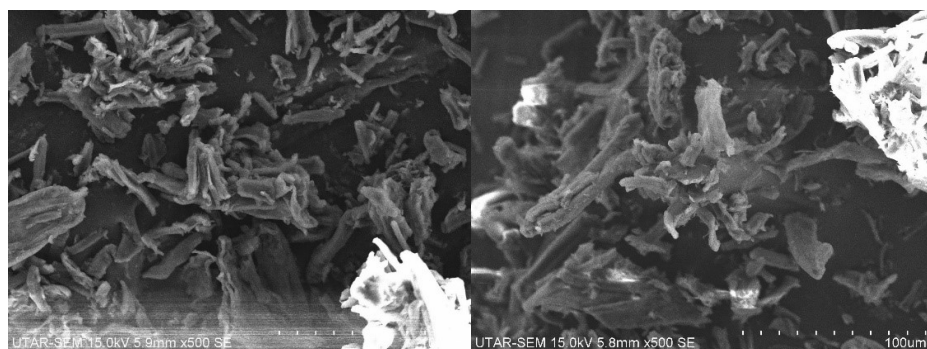Figure A-8: C-300 under (a) 500 × and (b) 1000 × Magnification
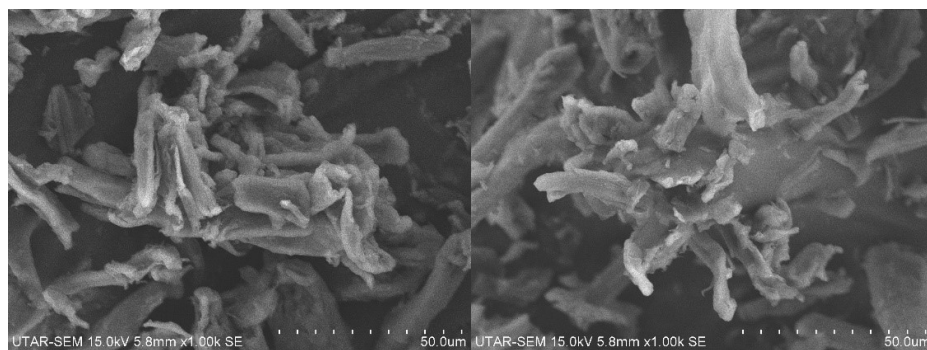

Figure A-9: M-300 under 500 × Magnification

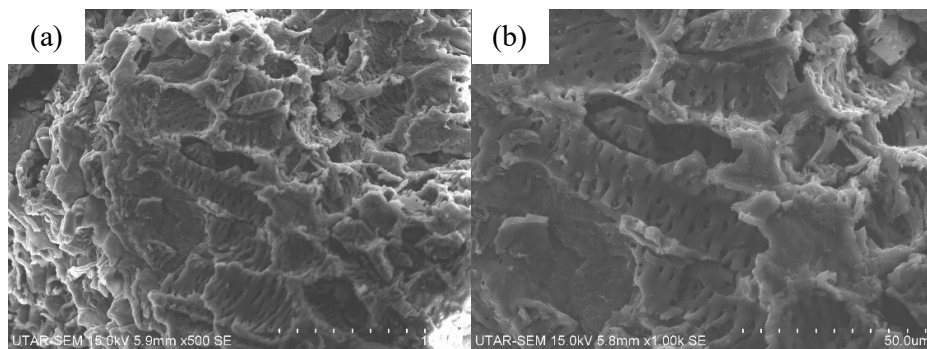Figure A-10: M-300 under 1000 × Magnification

Figure A-11: C-400 under (a) 500 × and (b) 1000 × Magnification
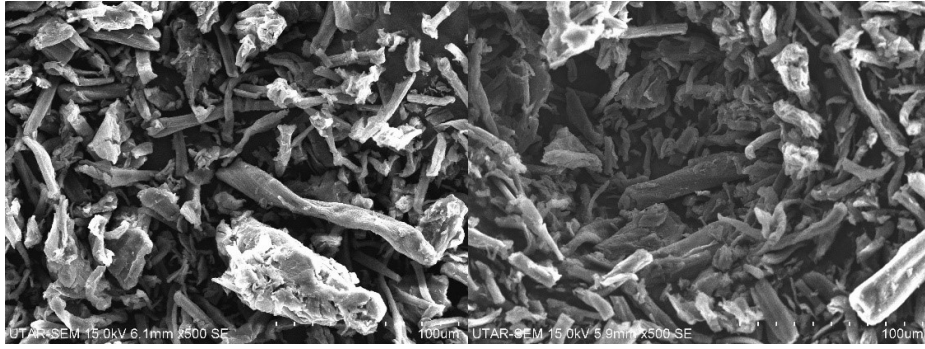
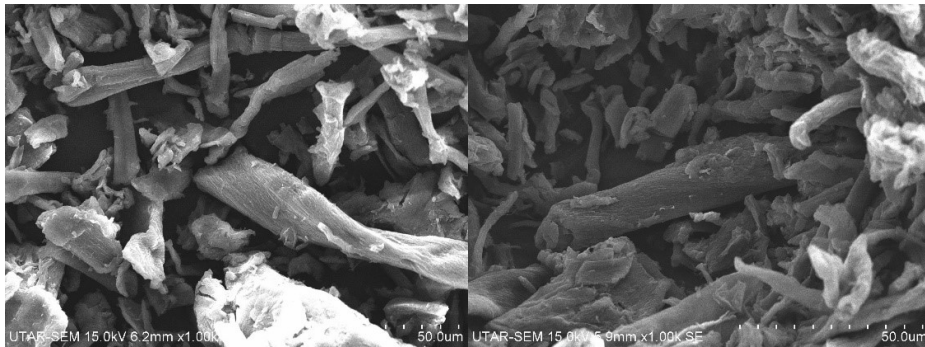Figure A-12: M-400 under 500 × Magnification

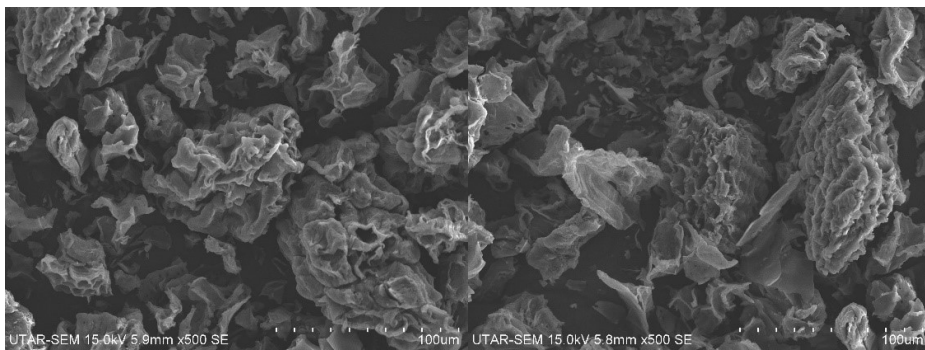Figure A-13: M-400 under 1000 × Magnification

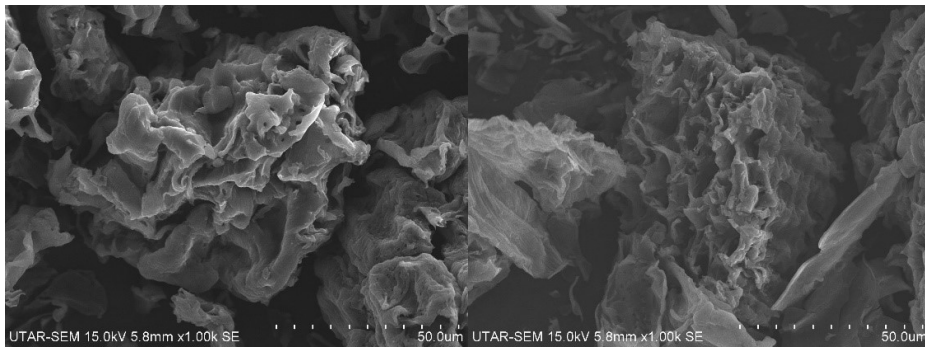Figure A-14: C-500 under 500 × Magnification

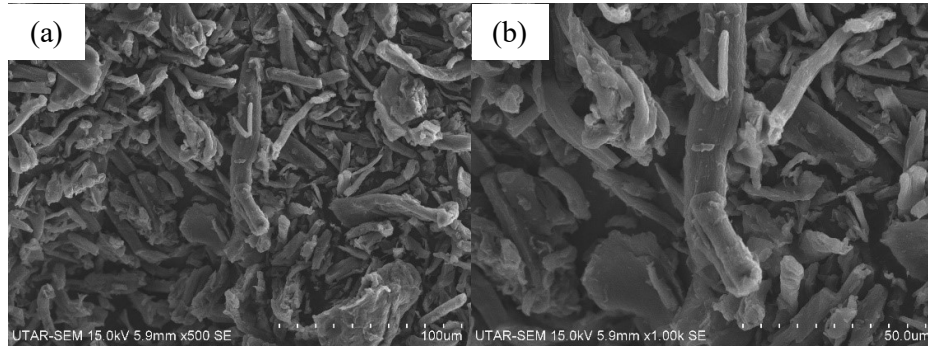Figure A-15: C-500 under 1000 × Magnification

Figure A-16: M-500 under (a) 500 × and (b) 1000 × Magnification

Appendix B: Sulfonic Group Density Test Results

Table B-1: Sulfonic Group Density Test Results for Varying Carbonisation
Temperature

`	Run				Sulfonic Group Density (mmol/g)
	1	2	3	Average	
M-200-100	2.5	2.4	2.6	2.5	1.00
M-300-100	1.3	1.3	1.3	1.3	0.52
M-400-100	1	1.1	0.9	1	0.40
M-500-100	0.7	0.8	0.9	0.8	0.32
C-200-100	2.7	2.5	2.6	2.6	1.04
C-300-100	1.5	1.5	1.5	1.5	0.60
C-400-100	0.7	0.5	0.9	0.7	0.28
C-500-100	0.2	0.6	0.4	0.4	0.16

Table B-2: Sulfonic Group Density Test Results for Varying Sulfonation
Temperature

Samples	Run				Sulfonic Group Density (mmol/g)
	1	2	3	Average	
M-200-100	2.5	2.4	2.6	2.5	1.00
M-200-150	2.3	2.7	2.5	2.5	1.00
M-200-200	1.0	2.1	1.9	2.0	0.80
C-200-100	2.6	2.6	2.6	2.6	1.04
C-200-150	2.5	2.4	2.6	2.5	1.00
C-200-200	1.0	0.8	0.9	0.9	0.36

Appendix C: Acid Value Test Results

Table C-1: Acid Value Test Results for Interesterification Parameter Studies

Sample	Catalyst Loading (wt%)	Reaction Time (h)	V_{KOH} (mL)			AV_1	X (%)	Y (%)
			1	2	Average			
Control	0	4	1.8	1.9	1.85	51.90	3	3
C-200-100	5	4	4.9	4.9	4.90	39.28	26	27
	10	4	4.0	3.8	3.90	11.22	79	82
	15	4	4.1	4.2	4.15	18.24	66	68
	10	2	3.9	4.3	4.10	16.83	68	71
	10	6	3.9	3.8	3.85	9.82	82	84
M-200-100	5	4	2.9	2.8	2.85	15.43	71	74
	10	4	3.7	3.8	3.75	40.68	24	25
	15	4	4.1	4.0	4.05	49.10	8	8
	5	2	3.2	3.2	3.20	25.25	53	54
	5	6	2.8	2.9	2.85	15.43	71	74

Table C-2: Acid Value Test Results for Reusability Study

Sample	V_{KOH} (mL)			AV_1	X (%)	Y (%)
	1	2	Average			
C-200-100	4.2	4.2	4.20	19.64	63	65
M-200-100	3.5	3.3	3.40	30.86	42	44